Superconducting RF cavities for accelerators

Fritz Caspers / Manfred Wendt / Michele Bozzolan

with many slides by: Sergio Calatroni, Wolfgang Weingarten, Tobias Junginger, Sarah Aull, Benedikt Peters, Michael Bartel and others

JUAS lecture 2020

OUTLINE OF LECTURE

- Basics of superconductivity

- Basics of RF cavities

- Interaction of the cavity with the beam

- Technological issues

- Diagnostics

- State of the art SRF research

Basics of superconductivity

- Motivation

- Historical remarks

- Surface impedance and plane waves in normal conductors

- Basics of RF superconductivity

  - Meissner effect

  - Two kinds of superconductors

  - Materials

  - Two fluid model

  - London equations and penetration depth

  - Complex conductivity, surface impedance and BCS theory

  - How to measure the surface impedance

  - Critical fields

- Summary

- Recommended Literature

Motivation (1/5)

Why was LEP so Big? Why SC RF?

Losses due to Synchrotron Radiation

EO = .511MeV for electrons and 938.256 for protons

$$U_0 \propto \frac{E_b^4}{E_0^4}\frac{1}{\rho} = V_{RF} \sin \varphi_s$$

ρ = machine radius

Power Dissipated in the walls of the Cu cavities

$$P_{Cu} \propto \frac{V_{RF}^2}{lr_{sh}} \propto \frac{E_b^8}{E_0^8}\frac{1}{\rho^2}\frac{1}{lr_{sh}}$$

lr_{sh} stands for

Longitudinal shunt impedance

Power to Beam from the SC cavities…..

$$P_{sc} \propto I_{tot}U_0 \propto \frac{E_b^4}{E_0^4}\frac{I_{tot}}{\rho}$$

So to minimise power you need ρ to be as large as possible **i.e. large radius.** The radius for LEP1 was optimised for around 80GeV with Cu cavities

For sc cavities the power needed is "only" proportional to the 4th power of energy. NOTE to operate LEP at 103 GeV with copper cavities would have needed 1280 cavities and 160MW of RF power!! Impossible for many reasons

LHC For protons since E_0 is a factor of 1836 higher, the RF power is not an issue and the bending radius can be made as low as is technically possible. i.e. High fields

28th November 2019, CERN   S.Myers LEP 30 Colloquium   9

Motivation (2/5)

Why use superconducting cavities?

- The reason is very simple: to obtain very high accelerating fields in continuous mode, the power dissipated by normal conducting (i.e copper) cavities becomes too large. Remember that there can be a 10^5 difference in R_s, thus in dissipated power, for the same surface fields.

- This is valid also taking into account the efficiency of the cryogenic plant. The Carnot efficiency of a perfect cooler working between 300 K and T is:

$$\eta_c = \frac{T}{300 - T}$$

- For T=4.2 K, η_c=0.014. A modern cryoplant has a technical efficiency that can reach about 30% of the ideal one, thus η_{real}=0.0042. Even taking this into account the energy savings are huge.

- Moreover, SC cavities allow designs with larger beam pipes which, are beneficial for beam stability although reducing R_a. This would be unacceptable for NC cavities, but owing to the huge Q_0 the performance of SC cavities don't suffer much.

- LEP case: Cu hypothesis   3 MW/m @ 5 MV/m accelerating field
  Nb case: 30 W/m @ 5 MV/m accelerating field
                  7 kW/m including cryogenic losses

Sergio Calatroni – CERN

Electrodynamics and Superconducting Cavities

JUAS 2020: SC RF - Caspers/Wendt/Bozzolan

Motivation

LEP2 Increase of accelerating Voltage

- 48 copper cavities
    - giving absolute maximum 150 MV
    - more reasonable level   120 MV
- 72 superconducting modules, each of 4 cavities
    - 68*41 + 4*34   giving design maximum   2910 MV
    -                                      applying .96 av. gradient   2790 MV
    -                                      allowing 2 units to trip   2630 MV
- For good quantum lifetime (i_b 0.7mA, Qs 0.1,102/90)
    - running "as in 98" 2750 MV   E = 96.0 GeV (J_x = 1)
    - pushing to 6.5MV/m   2980 MV   E = 98.0 GeV
    - pushing to 7.0MV/m   3200 MV   E = 100 GeV
    - staying at 6.8MV/m   3120+80 MV with only 1 unit reserve

JUAS 2020: SC RF - Caspers/Wendt/Bozzolan

Motivation

The RF group's 1999 collection

- Q: 102GeV: How did we get there??
  - A "by lowering luminosity and breaking cavities".
- Q: Can we go further??
  - A: "Yes, by further lowering the luminosity and breaking MORE cavities".

S. Myers, Twelve years of beam in LEP, —, LEP Fest 2000, CERN, (LEPFest2000.ppt), October 2000.

65

JUAS 2020: SC RF - Caspers/Wendt/Bozzolan

The abridged story of 2000

- 14th June: First candidate event 206.7 GeV
  - Reconstructed Higgs mass 114.3 GeV/c2
- 20th July: LEP Committee
  - ALEPH present excess at high masses
- 31st July & 21st Aug: events 2 & 3 for ALEPH
  - Things are heating up!
- 5th September: LEP Committee
  - Excess only in ALEPH, only 4 jets
- September 14th: Research board:
  - ONE MONTH run extension GRANTED (LHC startup)

We were not far from getting the HIGGS

28th November 2019, CERN   S.Myers LEP 30 Colloquium   68

Historical remarks

- 1908 Liquefaction of helium (4.2 K)

- 1911 Zero resistance

- 1933 Meissner effect

- 1935 Phenomenological theory of H & F. London

- 1950 Ginzburg – Landau theory

- 1951 – 2 TYPE II superconductors (Abrikosov)

- 1957 Bardeen – Cooper – Schrieffer theory

- 1960 Magnetic flux quantisation

- 1962 Josephson effect

- 1986 High temperature superconductors (Bednorz – Müller)
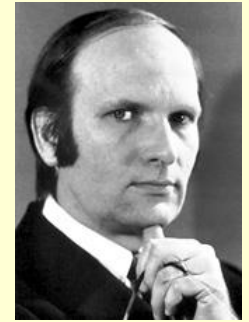
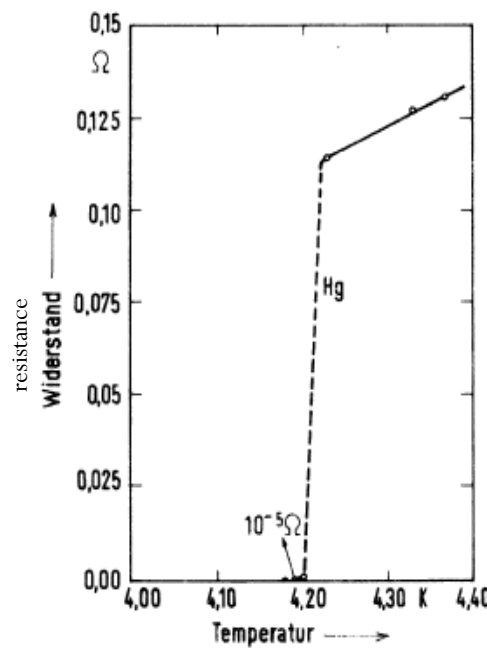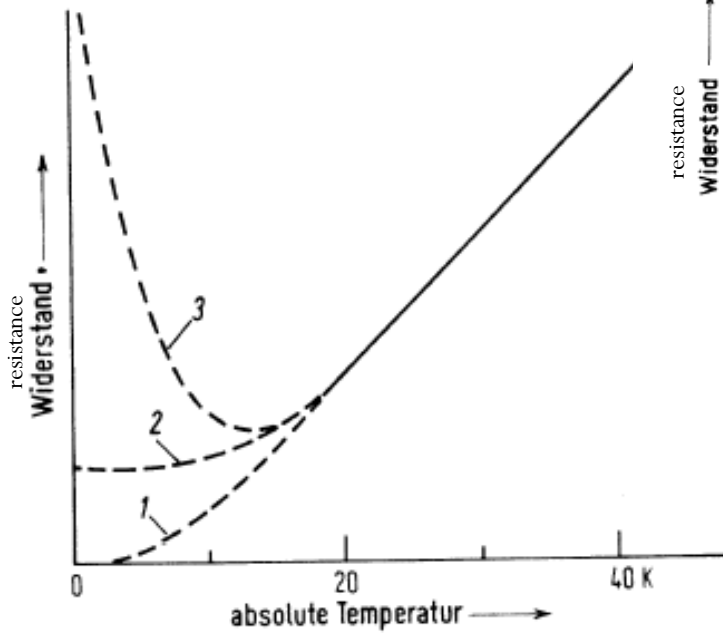Bardeen – Cooper – Schrieffer (BCS)
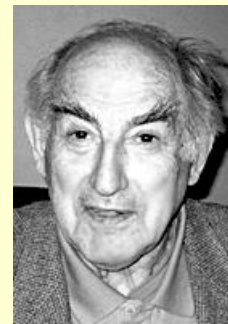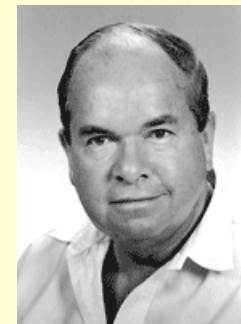
Ginzburg   Abrikosov

Bednorz   Müller

JUAS 2020: SC RF - Caspers/Wendt/Bozzolan
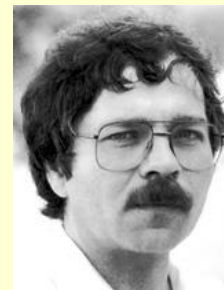
Nobel prize for « his investigations on the properties of matter at low temperatures which led, inter alia, to the production of liquid helium »
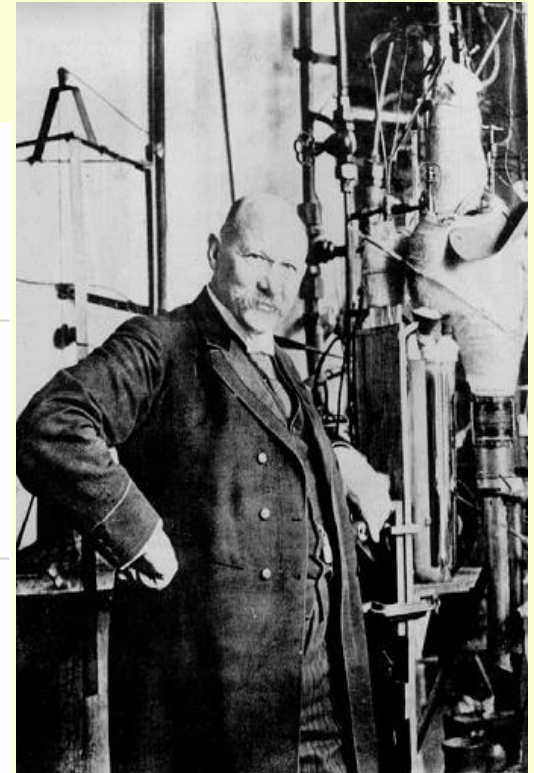
H. Kamerling – Onnes
in his laboratory at Leiden (NL)

- Zero resistivity
- Meissner effect
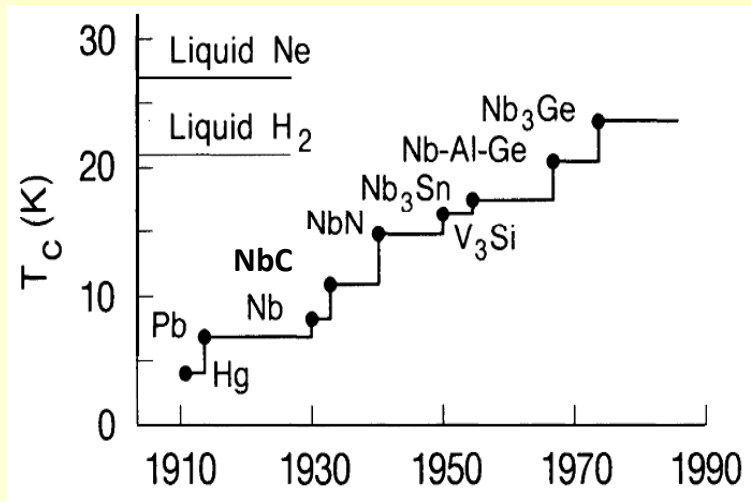

$H - T$ diagram for the
superconducting state
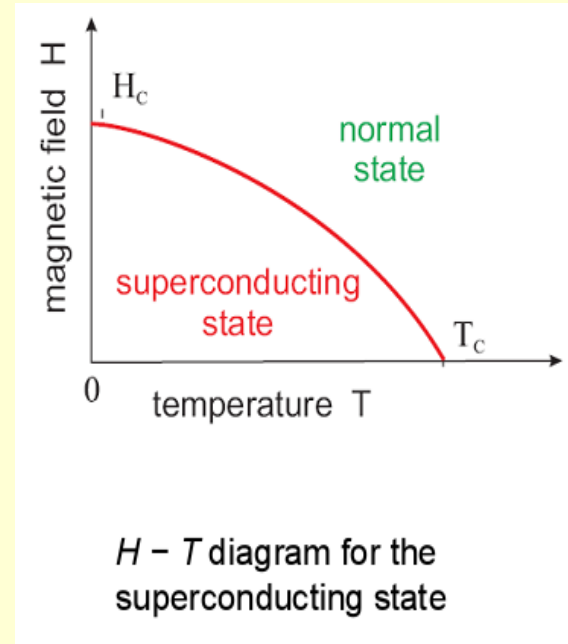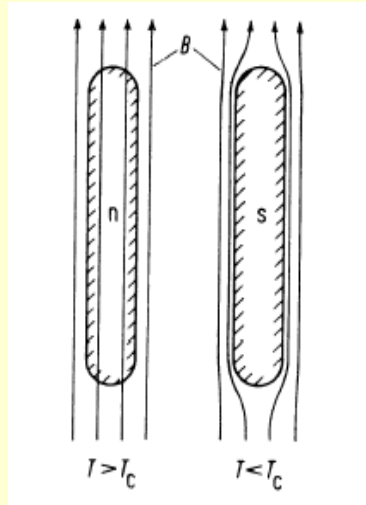
Superconductivity is destroyed:

- by increasing temperature at $T > T_c$
- by large magnetic field $H > H_c$

$$\frac{H_c(T)}{H_c(0)} = \left[1 - \left(\frac{T}{T_c} \right)^2 \right]$$

11

Development of the superconducting transition temperatures after the discovery of the phenomenon in 1911. The materials listed are metals or inter-metallic compounds and reflect the respective highest T_c's - Adapted from G. Bednorz – Nobel lecture
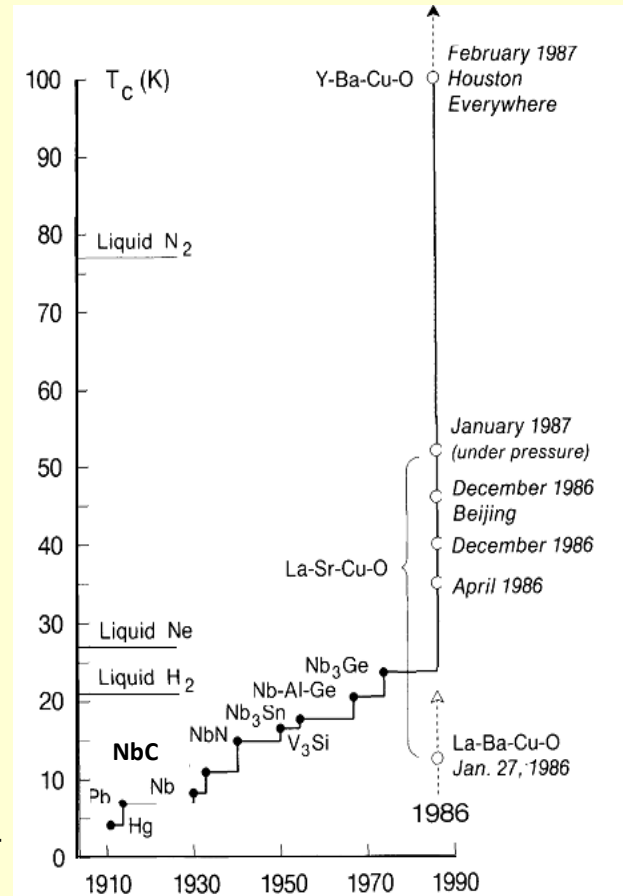
Figure 1.13. Evolution of the superconductive transition temperature subsequent to the discovery of the phenomenon. From [1.29], © 1987 by the American Association for the Advancement of Science.
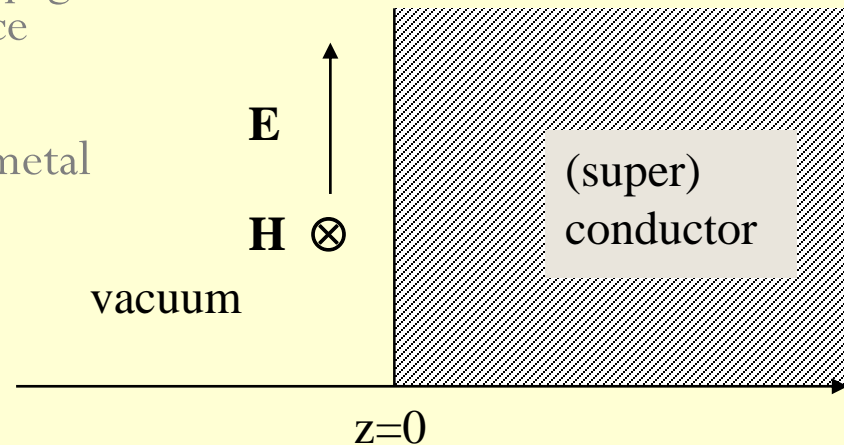
Surface Impedance

For a plane EM wave incident on a semi-infinite flat metallic surface:

$$Z_S = R_S + jX_S = \frac{E_{\parallel}(0)}{H_{\parallel}(0)}$$

- **E**, *H* always in complex notation
- **E**, *H* parallel to the surface
- R_s and X_s are real and imaginary part of the surface impedance respectively
- The homogeneous plane wave propagates in z-direction i.e. normal incidence

Reference frame coordinates:

- x, y parallel to the surface of the metal
- z perpendicular to the surface
  - z=0: on the surface

E

H ⊗

vacuum

(super) conductor

z=0

Plane Waves in Vacuum

From Maxwell's equations:

$$E = E_0 \, e^{j(kz - \omega t)} \qquad H = H_0 \, e^{j(kz - \omega t)} \qquad \text{and:} \qquad H = E_0 \frac{k}{\omega \mu_0} e^{j(kz - \omega t)}$$

with the wavenumber:
$$k = \frac{2\pi}{\lambda} = \frac{\omega}{c} = \omega \sqrt{\varepsilon_0 \mu_0}$$

follows the wave equation in free space:
$$E = E_0 \, e^{j(kz - \omega t)} \qquad H = E_0 \sqrt{\frac{\varepsilon_0}{\mu_0}} \, e^{j(kz - \omega t)}$$

with the free space impedance:
$$Z = \frac{|\mathbf{E}|}{|\mathbf{H}|} = \sqrt{\frac{\mu_0}{\varepsilon_0}} = 376.7 \, \Omega$$

Plane Waves in Metals

Generalized wavenumber: $\qquad k^2 = \omega^2 \varepsilon\mu + \mathrm{j}\,\omega\sigma\mu \qquad Z = \dfrac{|\mathbf{E}|}{|\mathbf{H}|} = \sqrt{\dfrac{\mu}{\varepsilon}} = \dfrac{\omega\mu}{k}$

Local current density and E-field: $\qquad \mathbf{J}(\vec{x}, t) = \sigma\,\mathbf{E}(\vec{x}, t)$

$\mathbf{J}$ =surface current density
not to be confounded with j=$\sqrt{-1}$

Conductivity in the metal: $\qquad \sigma(\omega) = \dfrac{\sigma_0}{(1 + \mathrm{j}\,\omega\tau)} \qquad$ with: $\; \sigma_0 = \dfrac{ne^2\ell}{m_e v_F} = \dfrac{ne^2\tau}{m_e}$

In practice σ is assumed to be frequency independent ($\omega\tau \ll 1$):

$$\omega\sigma\mu \gg \omega^2\varepsilon\mu \Rightarrow k^2 = \mathrm{j}\,\omega\sigma\mu$$

Wave equation in metals: $\qquad E = E_0\,\mathrm{e}^{\mathrm{j}(kz - \omega t)} = E_0\,\mathrm{e}^{\mathrm{j}(\alpha z - \omega t)}\mathrm{e}^{-\beta z}$

with: $\qquad \dfrac{1}{\beta} = \sqrt{\dfrac{2}{\sigma\omega\mu}} = \delta \qquad$ being the field penetration or skin depth

Surface Impedance in "normal" Metals

- The surface impedance Z_s is defined at the interface between two media. It can be calculated in a similar way as for continuous media.

- You take Maxwell's equation, set the appropriate boundary conditions for the continuity of the waves (incident, reflected, transmitted), and you get:

$$Z_S = \frac{E_{\parallel}(0)}{H_{\parallel}(0)} = \sqrt{\frac{j\omega\mu_0}{\sigma}} = \sqrt{\frac{\omega\mu_0}{2\sigma}} + j\sqrt{\frac{\omega\mu_0}{2\sigma}} = R_S + jX_S$$

- Introducing appropriate numbers, e.g. for copper at ambient for $f = 1\ GHz$:

$$\sigma_{Cu} = 58.5e6\ \text{S/m} \qquad\qquad R_s = 8.2\ \text{m}\Omega \text{ per unit square}$$

What is the skin depth?

Surface Resistance

Since we will deal a lot with the surface resistance R_s,
here is a simple DC model that gives a rough idea of what it means:

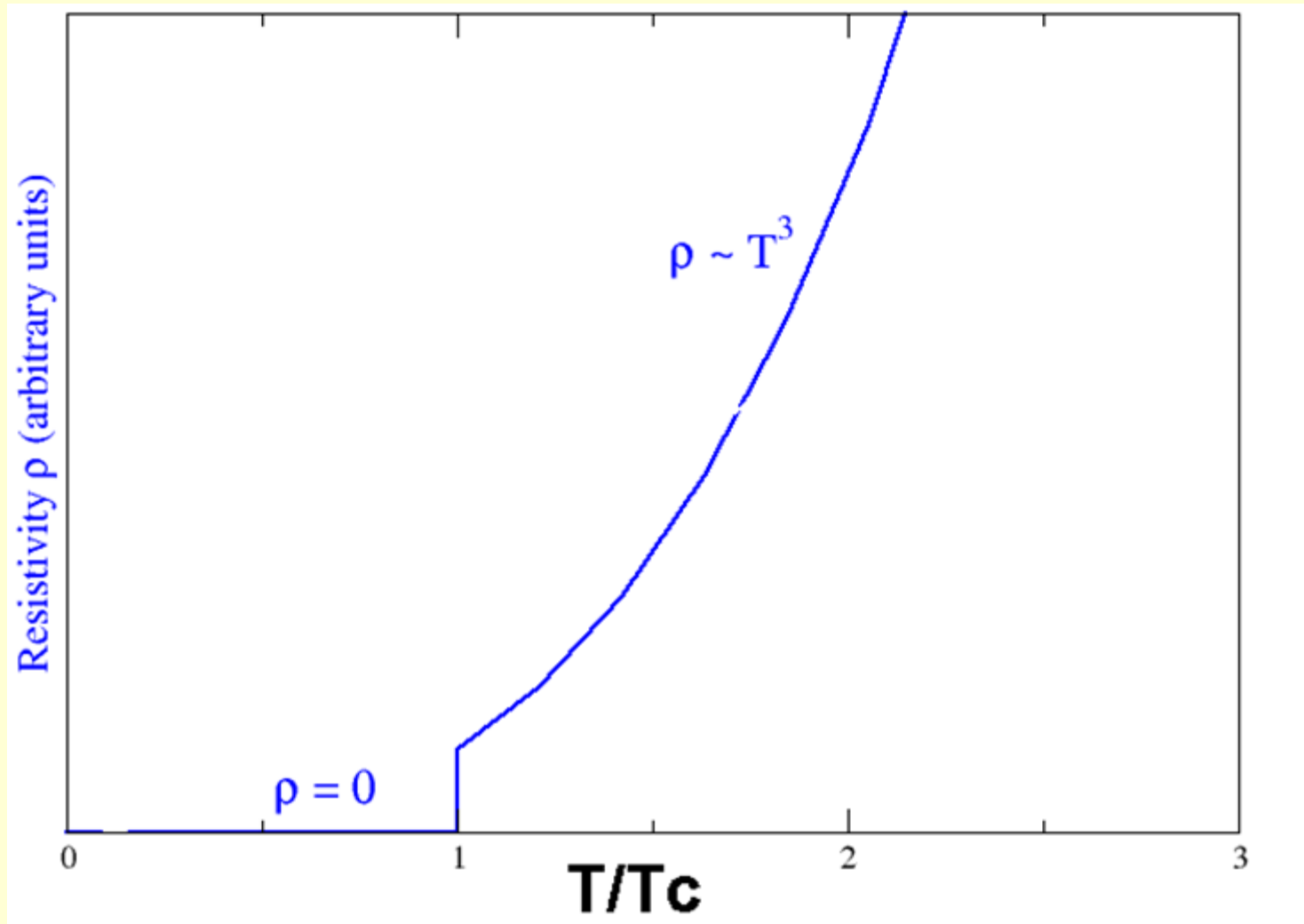Consider a square sheet of metal and calculate its resistance to a transverse current flow:
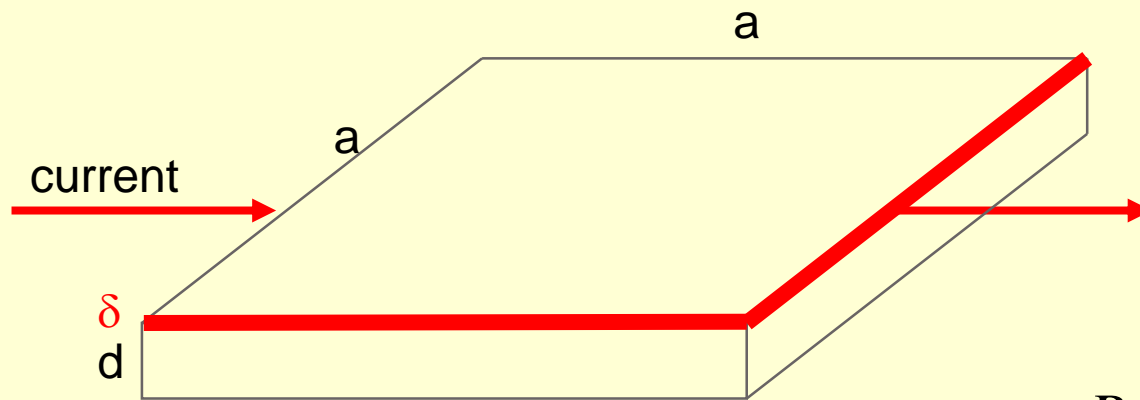
$$R = \frac{\rho \, \cancel{a}}{d \, \cancel{a}} = \frac{\rho}{d}$$

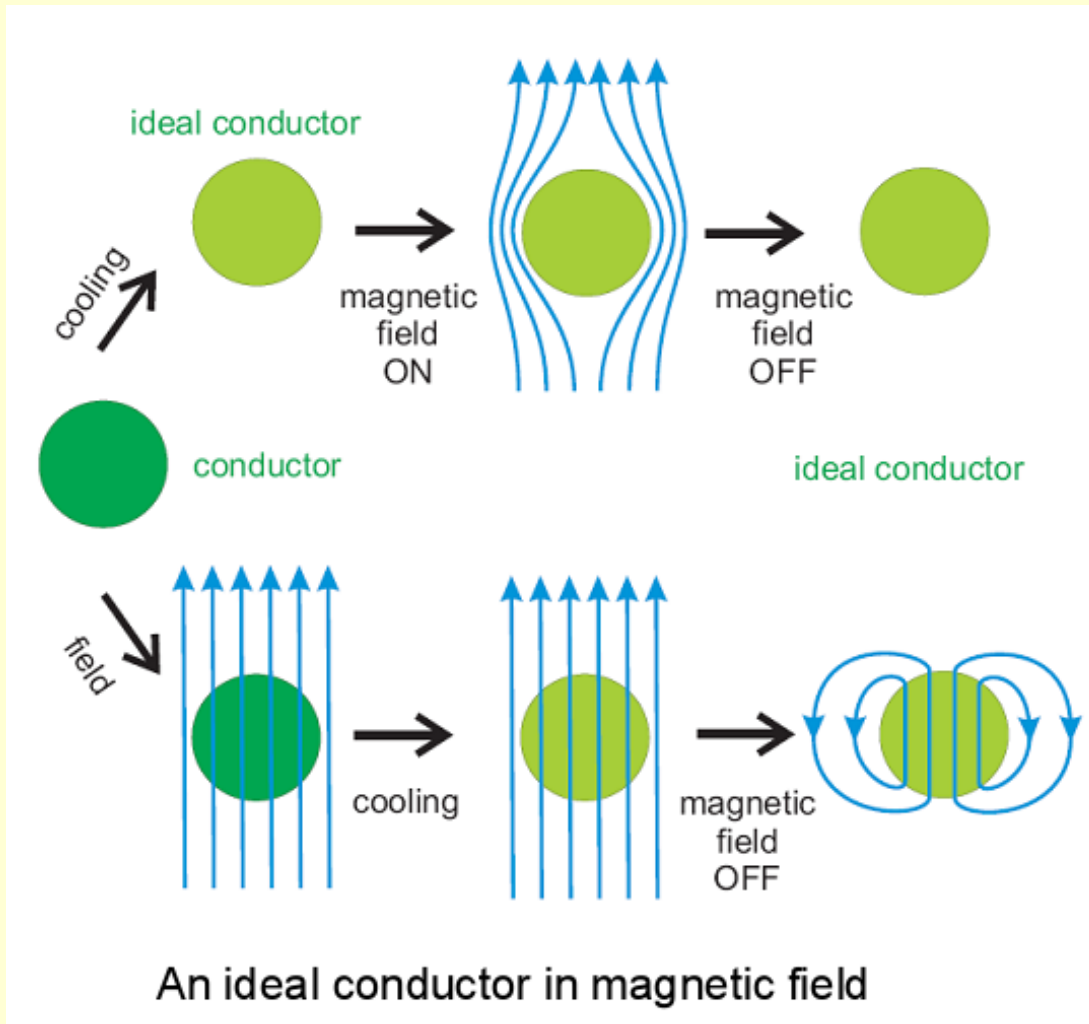$$R_s = \sqrt{\frac{\mu_0 \omega}{2\sigma}} = \frac{1}{\sigma \delta} = \frac{\rho}{\delta}$$

- The surface resistance R_s is the resistance that a square piece of conductor opposes to the flow of the currents induced by the RF wave, within a layer δ

- ρ is the specific electrical resistance, given in [Ωm].

    For copper: $\rho_{Cu} = 17 \cdot 10^{-3} \; \Omega \cdot mm^2/m = 17 \; n\Omega \; m$ (A one meter long Cu-wire of 1 mm^2 cross-section has 17 mΩ)

Superconductivity

$\rho \sim T^3$

$\rho = 0$

Resistivity ρ (arbitrary units)

T/Tc

Meissner effect 1/3

ideal conductor

cooling

conductor

magnetic field ON

magnetic field OFF

ideal conductor
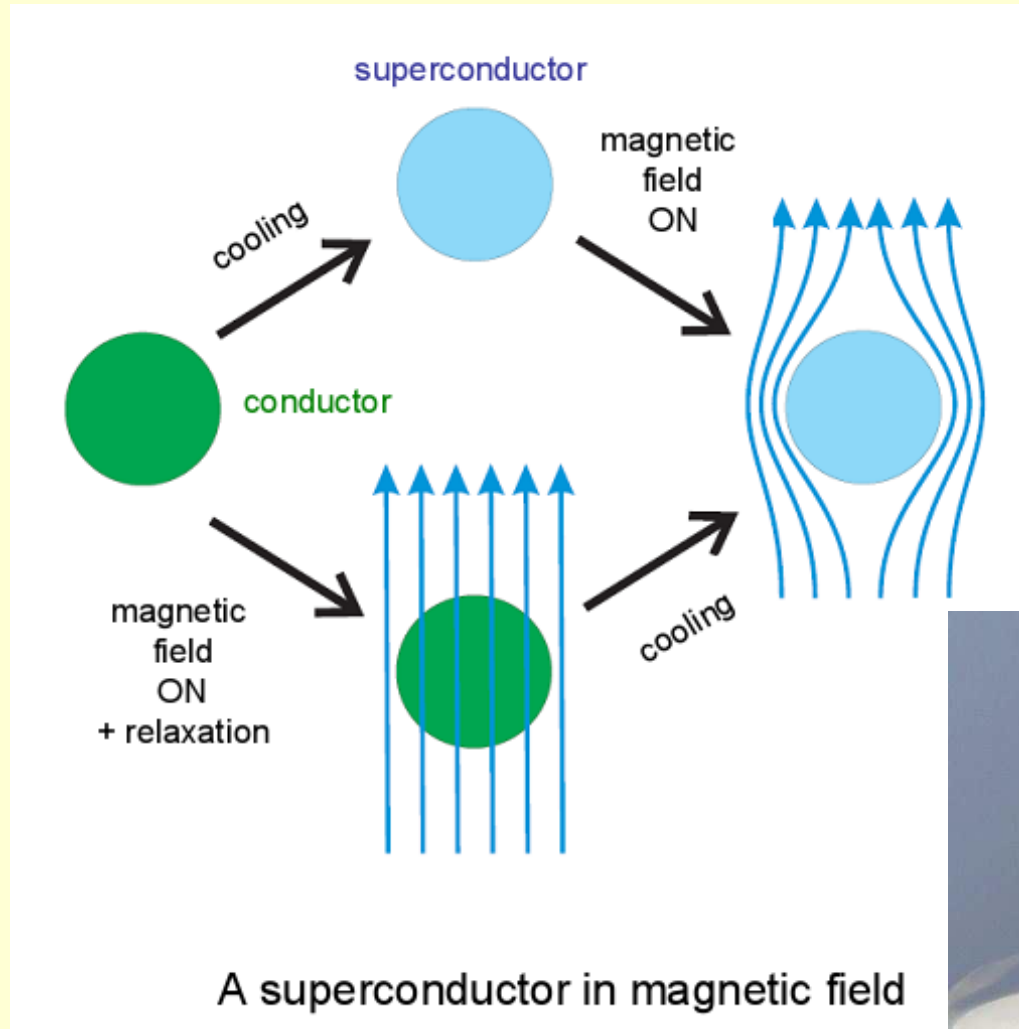
field

cooling

magnetic field OFF

An ideal conductor in magnetic field

For a hypothetical ideal conductor any change (vs time) in the ambient magnetic field induces persistent surface currents. If cooled inside a magnetic field from ambient to cryo then there can be a strong magnetic field inside at cryo

Meissner effect

superconductor

cooling

conductor

magnetic field ON

magnetic field ON + relaxation

cooling

A superconductor in magnetic field

A superconductor (well, yes a conventional one) is always field free at cryo or not superconducting regardless of the " history"

JUAS 2020: SC RF - Caspers/Wendt/Bozzolan

Meissner effect 3/3

1. Magnetic lines of force outside a superconductor are always tangential to its surface

$$\text{div } \vec{B} = 0;$$

$$\text{Since } \vec{B}_n^{(i)} = 0 \Rightarrow \vec{B}_n^{(e)} = 0$$

2. A superconductor in an external magnetic field always carries an electric current near its surface

$$\vec{\nabla} \times \vec{B} = \mu_0 \vec{j} \Rightarrow \vec{j} = 0 \text{ inside the superconductor}$$

$$\oint \vec{B} \cdot \mathrm{d}\vec{l} = \mu_0 j_{\text{surf}} \cdot l_{1-2}$$

$$\oint \vec{B} \cdot \mathrm{d}\vec{l} = \mu_0 H_0 \cdot l_{1-2} \Rightarrow \vec{j}_{\text{surf}} = \vec{n} \times \vec{H}_0$$
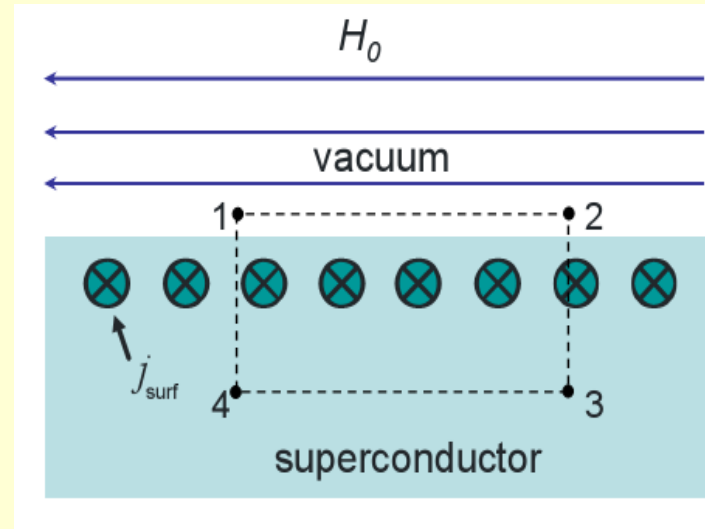
Thus, the surface current is completely defined by the magnetic field at the surface of a superconductor.

JUAS 2020: SC RF - Caspers/Wendt/Bozzolan

Theories of Superconductors

- Gorter & Casimir two fluid model
  - London Equations
  - Pippard's Coherence length ξ

- Ginzburg-Landau
  - Second order phase transition of complex order parameter Ψ

- BCS (Bardeen-Cooper-Schrieffer)
  - Microscopic theory
  - Two Fluid Model revised

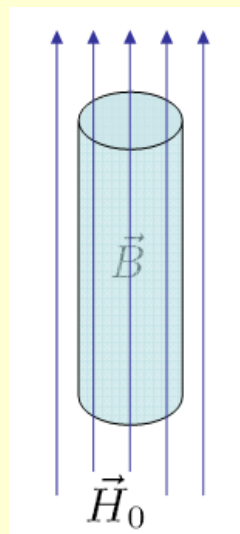- (Strong coupling – Elihasberg)

Two kinds of superconductors

Magnetic properties of a **type I superconductor**

Magnetic properties of a superconductor can be derived from $\rho = 0$ and $B = 0$

Type I superconductors are all elemental superconductors (except niobium)

$$\vec{B} = \mu_0 \cdot \left(\vec{H}_0 + \vec{M} \right)$$

The magnetization $\vec{M}$ compensates the external field H_0, thus the SC bulk is field free.

Magnetization curve
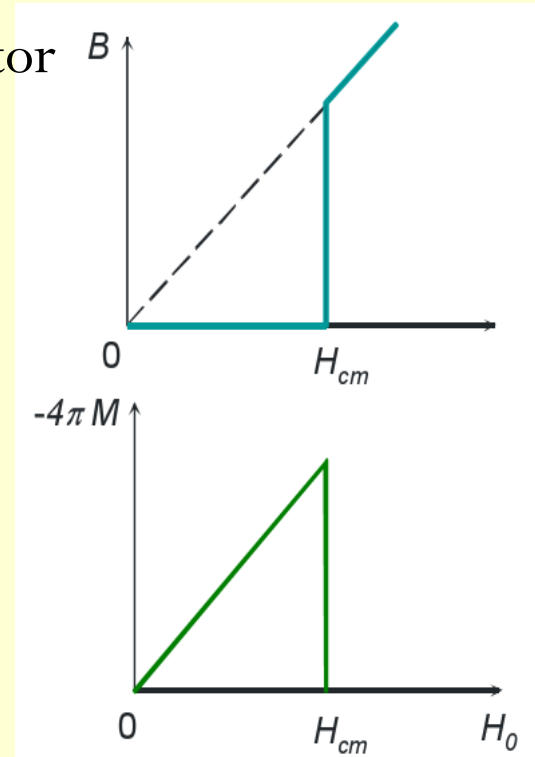
H_{cm} … critical field

JUAS 2020: SC RF - Caspers/Wendt/Bozzolan

- Type II superconductor

Magnetic properties of a **type II superconductor**

Above the 1st critical field H_{c1} magnetic flux penetrates into the bulk

Above the 2nd critical field H_{c2} the material is normal conducting (except for a thin surface layer that remains superconducting until the 3rd critical field H_{c3})
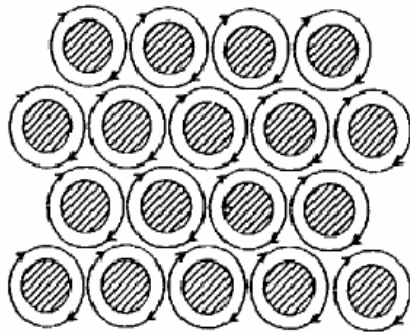
$$\vec{B} = \mu_0 \cdot \left(\vec{H}_0 + \vec{M} \right)$$
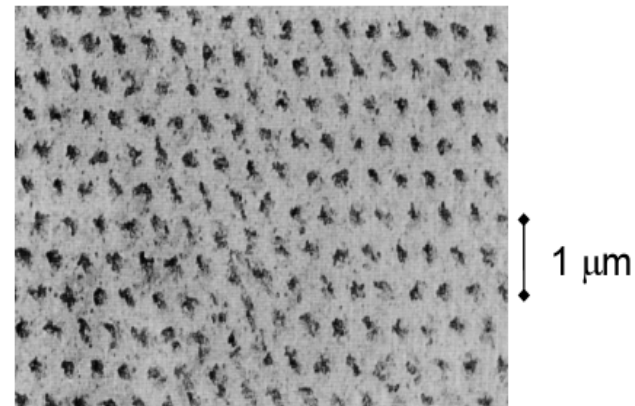
Magnetization curve

$-4\pi M$

Meissner state

mixed state (Abrikosov vortices)

H_0

0   H_{c1} H_{c2}

$\vec{B}$

$\vec{H}_0$
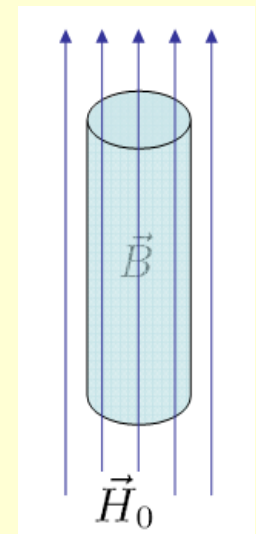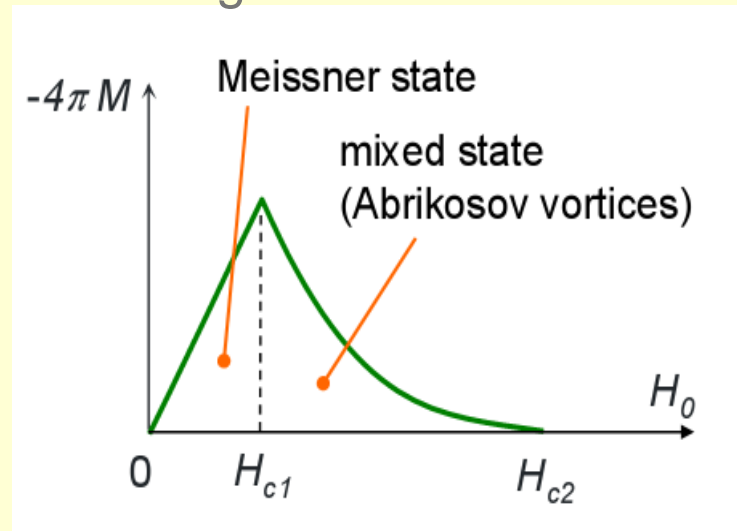
Two kinds of superconductors 3/3

Mixed state of a type II superconductor

Mixed state (Shubnikov phase) of a type II superconductor consists of a regular lattice of Abrikosov vortices.

Magnetic decoration image of a vortex lattice

1 μm

JUAS 2020: SC RF - Caspers/Wendt/Bozzolan

Materials 1/2

pure metals

material	T_c,K	H_c,Oe	year
Al	1.2	105	1933
In	3.4	280	
Sn	3.7	305	
Pb	7.2	803	1913
Nb	9.2	2060	1930

alloys

material	T_c,K	H_c,Oe	year
NbN	15	1.4×10^5	1940
Nb_3Ge	23	3.7×10^5	1971

ceramics

material	T_c,K	year
$La_{1.85}Ba_{0.15}CuO_4$	35	1986
$YBa_2Cu_3O_7$	93	1987
$Bi_2Sr_2CaCu_2O_{8+x}$	94	1988
$Ta_2Ba_2Ca_2Cu_3O_{10+x}$	125	1988

Cold liquids required for reaching low temperatures:

helium ^{4}He (4.2 K)
hydrogen H_2 (20 K)
neon   Ne (27 K)
nitrogen N_2 (77 K)

JUAS 2020: SC RF - Caspers/Wendt/Bozzolan
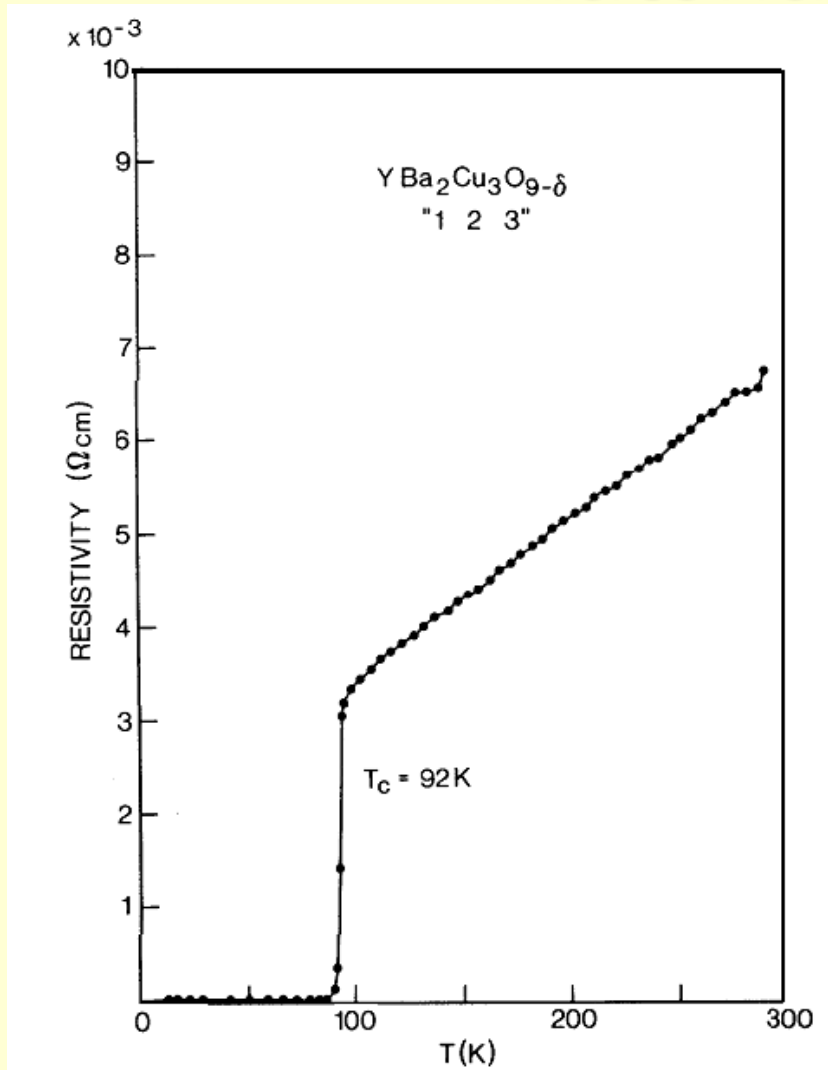
Resistivity of a single-phase $YBa_2Cu_3O_7$ sample as a function of temperature.

Two fluid model

Basic ingredients for RF superconductivity

Two fluid model (Gorter-Casimir)
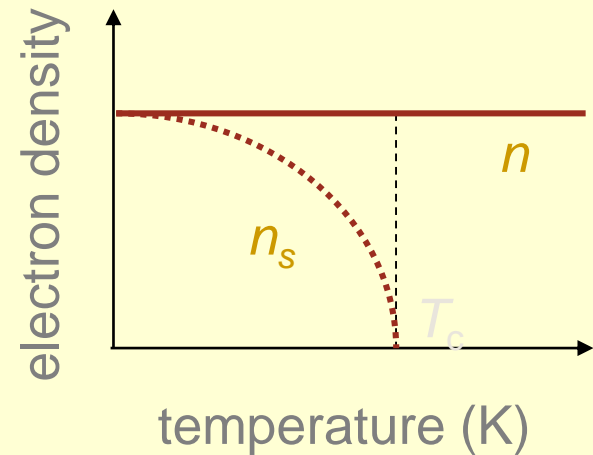Maxwell electrodynamics

Basic assumptions of two fluid model

- all free electrons of the superconductor are divided into two groups
  - □ superconducting electrons of density n_s
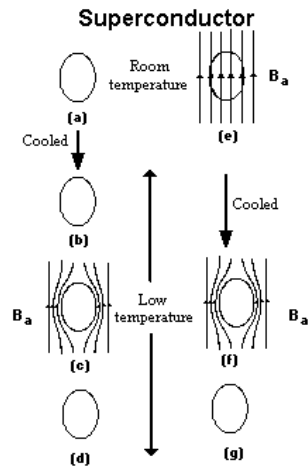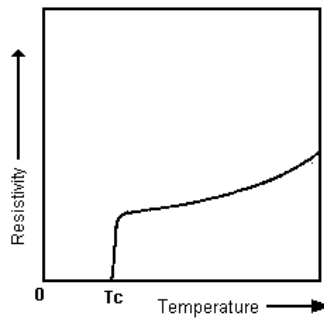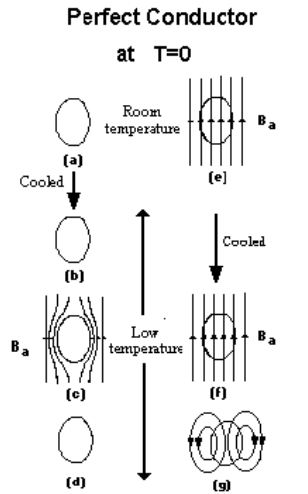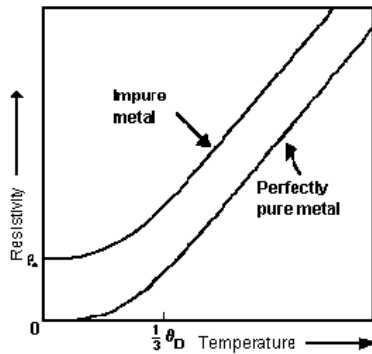 - □ normal electrons of density n_n

The total density of the free electrons is

$n = n_s + n_n$.

As the temperature increases from 0 to T_c, the density n_s decreases from n to 0.

$$n_s/n = 1 - \left(T/T_c\right)^4$$

London Equations

Postulated on plausibility arguments

$$\frac{\partial \mathbf{j}_s}{\partial t} = \frac{n_s e^2}{m} \mathbf{E} \qquad \nabla \times \mathbf{j}_s = -\frac{n_s e^2}{m} \mathbf{B}$$

Applying $\mathbf{B} = \nabla \times \mathbf{A}$
on the vector potential $\mathbf{A}$

$$\mathbf{j}_s = -\frac{n_s e^2}{m} \mathbf{A} = -\Lambda^{-1} \mathbf{A}$$

Applying Ampere's law
to London's 2nd eq gives:

$$\nabla^2 \mathbf{B} = \frac{1}{\lambda_L^2} \mathbf{B} \qquad \lambda_L = \sqrt{\frac{m}{\mu_0 n_s e^2}}$$
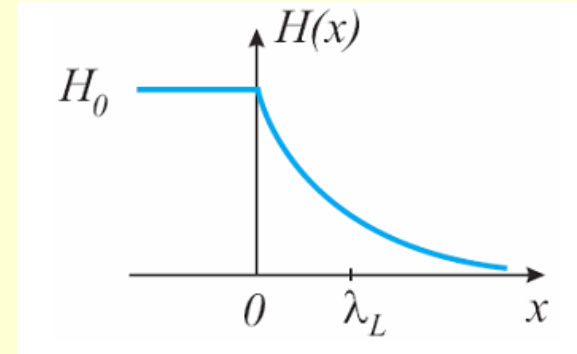
Exponential decay of the B-field
inside the superconductor

JUAS 2020: SC RF - Caspers/Wendt/Bozzolan

London penetration depth

On introducing the vector potential A via $\mathbf{B} = \nabla \times \mathbf{A}$

one obtains a relationship between the supercurrent and the vector potential, very similar to Ohm's law $\mathbf{j} = \sigma \mathbf{E}$

$$\Rightarrow \mathbf{j}_s = -\frac{1}{\Lambda}\mathbf{A} = -\frac{n_s e^2}{m}\mathbf{A}$$

with the London penetration depth $\lambda_L^2 = \Lambda/\mu_0 = m\big/\left(n_s e^2 \mu_0\right)$

Element	Al	Nb (crystal)	Nb (film)	Pb	Sn	YBCO
λ_L [nm]	50	47	90	39	51	170

Compare to
NC Cu skin depth:
2 μm @ 1 GHz

- You will probably be only half surprised to hear that a superconductor at T>0 has a $R_s \neq 0$.

- This can be understood in the framework of the previous two fluids model, where a population of normal electrons of density n_n and a population of "superconducting electrons" of density $n_s = n_0(1 - T^4/T_c^4)$ coexist such as $n_n + n_s = 1$ and both give a response to the varying EM fields.

- Let's "invent" the conductivity of superconducting electrons:

$$\sigma(\omega) = \frac{ne^2\tau}{m_e(1 + \mathrm{j}\omega\tau)} \qquad \lim_{\tau\to\infty} \sigma(\omega) = -\mathrm{j}\frac{ne^2}{m_e\omega}$$

Complex Conductivity

- Do you think the previous formula looks like a joke: conductivity of a perfect conductor is an imaginary number?

- There is indeed real physics behind it. Recall London equations, from which we can set-up the following equivalence, in the "dirty" limit:

Normal metal	Superconductor (London theory)
$\mathbf{j} = \sigma_0 \mathbf{E} = \dfrac{n_n e^2 \ell}{m v_F} \mathbf{E}$	$\mathbf{j}_s = -\Lambda^{-1} \mathbf{A} = -\dfrac{n_s e^2}{m} \mathbf{A}$

- The value of Λ is the expression of the kinetic inductivity of the "superconducting electrons": basically, the electron pairs have a mass, and they get accelerated by the RF wave. This is the same as what happens with the magnetic field produced inside an inductor.

London&London Proc. Roy. Soc A149 (1935) 71

Pippard Proc. Roy. Soc. A216 (1953) 547

- The conductivity of superconductors then becomes:

$$\sigma_s = \frac{n_0 e^2 \tau}{m}\left(T^4 \Big/ T^4_c\right) - \text{j}\frac{n_0 e^2}{m\omega}\left(1 - T^4 \Big/ T^4_c\right) = \sigma_1 - \text{j}\sigma_2$$

conductivity of "normal electrons"	conductivity of "superconducting electrons"

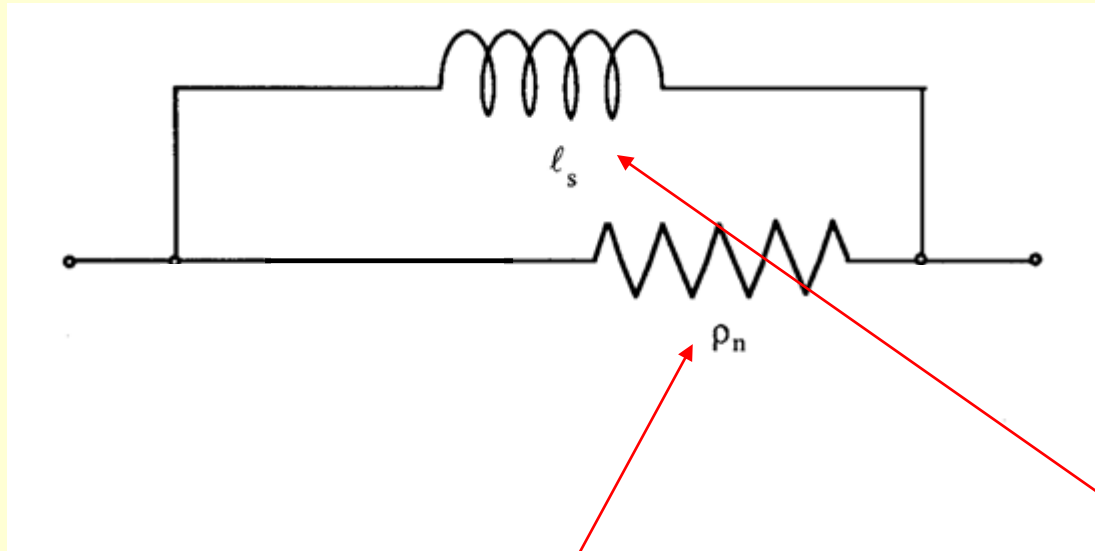- Where $n_s = n_0(1 - T^4/T_c^4)$ and $n_n = n_0(T^4/T_c^4)$ with n_0 total electron density
- Note:

$$\sigma_2 = \frac{\sigma_0}{\omega\tau} = \frac{1}{\mu_0 \omega \lambda_L^2} = \frac{1}{\Lambda\omega} \qquad \text{with} \quad \lambda_L^2 = \frac{\Lambda}{\mu_0}$$

Equivalent Circuit

Indeed if you take the time derivative of $\mathbf{j}_s = -\Lambda^{-1}\mathbf{A}$ you get the 1st London eq:

$$-\frac{\partial \mathbf{A}}{\partial t} = \mathbf{E} = \Lambda \frac{\partial \mathbf{j}_s}{\partial t}$$

Λ is interpreted as a specific inductance. This justifies representing the complex conductivity of a superconductor with an equivalent circuit of parallel conductors:

$$\sigma_s = \sigma_1 - j\sigma_2 = \sigma_n(T^4 \big/ T_c^4) - j\frac{\sigma_n}{\omega\tau}(1 - T^4 \big/ T_c^4)$$

JUAS 2020: SC RF - Caspers/Wendt/Bozzolan

Surface Impedance 1/2

- It is now possible, within the basic approximations we have made, to calculate the surface impedance of a superconductor.

- Take the formula for normal metals:

$$Z = (1+i)\sqrt{\frac{\mu_0 \omega}{2\sigma_n}}$$

- Perform the substitution: $\sigma_n \rightarrow \sigma_s = \sigma_1 - i\sigma_2$

- Calculate:

$$R_s = \sqrt{\frac{\mu_0 \omega}{\sigma_n}} \frac{\left[\left(\sigma_1^2 + \sigma_2^2\right)^{1/2} - \sigma_2\right]^{1/2}}{\left(\sigma_1^2 + \sigma_2^2\right)^{1/2}} \qquad X_s = \ldots\ldots$$

- In the approximation of small ℓ (small $\omega\tau \rightarrow \sigma_1 < \sigma_2$)

- and $0 < T < 0.5 T_c$ ($n_n < n_s \rightarrow \sigma_1 < \sigma_2$) it gives:

$$R_s = \frac{R_N}{\sqrt{2}} \frac{\sigma_1/\sigma_n}{\left(\sigma_2/\sigma_n\right)^{3/2}} = \frac{1}{2}\mu_0^2 \omega^2 \sigma_1 \lambda_L^3 \qquad X_s = X_N \frac{\sqrt{2}}{\left(\sigma_2/\sigma_n\right)^{1/2}} = \sqrt{\frac{\mu_0 \omega}{\sigma_2}} = \mu_0 \omega \lambda_L$$

- Which is a good description of the experimental data, but…

- How to generalize to larger ℓ ? Take:
  (Pippard Proc. Roy. Soc. A216 (1953) 547)

$$\mathbf{j}_s = -\Lambda^{-1}\mathbf{A} = -\frac{ne^2}{m}\mathbf{A}$$

- Introduce a parameter ξ
  in some way proportional to ℓ:

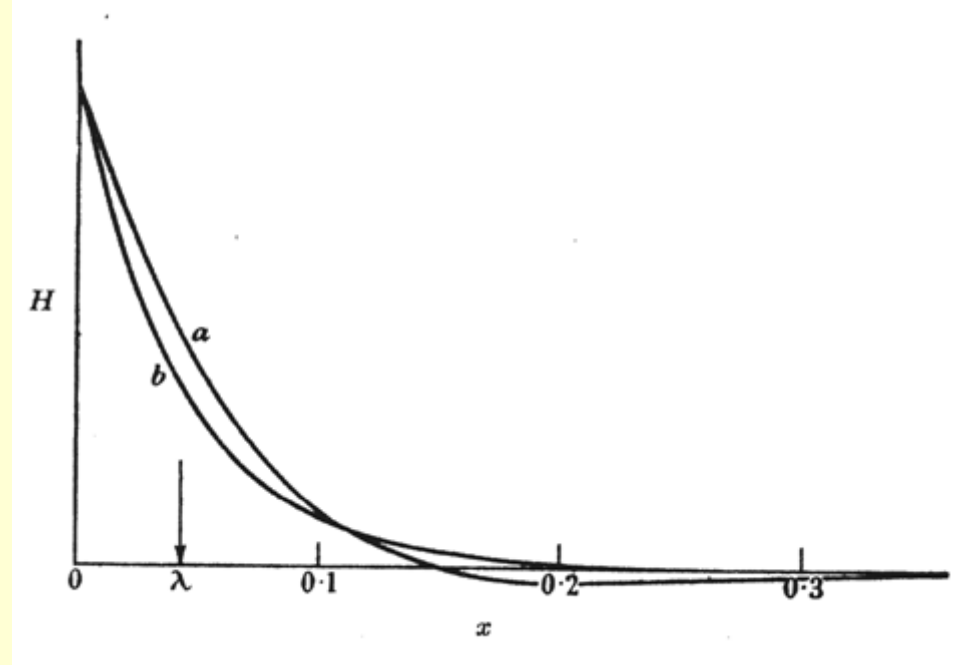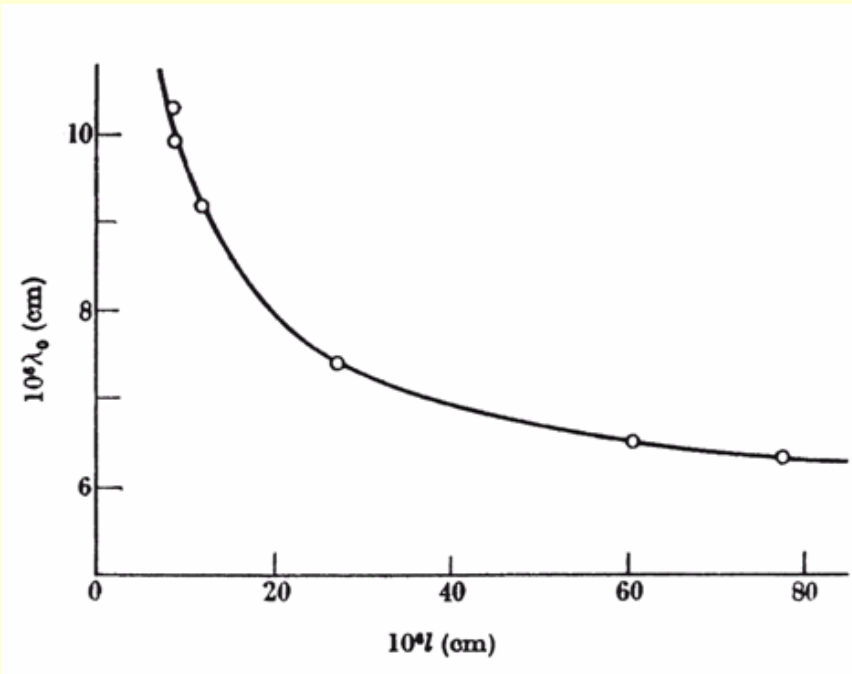$$\mathbf{j}_s = -\frac{\xi}{\xi_0}\Lambda^{-1}\mathbf{A}$$

- Then substitute corresponding quantities into Chambers' formula:

$$\mathbf{J}(\mathbf{r},t) = -\frac{3}{4\pi\xi_0\Lambda}\int_V \frac{\mathbf{R}\left[\mathbf{R}\cdot\mathbf{A}(\mathbf{r}',t-R/v_F)\right]e^{-R/\xi}}{R^4}\,\mathrm{d}\mathbf{v}'$$

- Pippard used this formula to fit his
  experimental data, and found:

$$\frac{1}{\xi} = \frac{1}{\xi_0} + \frac{1}{\ell} \qquad \xi_0 = 0.15\frac{\hbar v_F}{kT_c}$$

- This was the first definition ever of the coherence length ξ_0

Pippard's Data

We are now ready to go into the real ("heavy") stuff: the BCS formulation.

- In BCS theory the values for σ_1/σ_n and σ_2/σ_n can be calculated.
- These are then used to calculate the surface impedance

BCS Theory 1/2

Mattis & Bardeen, Phys. Rev. 111 (1958) 412

1st step:

$$\mathbf{j}(\mathbf{r},t) = \sum_\omega \frac{e^2 N(0)v_0}{2\pi^2 \hbar c}$$

$$\times \int \frac{\mathbf{R}[\mathbf{R}\cdot\mathbf{A}_\omega(r')]I(\omega,R,T)e^{-R/l}dr'}{R^4}, \quad (3.3)$$

is

$$I(\omega,R,T) = \int_{-\infty}^{\infty}\int_{-\infty}^{\infty}\left\{ L(\omega,\epsilon,\epsilon') - \frac{f(\epsilon)-f(\epsilon')}{\epsilon'-\epsilon} \right\}$$

$$\times \cos[\alpha(\epsilon-\epsilon')]d\epsilon d\epsilon', \quad (3.4)$$

2nd step:

$$\frac{\sigma_1 - i\sigma_2}{\sigma_N} = \frac{I(\omega,0,T)}{-\pi i\hbar\omega}.$$

3rd step:

$$\frac{\sigma_1}{\sigma_N} = \frac{2}{\hbar\omega}\int_{\epsilon_0}^{\infty}[f(E)-f(E+\hbar\omega)]g(E)dE$$

$$+\frac{1}{\hbar\omega}\int_{\epsilon_0-\hbar\omega}^{-\epsilon_0}[1-2f(E+\hbar\omega)]g(E)dE, \quad (3.9)$$

$$\frac{\sigma_2}{\sigma_N} = \frac{1}{\hbar\omega}\int_{\epsilon_0-\hbar\omega,-\epsilon_0}^{\epsilon_0}\frac{[1-2f(E+\hbar\omega)](E^2+\epsilon_0^2+\hbar\omega E)}{(\epsilon_0^2-E^2)^{\frac{1}{2}}[(E+\hbar\omega)^2-\epsilon_0^2]^{\frac{1}{2}}}.$$

$$(3.10)$$

JUAS 2020: SC RF - Caspers/Wendt/Bozzolan

BCS Theory 2/2

- (3.9) and (3.10) can be approximated for low frequencies $h\nu \ll 2\Delta$ as:

$$\frac{\sigma_1}{\sigma_n} = 2f(\Delta)\left\{1 + \frac{1}{kT}\ln\left(\frac{2\Delta}{\hbar\omega}\right)[1-f(\Delta)]\right\} \qquad \frac{\sigma_2}{\sigma_n} = \frac{\pi\Delta}{\hbar\omega}\tanh\left(\frac{\Delta}{2kT}\right)$$

- The surface impedance Z can be calculated from σ_1/σ_n and σ_2/σ_n

- However the formulas seen until now are approximate valid only in a very specific limit.

- Calculations can be done having a full validity range (but only for $H_{RF} \ll H_c$)

  - Abrikosov Gorkov Khalatnikov, JETP 35 (1959) 182
  - Miller, Phys. Rev. 113 (1959) 1209
  - Nam, Phys. Rev. A 156 (1967) 470
  - Halbritter, Z. Phys. 238 (1970) 466 and KFK Ext. Bericht 3/70-6

Halbritter's theoretical Predictions
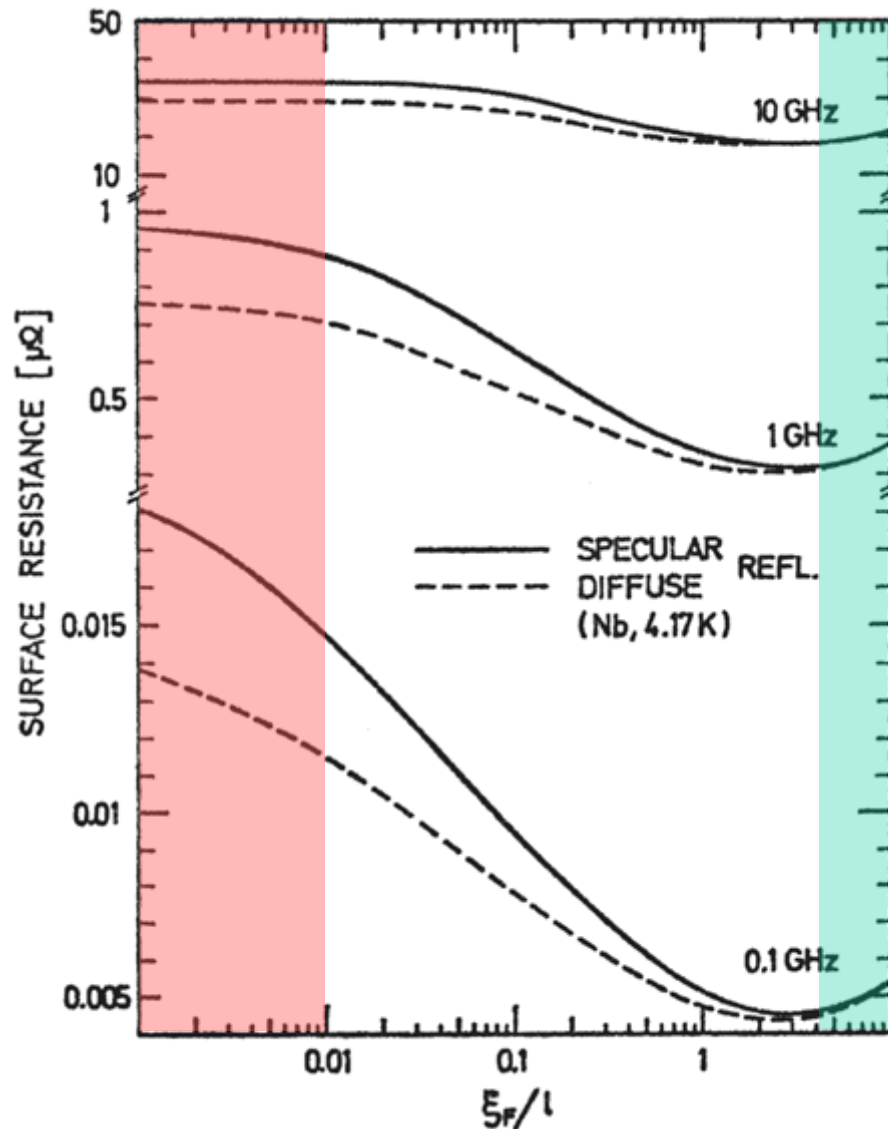
In the green region (small ℓ):

$$\frac{Z_s}{Z_n} = \left(\frac{\sigma_1}{\sigma_n} - i\frac{\sigma_2}{\sigma_n} \right)^{1/2}$$

$$R_s \propto \frac{\omega^2}{T\sqrt{\sigma}} \exp\left(-\Delta\!\big/_{kT}\right)$$

In the red region (large ℓ):

$$\frac{Z_s}{Z_n} = \left(\frac{\sigma_1}{\sigma_n} - i\frac{\sigma_2}{\sigma_n} \right)^{1/3}$$

$$R_s \propto \frac{\omega^{3/2}}{T} \exp\left(-\Delta\!\big/_{kT}\right)$$

JUAS 2020: SC RF - Caspers/Wendt/Bozzolan

BCS Surface Resistance

- Material parameter dependence of $R_s\ (T, f)$

Fig. 2: Surface resistance $R_s(T)$ of two 3 GHz cavities, fabricated from niobium of different purity. $R_s(T)$ is the sum of the temperature dependent part R_{BCS} and the residual resistance R_{res}.

RRR: residual resistance ratio

$$RRR = \frac{\rho_{300K}}{\rho_{oK}}$$
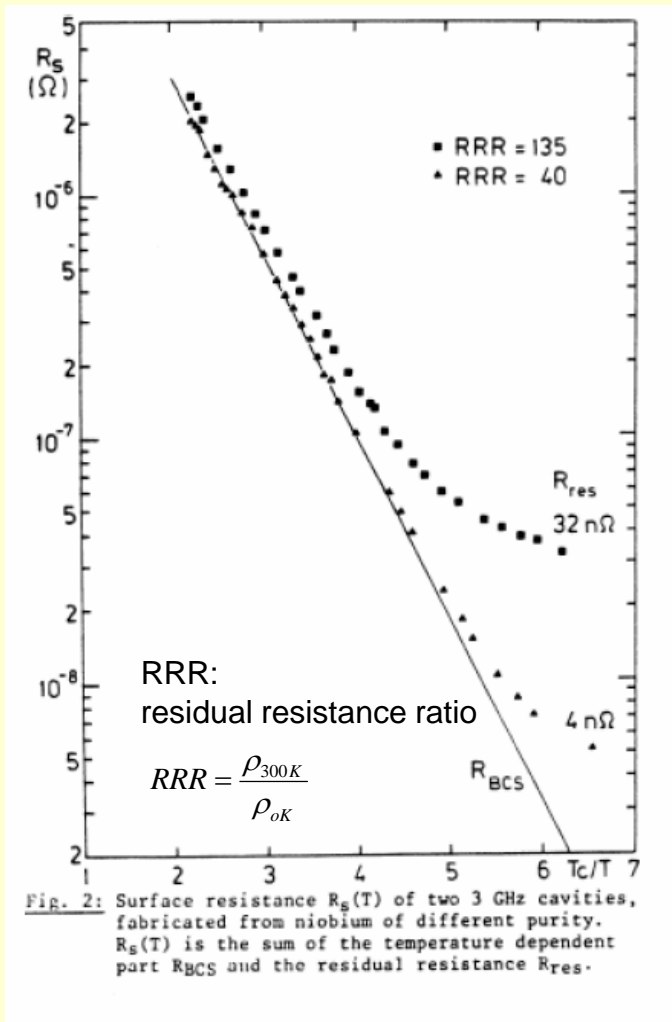
$$R_s^{BCS}(\omega, T) = \frac{A}{T}\omega^2 \exp\left(-\frac{\Delta}{kT}\right)$$

$$2\Delta \approx 3.5 \cdot kT_c$$

A depends on the material

$$R_s = R_s^{BCS} + R_{res}$$

An approximate expression for Niobium:

$$R_S^{BCS} = 3 \cdot 10^{-4}\Omega \cdot \left(\frac{f[MHz]}{1500\ MHz}\right)^2 \cdot 1/T \cdot \exp\left(-\frac{17.67\ K}{T[K]}\right)$$

Developed by *Mattis* and *Bardeen*, based on the SC theory of *Bardeen*, *Cooper* and *Schrieffer* (BCS theory).

- Normally some kind of resonator is applied for the samples

- You MUST avoid any sliding contacts since they have usually an undefined contact resistance and spoil the Q of the cavity and you should avoid any radiation losses

- Often a TE_{011} mode type resonator is used..works very well not sensitive to contact resistance due to azimuthal wall current only

- But of you would like to go to lower frequencies then the quadrupolar resonator is a good choice

- For even lower frequencies the shielded two wire coaxial resonator has been used (for the LHC beam screen)

• Small samples can be exposed to RF using a pill box cavity with demountable endplate

• Two possible techniques
  • Replacement
  • **Calorimetric**

TE$_{011}$ mode

B$_{\parallel}$

max

0

Demountable endplate

Flange

Host cavity

Figure by T. Junginger

Replacement = Q-measurement with copper cover/DUT

JUAS 2020: SC RF - Caspers/Wendt/Bozzolan
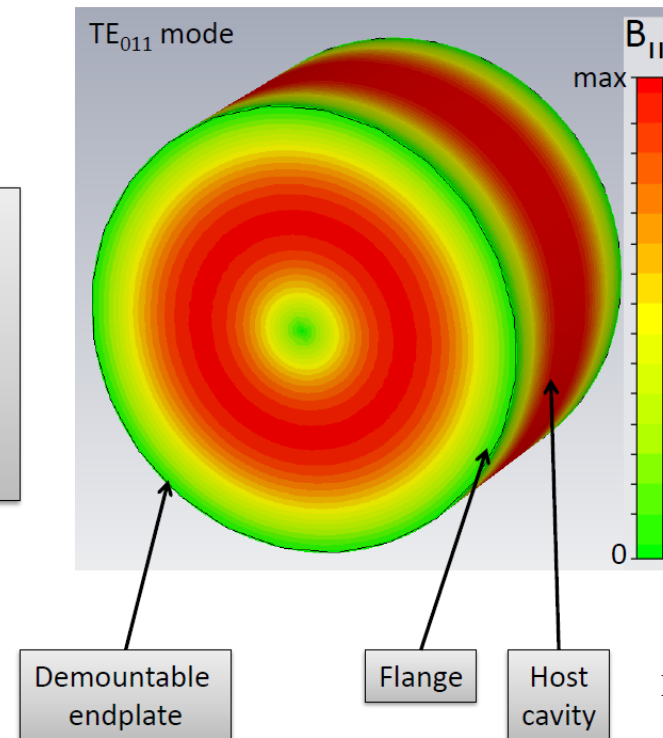
Figure by T. Junginger
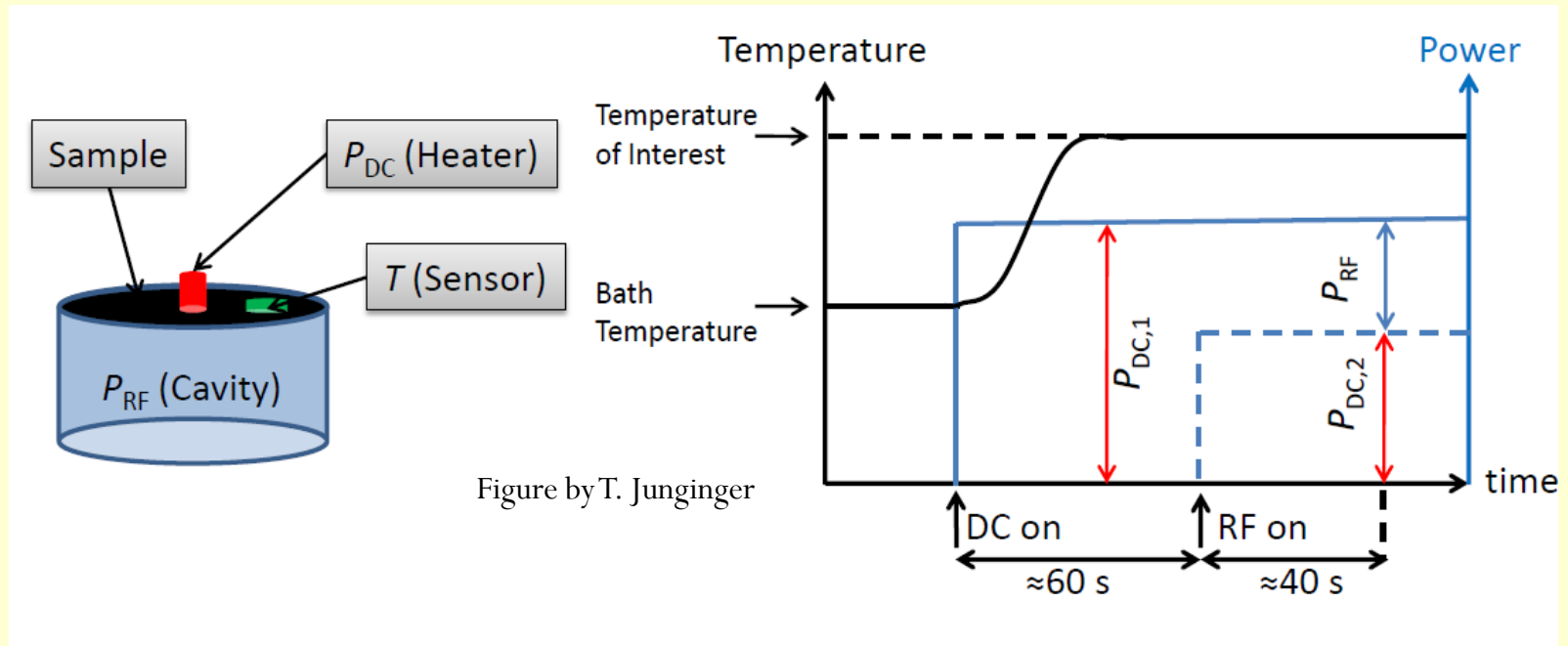
$$P_{RF} = P_{DC,1} - P_{DC,2} \approx 1/2\, R_{Surface} \int_{Sample} H^2 dS$$

$$R_{Surface} = \frac{2(P_{DC,1} - P_{DC,2})}{\int_{Sample} H^2 dS}$$

→ **Direct Measurement**

- Measurement of transmitted power P_t
- $P_t = c \int H^2 ds$, c from computer code
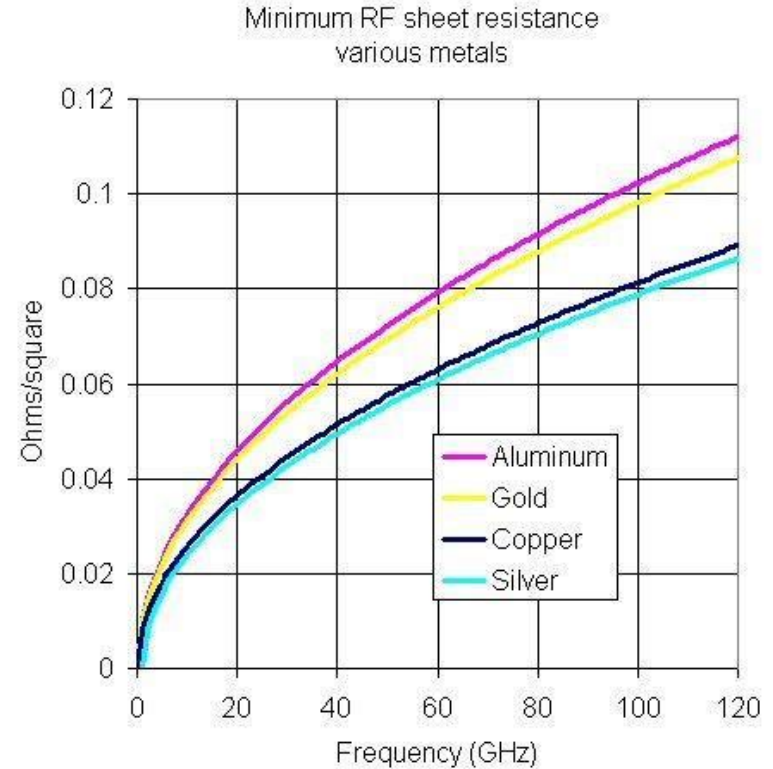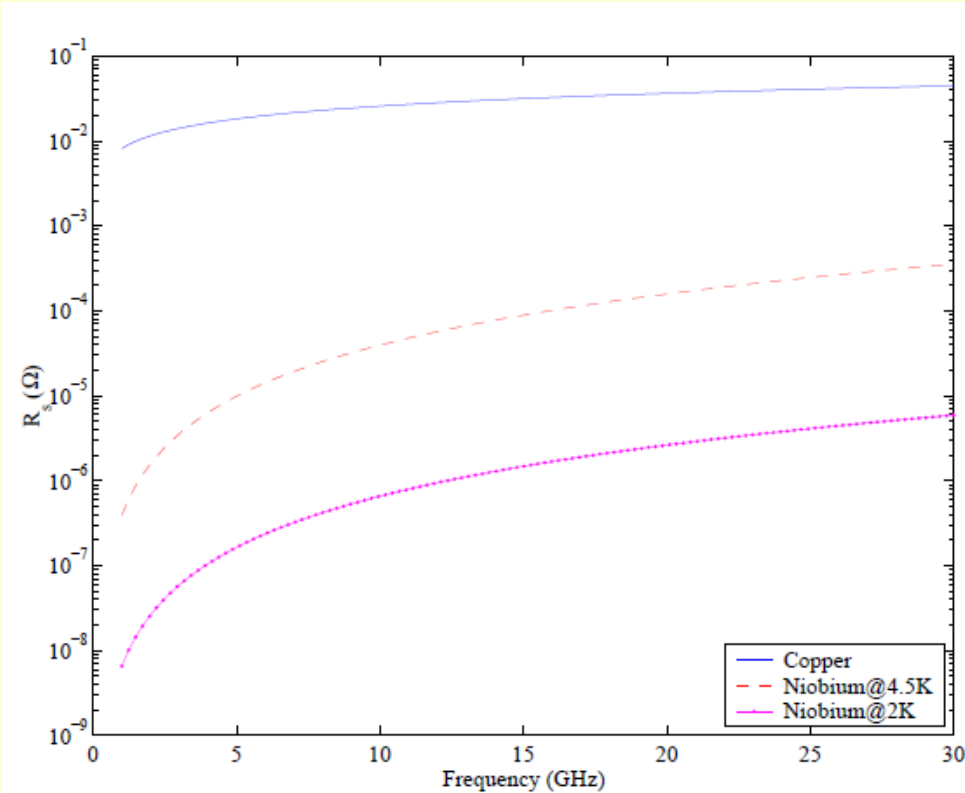
Surface resistance vs frequency for copper and Niobium at @2K and 4.5 K respectively (left graph by B. Tenenbaum)

How to measure RF Surface Impedance

Rods

361 mm

Sample, E-beam welded to cylinder

Tobias.Junginger@cern.ch

max B$_{||}$

0

[5] E. Mahner et al. -Rev. Sci. Instrum., Vol. 74, No. 7, July 2003)
[6] T. Junginger et. al – SRF 2009, Berlin Germany
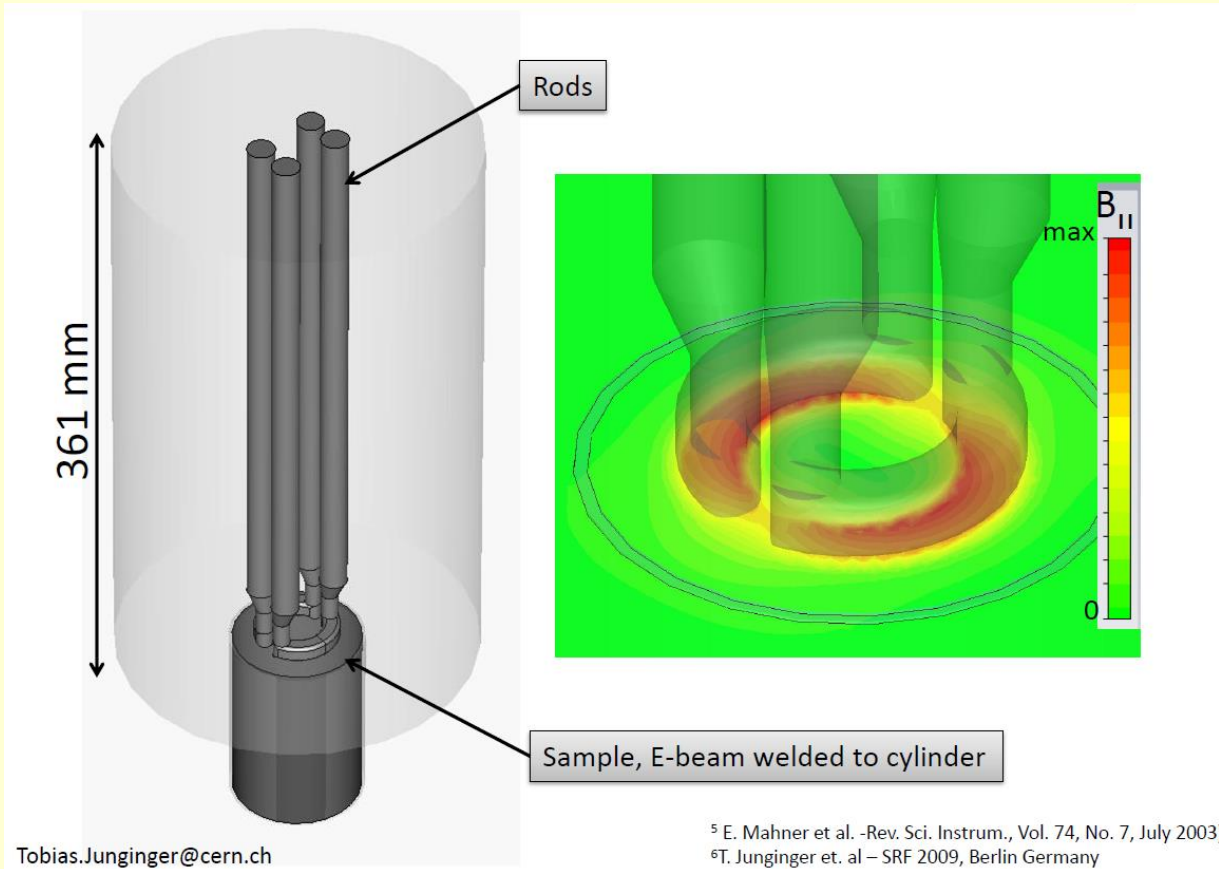
Why should we use this kind of resonator when we have the nice TE011 type pillbox?

Answer: It allows for lower frequencies or a smaller sample size compared to the pillbox resonator

The measurement principle is based on the so-called shielded pair technique [7], which consists of a one metre long cylindrical TEM cavity with two cylindrical inner conductors (see Figure 1). A detailed description of the experimental set-up is given in ref. [6]. Basically, processing of the loaded quality factors measured in the even and odd mode excitations, in steps of ~150MHz, yields the surface resistance of the outer tube and of the inner conductors, assuming that the latter have an identical copper coating.
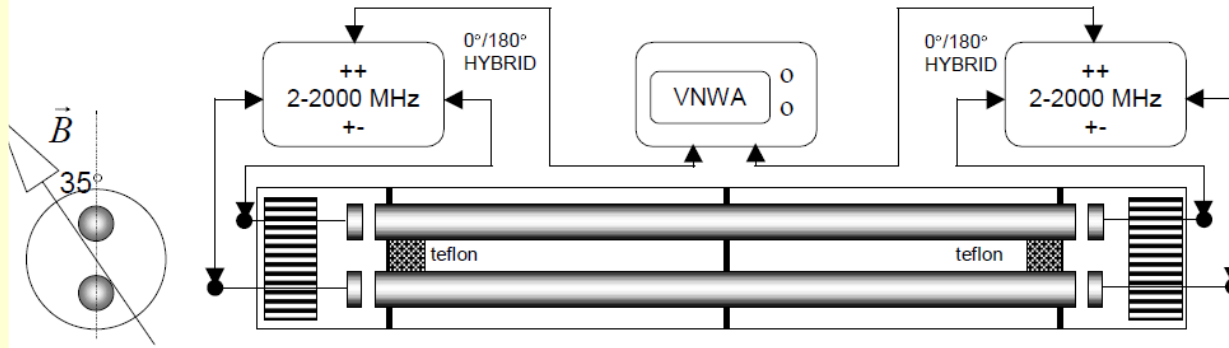
Figure 1: Cross section and side view of the experimental setup: a vector network analyser (VNWA) is used in conjunction with two hybrids, yielding either even (++) or odd (+-) mode excitation for a 1 m long cylindrical cavity with 2 inner conductors, held by 3 Teflon supports. The near degeneracy of even and odd modes is removed by 2 teflon blocks (splitters) placed between the inner conductors.

This setup has been intensively used for measurements of the normal conducting copper losses of the LHC beam screen at cryo temperature at with a strong static magnetic field; it now again under discussion for the FCC beam screen evaluation which may have high Tc superconducting coating (compatible with the strong DC magnetic field)

From: F. Caspers et al; Surface resistance measurements… LHC project report 307

How to measure RF Surface Impedance

- The examples shown so far are by no means exhaustive

- For the design of new measurement setups e.g. related to the evaluation of surface roughness impact, one may have to take anisotropy issues into account , depending on the structure of the surface roughness (e.g. laser erosion for multipactor reduction)

- For very high frequencies confocal resonator (Fabry Perot type) setups were used.

- For tube-like (beam-pipe style) samples the first resonance frequency of often too high to cover the frequency range of interest. In this case one may insert a sapphire rod which at cryo has extremely low RF losses and an epsilon around 10 (caveat: anisotropic)

JUAS 2020: SC RF - Caspers/Wendt/Bozzolan

Critical field (s)

Critical field of superconductors studied for RF

Material	T_c [K]	B_{cth0} [mT]	B_{c10} [mT]	B_{c20} [mT]	B_{sh0} [mT]	B_{exp0} [mT]
Sn	3.7	30.9	–	–	68	30.6
In	3.4	29.3	–	–	104	28.4
Pb	7.2	80.4	–	–	105	112
Nb	9.2	200	185	420	240	160
Nb_3Sn	18.2	535	$\approx$ 20	2400	400	106

Critical fields in DC and RF superconductivity

B_c	Critical magnetic field of type-I superconductor
B_{c1}	Lower critical magnetic field of type-II superconductor
B_{c2}	Upper critical magnetic field of type-II superconductor
B_{cth}	Thermodynamic critical field
B_{sh}	Superheating critical field
B_{exp}	Experimentally obtained maximum field in RF
An index "0" following any of the above symbols refers to the temperature T = 0 K, tacitly assuming $B(T) = B_0 [1 - (T/T_c)^2]$.	

JUAS 2020: SC RF - Caspers/Wendt/Bozzolan

Other deterministic parameters for cavity performance

Until till now we discussed the role of the RF frequency, lHe bath temperature, and sc material with its characteristic critical field and temperature. There are still other (less important) parameters that determine the performance of the cavity as well:

Influencing quantity	Impact quantity	Physical explanation	Cure
External static magnetic field B_{ext}	Residual surface resistance	Creation of vortices	Shielding of ambient magnetic field by Mu-metal / Cryoperm
Residual resistivity ratio RRR	BCS surface resistance	Mean free path dependence of R_{res}	Annealing steps during ingot production/after cavity manufacture
Ratio peak magnetic field to accelerating gradient B_p / E_a	Max. accelerating gradient	Critical magnetic field as ultimate gradient limitation	Optimization of cavity shape
Nb-H precipitate	Q-value / acc. gradient (Q-disease)	Lowering of T_c / B_c at precipitates of Nb-H	T-control during chemical polishing Degassing @ 700 °C Fast cool-down

JUAS 2020: SC RF - Caspers/Wendt/Bozzolan

Summary

Superconducting materials:
- are characterized by zero resistivity (in DC) and the Meissner effect;
- Show the (thermodynamic) phase transition into the superconducting state below a critical temperature and below a critical field;
- have a non-zero surface resistance for RF which can be understood by the two-fluid model and the London theory
- are subdivided into type I and type II, depending on the value of the Ginzburg-Landau parameter κ;
- may be alloys or elements, for which they are of type I, except Nb, the technically most important one, which is type II and has the largest critical temperature and critical field;

Learning targets

After this chapter you should
- be familiar with the motivation for using RF superconducting cavities in accelerators
- be able to dicuss why SC Rf cavity technology is barely used outside the accelerator field
- see the benefits but also the problems related to RF SC technology
- have understood the main difference between DC and RF superconductivity
- be able to calculate the RF surface impedance of a given material vs frequency
- have understood the concept of the resistance and impedance per unit square
- be able to name some of the materials used for RF SC applications
- have understood the principal difference wrt conventional Rf superconductors and high temp RF superconductors
- be familiar with the basics, history and important milestones of superconducting technology in general
- be able to describe the meaning and relevance of vortices in the context of SC technology
- know the difference between type I and type II superconductors

Basics of RF cavities (slightly different wrt the RF lecture)

- Variety of RF cavities (examples)
- Cavity characteristics
  - Cavity characteristics (peak fields, stored energy, …)
  - Pillbox resonator –basics, field distribution
  - Computer codes to determine the cavity parameters
  - Different mode families
- Transmission line
- Response of a sc cavity to RF (determination of Q_0, E_{acc}, …)
- Measuring setup ($Q(E_{acc})$ curve, …)
- Pass-band modes
- Typical example of storage ring cavity (LEP)
- Summary

JUAS 2020: SC RF - Caspers/Wendt/Bozzolan

Examples of RF cavities

Fig. 1 A spectrum of superconducting cavities.

(from H. Padamsee, CERN-2004-008)

LHC - CERN

- f_{res} = 400 MHz
  - R/Q = 89 Ω
  - Q_0 = 2 x 10^9
  - E_{acc} = 5.33 MV/m
  - P_{in} = 116 kW (CW)
- Niobium-film on Cu
  - 1-2 μm thickness
- 4 single-cell cavities per cryomodule
  - Each resonator delivers 2 MV
  - Blade tuner
  - «Doorknob» power coupler, 75 Ω coaxial
- Total of 8 cavities per beam: 16 MV
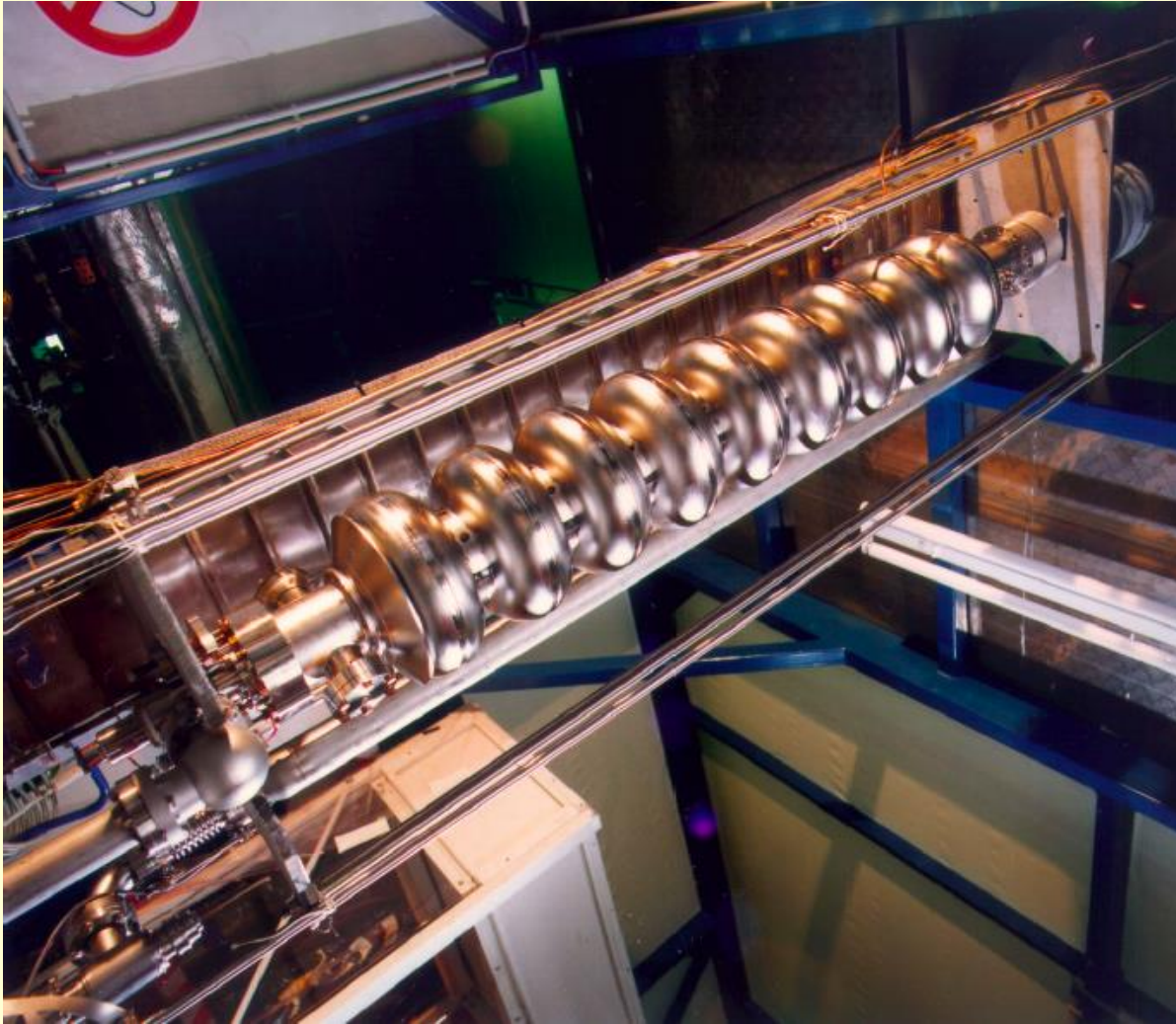
- f_{res} = 1300 MHz
  - R/Q = 89 Ω
  - Q_0 = 2 x 10^9
  - E_{acc} = 5.33 MV/m
  - P_{in} = 116 kW (CW)
- Niobium-film on Cu
  - 1-2 μm thickness
- 4 single-cell cavities per cryomodule
  - Each resonator delivers 2 MV
  - Blade tuner
  - «Doorknob» power coupler, 75 Ω coaxial
- Total of 8 cavities per beam: 16 MV

XFEL cryomodule assembly of eight 9-cell cavities, quadrupole and BPM in a cleanroom

JUAS 2020: SC RF - Caspers/Wendt/Bozzolan

Cryomodule installation in the tunnel (the XFEL consists out of 101 cryomodules)

JUAS 2020: SC RF - Caspers/Wendt/Bozzolan

CEBAF - JLAB

JUAS 2020: SC RF - Caspers/Wendt/Bozzolan

SPL - CERN/ SNS - ORNL

Prototype Beta 0.61 and .81 Cavities
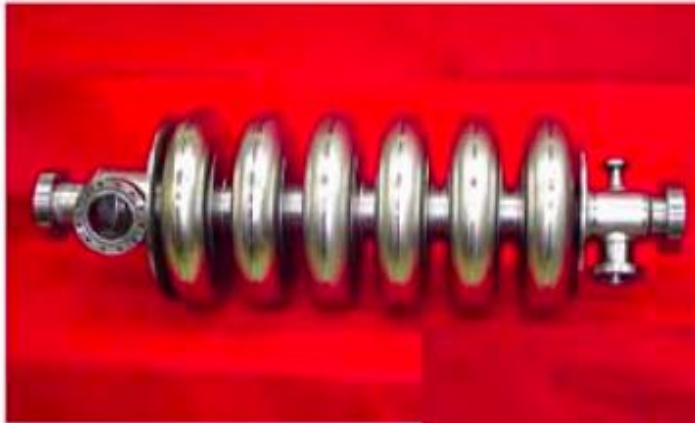
Development led by P. Kneisel with aid from colleagues all over the world

704 MHz SRF cavity R&D study to upgrade the CERN injectors with a high intensity superconducting RF proton linac (SPL)

Heavy Ion accelerators ATLAS - ANL

JUAS 2020: SC RF - Caspers/Wendt/Bozzolan

Shapes of heavy ion accelerator cavities

JUAS 2020: SC RF - Caspers/Wendt/Bozzolan
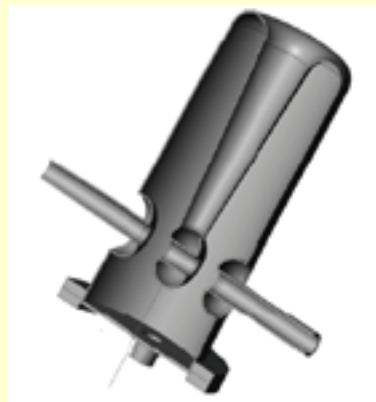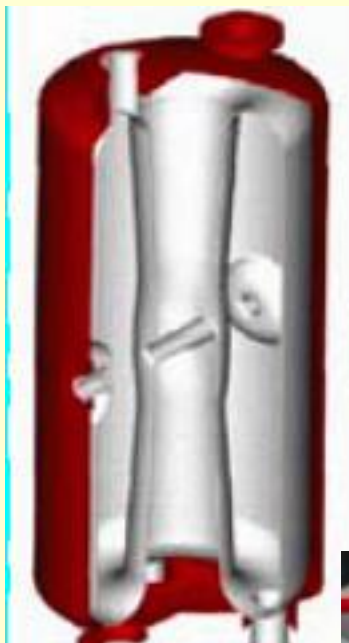
Pill box resonator
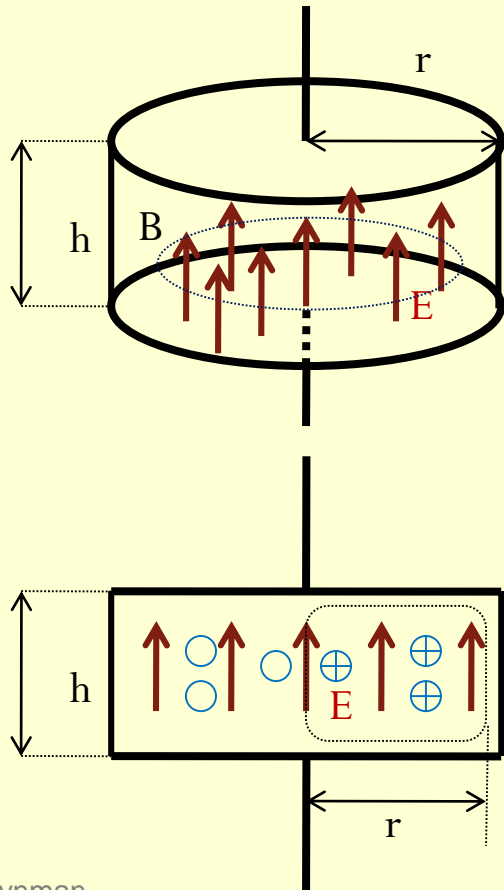
Field distribution TM$_{010}$ mode:

J_0 …. Bessel function of 0th order
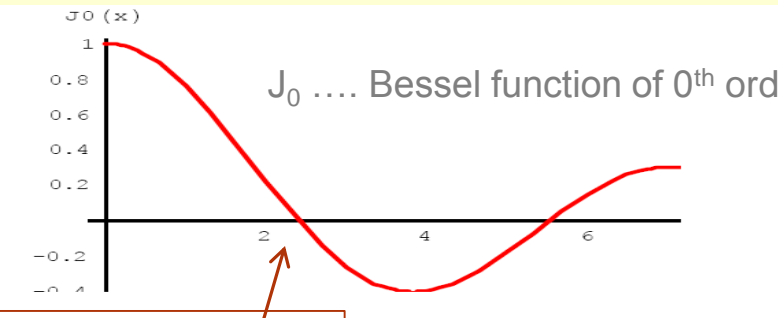
$$\frac{\omega_0 \cdot R}{c} = 2.405$$

Resonance-condition

J_1 ... Bessel function of 1st order
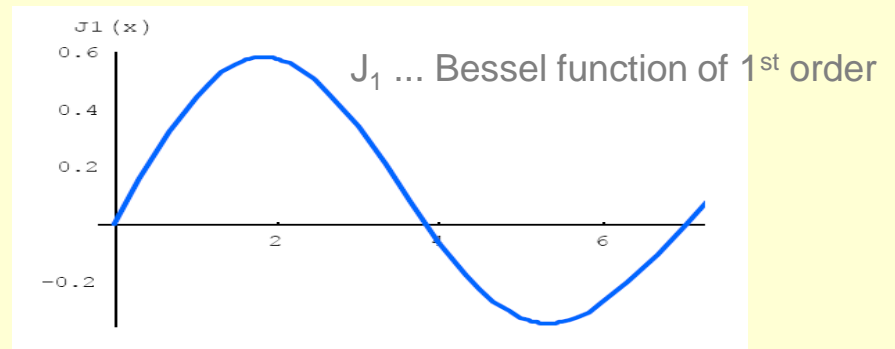
Source: The Feynman
Lectures on Physics, Vol. II

Pill box resonator

$$h = \beta \cdot \frac{\lambda}{2}$$

B

beam

E

$$E(r,t) = J_0\left(\frac{2.405 \cdot r}{R}\right) \cdot E_0 \sin(\omega_0 \cdot t) \qquad B_\varphi(r) = \frac{i}{c} J_1\left(\frac{2.405 \cdot r}{R}\right) \cdot E_0 e^{i\omega_0 t}$$

$$t(z) = z / (\beta \cdot c)$$

Stored energy U: $\quad U = \dfrac{\varepsilon_0}{2} \displaystyle\int_0^{2\pi} d\varphi \int_0^h dz \int_0^R rdr \cdot |E(r)|^2 = \dfrac{\varepsilon_0}{2} \cdot \underbrace{\pi R^2 h}_{V} |E_0|^2 \cdot \left| \underbrace{J_1(2.405)}_{0.581865} \right|^2$ $\qquad \boxed{\eta = \sqrt{\dfrac{\mu_0}{\varepsilon_0}}}$

Dissipated power P:

$$P = \frac{R_s}{2\mu_0^2} \int_0^{2\pi} d\varphi \cdot \left(\int_0^h dz |B_\varphi(R)|^2 + 2 \cdot \int_0^R rdr |B_\varphi(r)|^2 \right) = R_s \frac{1}{\eta^2} |E_0|^2 \cdot \pi R \cdot (h+R) \cdot \left| \underbrace{J_1(2.405)}_{0.581865} \right|^2$$

Q factor: $\qquad Q = \dfrac{\text{Stored energy } U}{\text{Energy lost during 1 RF period}} = \omega \dfrac{U}{P} \qquad\qquad Q = \omega \cdot \dfrac{\varepsilon_0 \cdot \eta^2}{2 R_s \cdot \left(\dfrac{1}{R} + \dfrac{1}{h} \right)}$

Cavity characteristics

shunt impedance R:

$$R = \frac{V_a^2}{2 \cdot P}$$

R/Q **measures the interaction of the cavity with the beam:**

$$\frac{R}{Q} = \underbrace{\frac{V_a^2}{2 \cdot P}}_{R} \cdot \underbrace{\frac{P}{\omega \cdot U}}_{1/Q} = 7.10 \frac{4}{\pi^3} \cdot \frac{h}{R} \cdot \eta \qquad \eta = 377 \text{ Ohm}$$

The **peak surface electric and magnetic fields** constitute the ultimate limit for the accelerating gradient => minimize the ratio E_p/E_a and B_p/E_a.
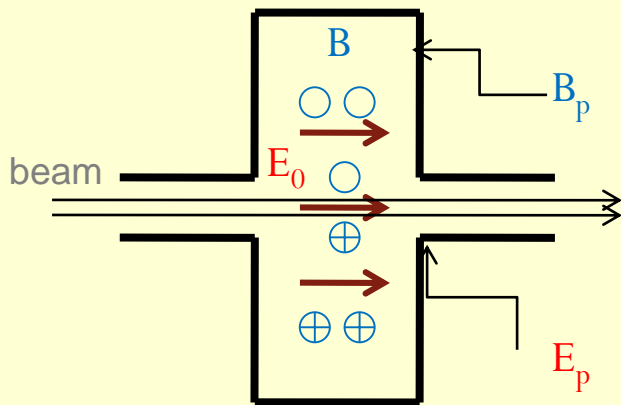
$$E_a = \frac{2E_0}{\pi}$$

$$\frac{B_p}{E_a} = 3.07 \left[\frac{\text{mT}}{\text{MV/m}} \right]$$

$$\frac{E_p}{E_a} = \frac{\pi}{2} \approx 1.57$$

JUAS 2020: SC RF - Caspers/Wendt/Bozzolan

Cavity characteristics - Summary

Symbol	Name	Definition	Pillbox cavity [0.35 GHz, 4.2 K, Nb]	Accelerating cavity [0.35 GHz, 4.2 K, Nb]
E_p/E_a	Peak normalized surface electric field	n/a	1.6	2
B_p/E_a [mT/(MV/m)]	Peak normalized surface magnetic field	n/a	3.1	4
R_s [nΩ]	Surface resistance	E_x/H_y	40	40
h [m]	Cavity length	$h=\lambda/2$	0.43	0.43
E_a [MV/m]	Accelerating gradient	$(1/e)\cdot$Energy gain/length	10	10
V [MV]	Accelerating voltage	$V=E_a\cdot h$	4.3	4.3
G [Ω]	Geometry factor	$G=R_s\cdot Q$	260	275
Q [10^9]	Quality factor	$Q=\omega U/P$	6.5	6.9
R/Q [Ω]	(R/Q) factor	$(R/Q)=V^2/(2\omega U)$	450	280
R [MΩ]	Shunt impedance	$R=V^2/(2P)$	$3\cdot 10^6$	$2\cdot 10^6$
U [J]	Stored energy	$U=V^2/[2\omega(R/Q)]$	9	15
P [W]	Dissipated power	$P=\omega U/Q$	3	5
h/R	Ratio cavity length to radius	n/a	1.3	0.5

JUAS 2020: SC RF - Caspers/Wendt/Bozzolan

Computer codes for RF cavities

Computer codes to determine the cavity parameters

For real structures with contoured shapes, beam apertures and beam pipes, it is necessary to use field computation codes, such MAFIA and Microwave Studio. Figure 10 shows the electric and magnetic fields computed by Microwave Studio for the accelerating mode of a pillbox cavity with a beam hole, and for a round wall cavity. Such codes are also necessary for computing the fields in the higher order modes of a cavity that can have an adverse effect on beam quality or cause instabilities. Figure 11 shows the electric and magnetic fields of the first monopole HOM. Beam induced voltages are also proportional to the R/Q of HOMs.

TM010

$f = 1323$ MHz
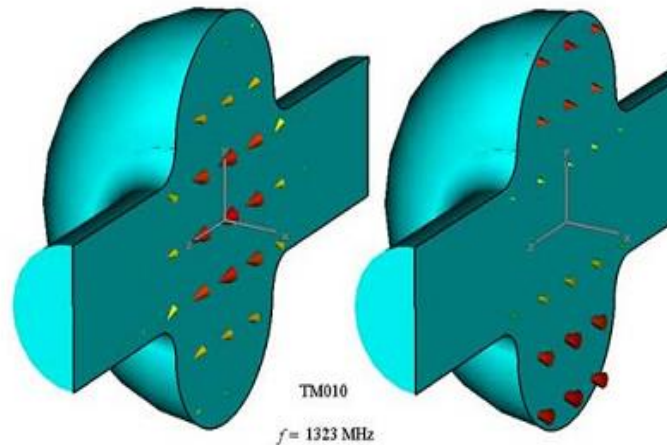
Fig.10 (Left) Electric and (Right) Magnetic fields for a round cavity with beam holes.

Cavity characteristics – Summary table

Table: Equivalence of cavity and lumped-element circuit parameters
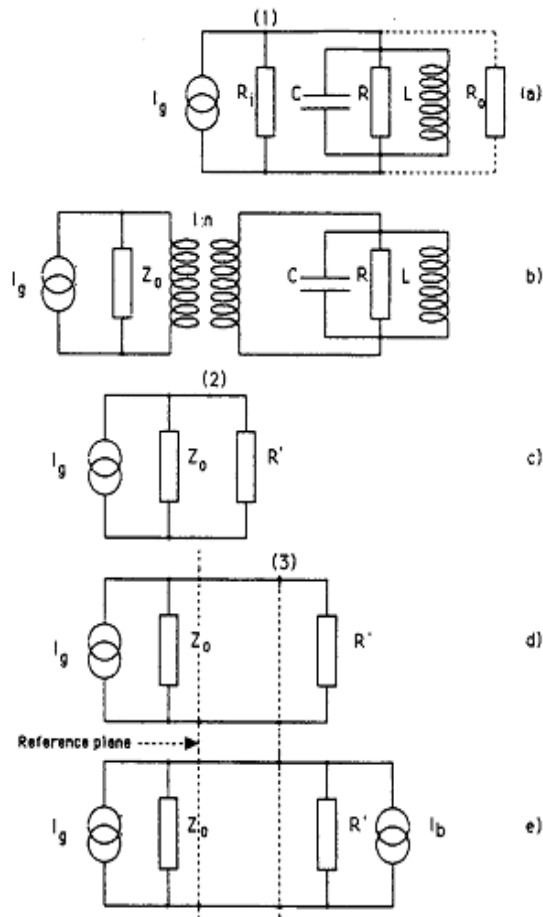
Fig. 8 Lumped element equivalent circuit model of an accelerating cavity resonator

Cavity	Lumped-element circuit
Accelerating voltage V	Peak voltage V
Resonant frequency ω_0	$\omega_0 = 1/\sqrt{(LC)}$
Stored energy U	$U = (1/2)CV^2$
Dissipated power P_c	$P_c = (1/2)\,V^2/R$
Radiated power P_{rad}	$P_{rad} = (1/2)\,V^2/R_i$
Shunt impedance $R = V^2/(2 \cdot P_c)$	R
Unloaded Q - value $Q_0 = \omega_0 \cdot U/P_c$	$Q_0 = \omega_0 \cdot RC$
External Q - value $Q_{ext} = \omega_0 \cdot U/P_{rad}$	$Q_{ext} = \omega_0 \cdot R_i C = R_i/(R/Q)$
(R/Q) value $R/Q = V^2/(2\,\omega_0 \cdot U)$	$R/Q = \sqrt{(L/C)} = 1/(\omega_0 \cdot C)$
Coupling factor $\beta = Q_0/Q_{ext}$	$\beta = R/R_i$
Loaded Q - value $Q_L = Q_0/(1+\beta)$ (because $Q_L^{-1} = Q_0^{-1} + Q_{ext}^{-1}$)	$Q_L = \omega_0 \cdot RC/(1+\beta)$
Turns ratio $n = \sqrt{[(R/Q) \cdot Q_{ext}/Z_0]}$	$n = \sqrt{(R_i/Z_0)}$
Wave impedance $Z_0 = 50\ \Omega$	

From W. Weingarten, CERN-1992-03

JUAS 2020: SC RF - Caspers/Wendt/Bozzolan

Measuring setup

- Q determined by measuring the decay time of the cavity response
- Measurement of Q vs E_{acc}

p: power meter
f: frequency counter
ϕ: phase shifter
i: incident
r: reflected
t: transmitted
ant1: pickup antenna no. 1
ant2: pickup antenna no. 2
VCO: voltage controlled oscillator

Q(E$_{acc}$) curve
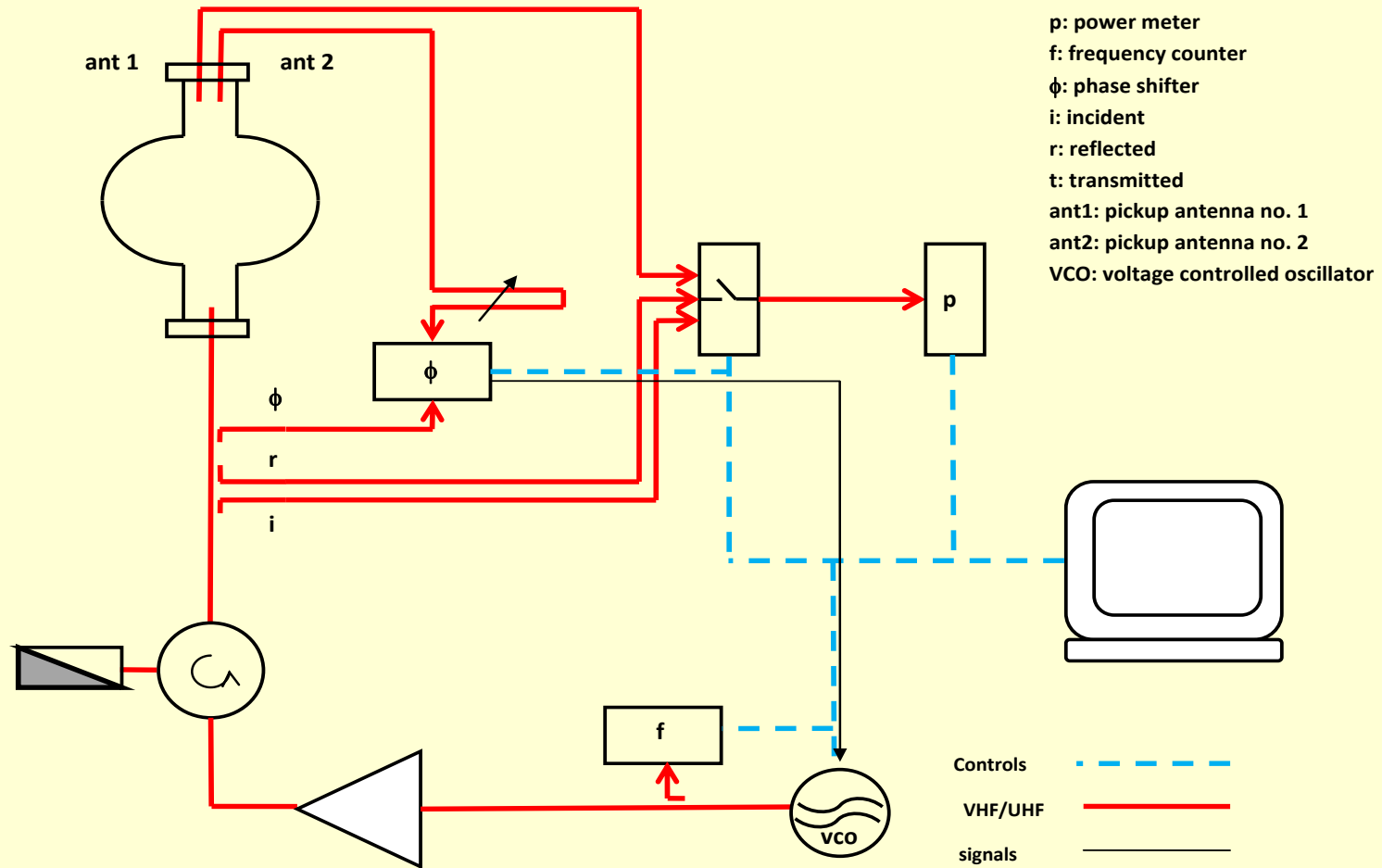
Electropolishing and in-situ Baking of 1.3 GHz Niobium Cavities

L. Lilje[+], D. Reschke, K. Twarowski, DESY, Notkestraße 85, 22607 Hamburg
P. Schmüser, Universität Hamburg
D. Bloess, E. Haebel, E. Chiaveri, J.-M. Tessier, H. Preis, H.Wenninger, CERN, Geneva
H. Safa, J.-P. Charrier, CEA, Saclay
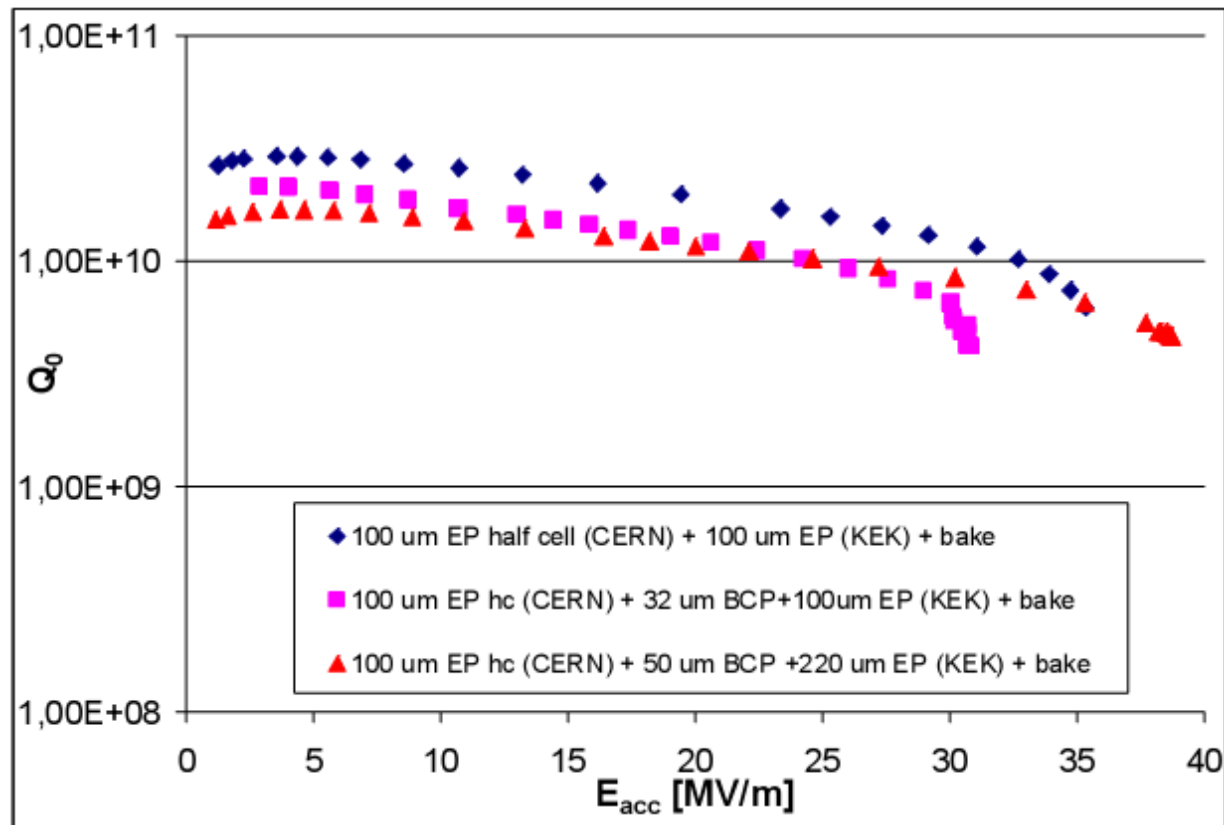
Figure 6: The cavities after bakeout show no Q-drop. One cavitiy is limited at 30 MV/m due to strong field emission and available RF power.

JUAS 2020: SC RF - Caspers/Wendt/Bozzolan

Passband modes

π/4

2π/4

3π/4

4π/4
π
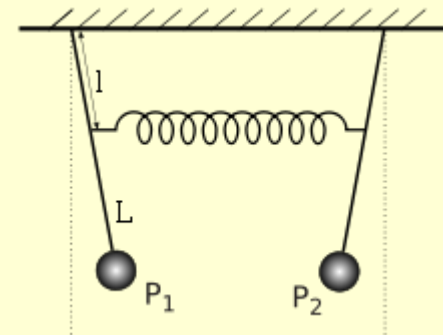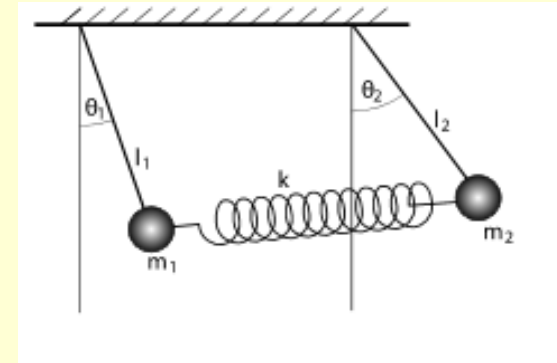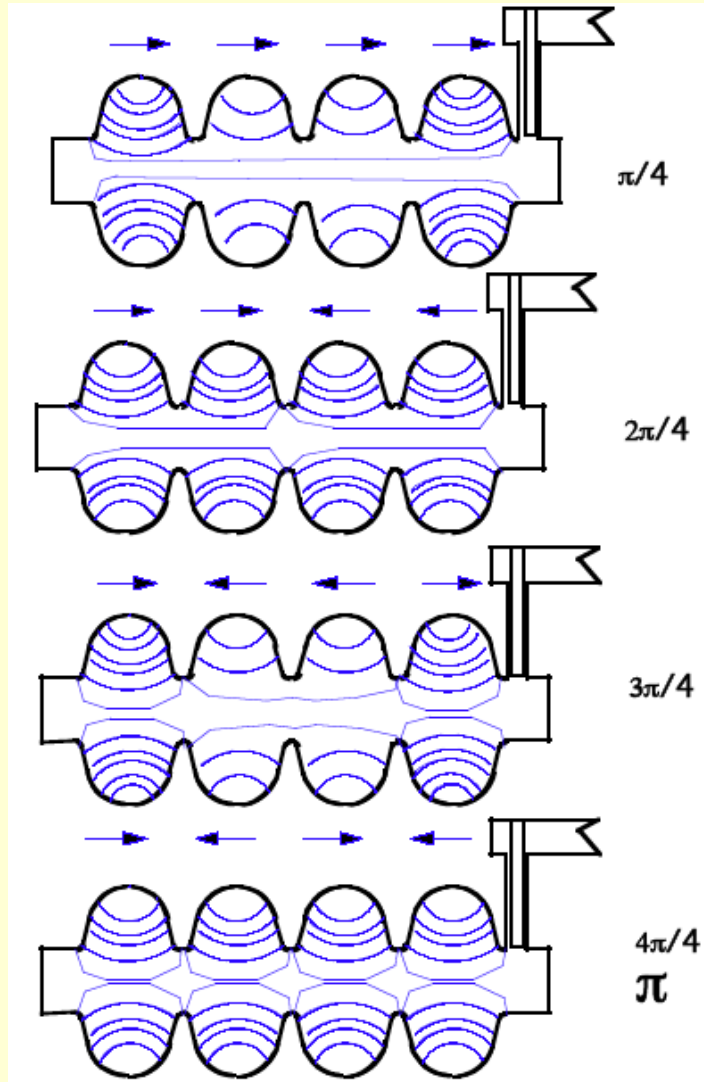
http://de.wikipedia.org/wiki/Gekoppelte_Pendel

JUAS 2020: SC RF - Caspers/Wendt/Bozzolan

- http://www.youtube.com/watch?v=IAPWpViY19A

JUAS 2020: SC RF - Caspers/Wendt/Bozzolan

Typical storage ring cavity (LEP)

JUAS 2020: SC RF - Caspers/Wendt/Bozzolan
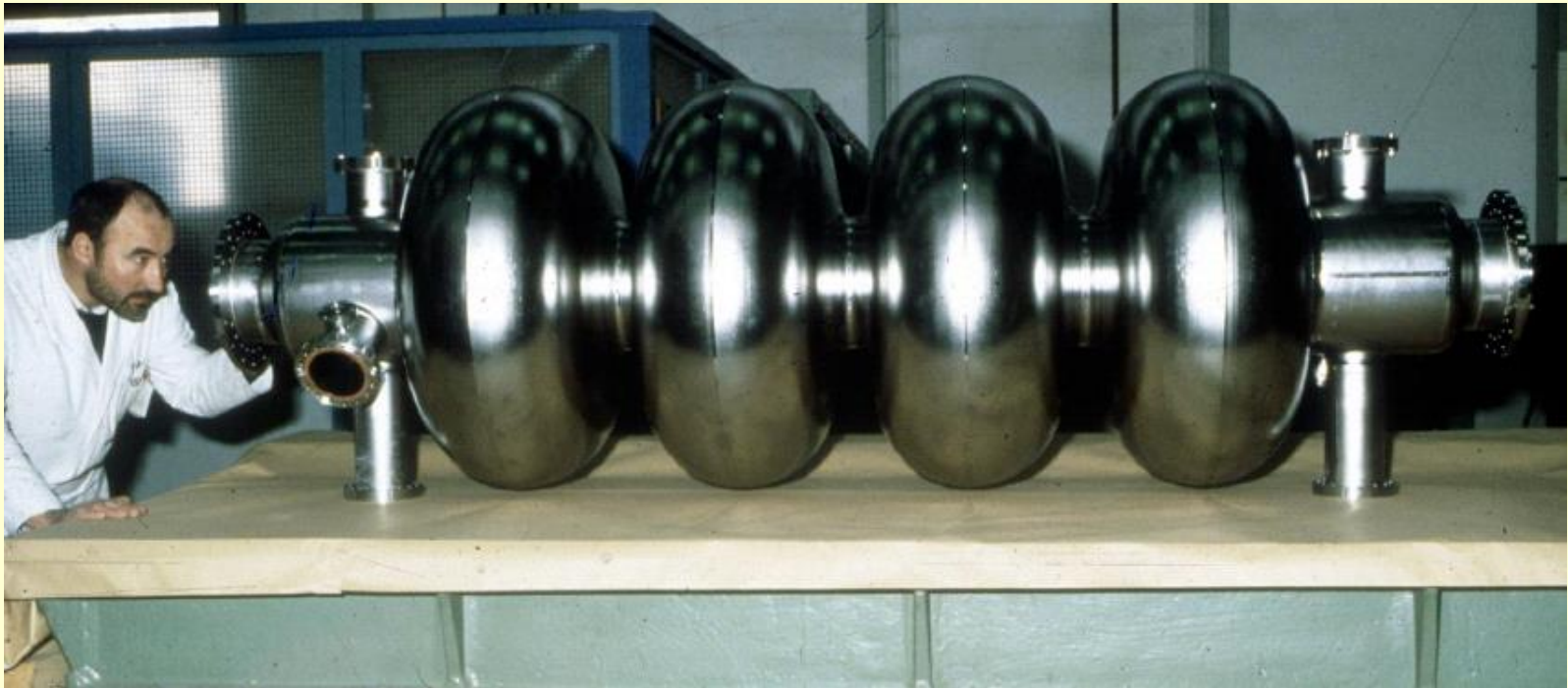
Summary

- The pillbox resonator (TM_{010} mode) allows – as a paradigm - the analytical description of typical accelerator parameters, such as peak surface fields (E and H), power loss and Q-value, shunt impedance, geometrical shunt impedance, geometry factor, etc.

- « Real » accelerator cavities are designed by making use of computer codes such as Microwave Studio, MAFIA, SUPERFISH, etc.

- The response of a cavity to an RF pulse is well described by lumped circuit networks, in particular by the transmission and reflection of an electromagnetic wave at a discontinuity in the line.

- An algorithm is presented to determine the coupling factor β (or the reflection factor ρ), and finally the unloaded Q-value Q_0, the accelerating voltage V (accelerating gradient E_a) and the surface resistance R_s.

Learning targets

After this chapter you should

- Have an idea about SC muliple cell resonator structures and their mechanical implementation
- Know that for coupled resonators the resonance frequencies are splitting up
- Have understood the concept of the test setup for the amplitude dependent Q measurement on a SC cavity in particular proper control of all parameters
- Know that the Q value of superconducting cavities is field strength dependent
- Be able to understand and mutually convert different notations and symbols for RF cavities
- Be able to give some examples of typical shapes for SC cavities

-

Recommended literature

Literature

W. Buckel and R. Kleiner, « Superconductivity: Fundamentals and applications, Wiley VCH 2004

V. V. Schmidt « The physics of superconductors », Springer 1997

M. Tinkham, « Introduction to superconductivity », McGraw-Hill 1996, and many others

Nobel lectures (http://nobelprize.org/nobel_prizes/physics/laureates/)

Interaction of cavity with beam

- Descriptive introduction

- Analytical introduction

- Transfer of RF power from the cavity to the beam
  - The fundamental mode power coupler

- Transfer of RF power from the beam to the cavity
  - Higher order modes and their damping

- The frequency tuner

- Summary

JUAS 2020: SC RF - Caspers/Wendt/Bozzolan

Descriptive Introduction

THE SUPRACONDUCTIVITY

LIKE THE WAVE PROPELS THE SURFER ELECTROMAGNETIC WAVES ACCELERATE PARTICLES

THE USE OF SUPRACONDUCTIVITY TO INCREASE PERFORMANCES AND CONSIDERABLY REDUCE ELECTRICITY CONSUMPTION

ACCELERATING ELECTROMAGNETIC WAVE

SUPERCONDUCTING ACCELERATING CAVITY MADE OF NIOBIUM

LIQUID HELIUM COOLED TO - 269° C

JUAS 2020: SC RF - Caspers/Wendt/Bozzolan
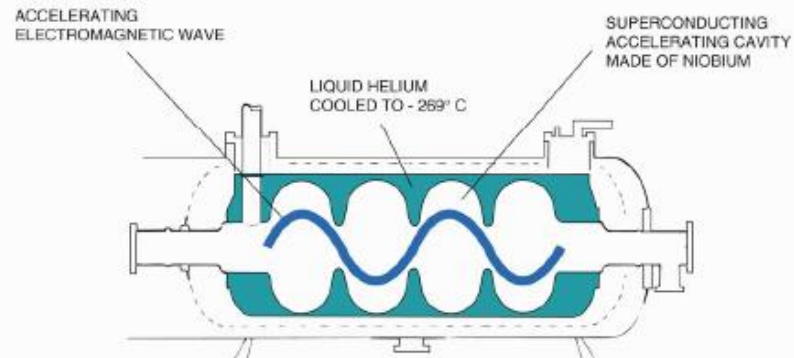
Particle passing through cavity

JUAS 2020: SC RF - Caspers/Wendt/Bozzolan

Analytical Introduction

t=3T/8
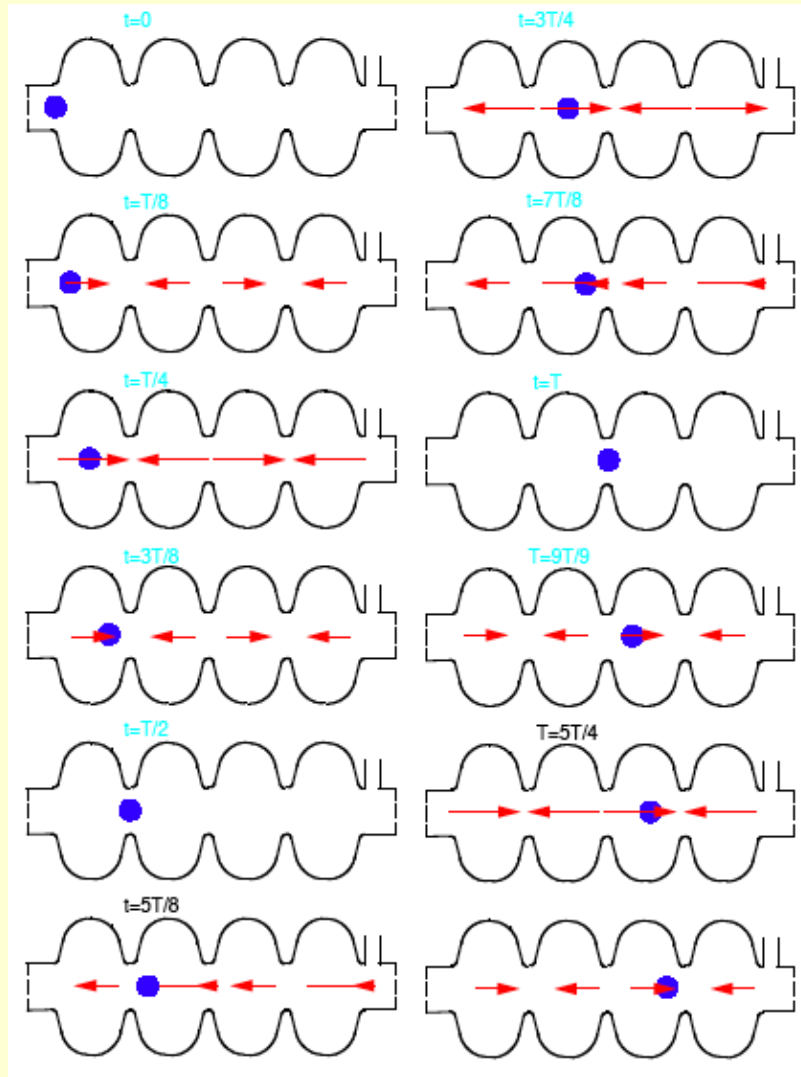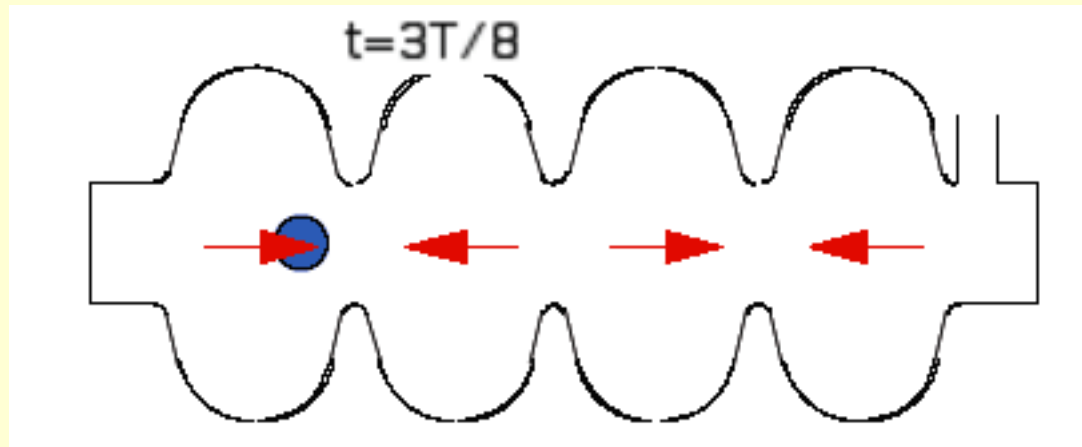
$$V = E(z_1, t_1)\Delta z_1 + E(z_2, t_2)\Delta z_2 + \ldots\ldots$$

$$\Rightarrow V = \int_{-\infty}^{+\infty} E(z, \ t \ (z) \ ) \ dz$$

$$E(z,t) = E(z) * \cos(\omega t + \varphi)$$

$$t = z/v$$

$$V(\varphi) = \int_{-\infty}^{+\infty} E(z) * \cos(z\omega/v + \varphi) \ dz$$

JUAS 2020: SC RF - Caspers/Wendt/Bozzolan

$$I_r - I_g + I_k = \frac{V}{Z} \Bigg\} \Rightarrow I_r + I_g = \frac{V}{Z}$$

$$I_k = 2I_g$$

A circulator guarantees that under no circumstances there is no reflected wave impinging to the RF generator

$$I_{LCR} = I_g - I_r - I_{b,RF} = 2I_g - I_{b,RF} - \frac{V}{Z}$$

$$I_{LCR} = V\left(\frac{1}{i\omega L} + i\omega C + \frac{1}{R}\right)$$

$$\omega_0 = \frac{1}{\sqrt{LC}}$$

With $\omega_0^2 - \omega^2 \approx 2\omega_0 \Delta\omega$ and $\Delta\omega \prec \omega$

$$\Rightarrow V\left(-\frac{2\Delta\omega}{\omega} + \frac{1}{i\omega C}\left(\frac{1}{R} + \frac{1}{Z}\right)\right) = \frac{2I_g - I_{b,RF}}{i\omega C}$$

JUAS 2020: SC RF - Caspers/Wendt/Bozzolan

Re-write preceding equation

$$V\left(-\frac{2\Delta\omega}{\omega} + \frac{1}{i\omega C}\left(\frac{1}{R} + \frac{1}{Z}\right)\right) = \frac{2I_g - I_{b,RF}}{i\omega C}$$

in cavity parameters

$$V\left(\frac{1}{2(R/Q)}\left(\frac{1}{Q_{ext}} + \frac{1}{Q_0}\right) - i\frac{\Delta\omega}{\omega(R/Q)}\right) = I_g - \frac{1}{2}I_{b.RF}$$

- Minimize reflected power

$$V\left(\frac{1}{2(R/Q)}\left(\frac{1}{Q_{ext}}+\frac{1}{Q_0}\right)-i\frac{\Delta\omega}{\omega(R/Q)}\right)=I_g-\frac{1}{2}I_{bRF}$$

$$\Rightarrow I_g = \frac{V}{2(R/Q)}\left(\frac{1}{Q_{ext}}+\frac{1}{Q_0}\right)+I_{DC}\cos\Phi-i\left(I_{DC}\sin\Phi+\frac{V\Delta\omega}{\omega(R/Q)}\right)$$

$$\frac{1}{Q_0}\prec\frac{1}{Q_{ext}}\text{ for sc cavities}$$

$$I_r = \frac{V}{Q_{ext}\cdot(R/Q)}-I_g = \frac{V}{2\cdot(R/Q)}\left(\frac{1}{Q_{ext}}-\frac{1}{Q_0}\right)-I_{DC}\cos\Phi-i\left(I_{DC}\sin\Phi+\frac{V\Delta\omega}{\omega(R/Q)}\right)$$

Actions: 1) compensate « reactive beam loading » to zero by detuning $\Delta\omega$

$$\Delta\omega = -\omega\frac{(R/Q)\cdot I_{DC}}{V}\sin\Phi$$

2) define optimum Q_{ext} for nominal beam current for $I_r = 0$

$$Q_{ext,opt} = \frac{V}{2\cdot(R/Q)I_{DC}\cos\Phi}$$

RF power $\quad P_{g,r} = \frac{1}{2}Z|I_{g,r}|^2 = \frac{1}{2}(R/Q)\cdot Q_{ext}\cdot|I_{g,r}|^2$

Check: $\quad P_{beam,r} = P_{g,r}-P_{r,r} = V\cdot I_{DC}\cdot\cos\Phi$

The fundamental mode power coupler

Air cooling inlet

Air inlet antenna

Displacement mechanism

Air pressure interlock

RF screen

Bellows

Motor drive

Capacitor for DC bias

RF input

Short circuit

Ceramic window

Antenna (copper)
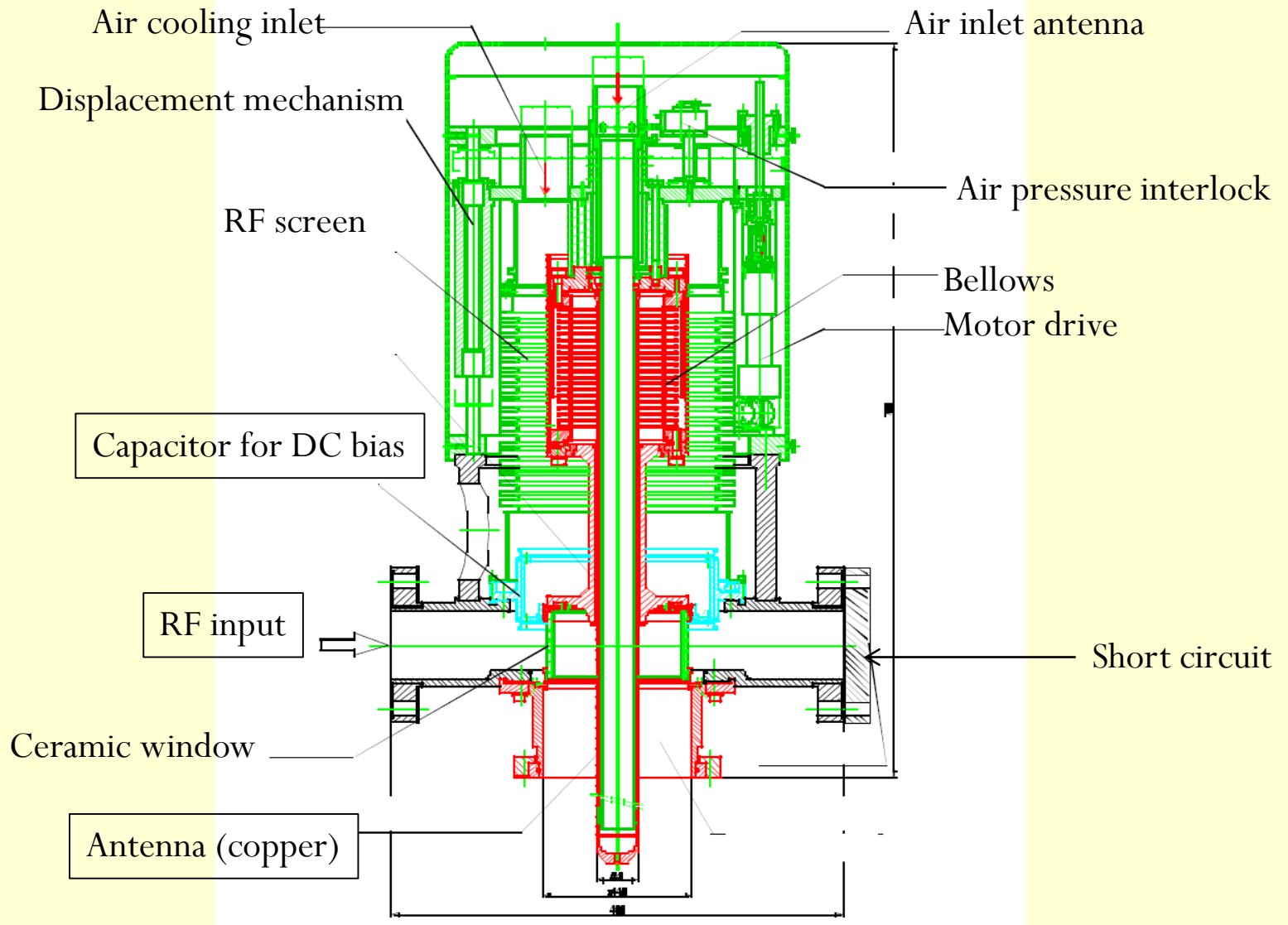
LHC solution of the power coupler

JUAS 2020: SC RF - Caspers/Wendt/Bozzolan
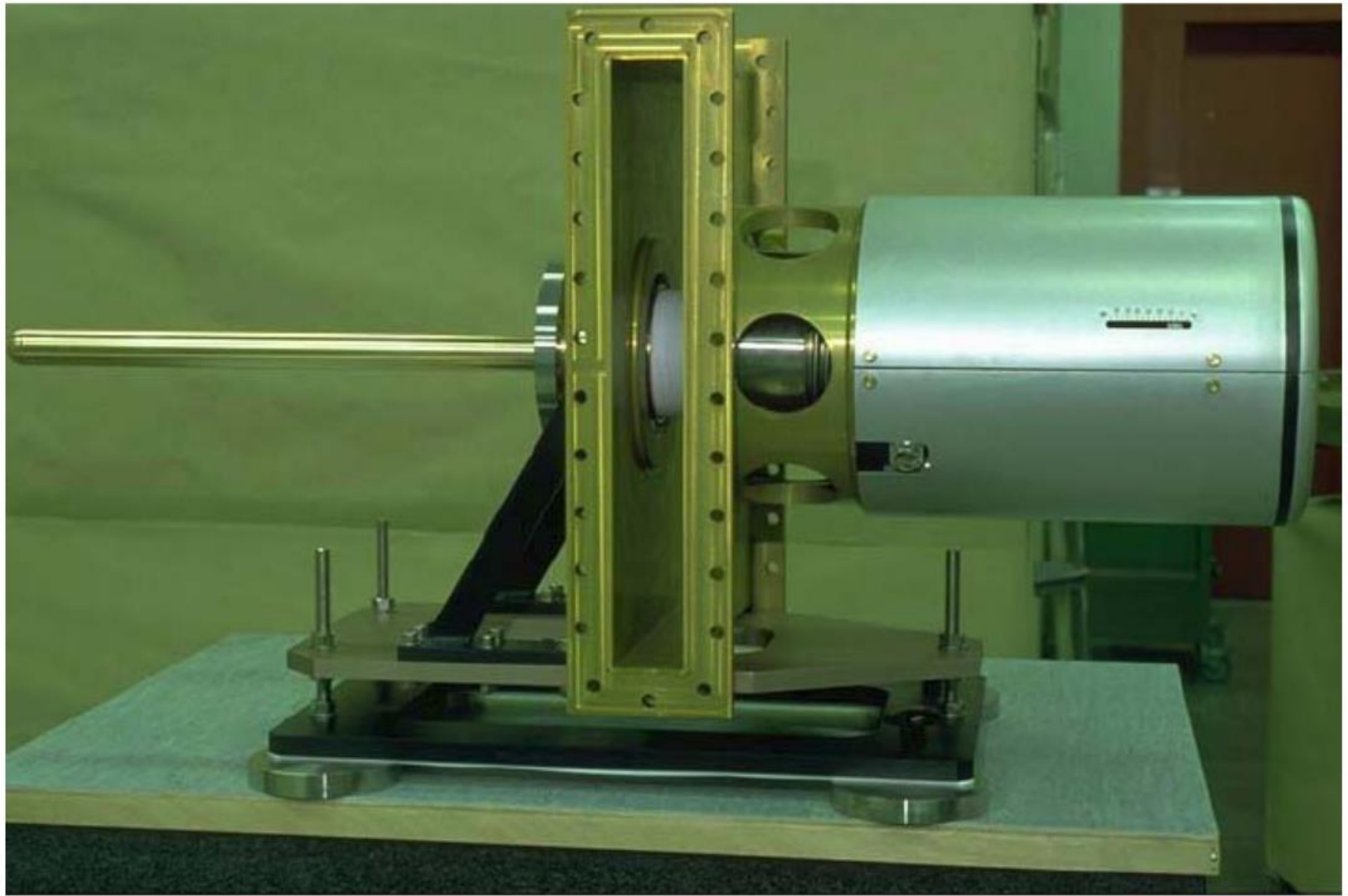
Transfer of RF power from the beam to the cavity

- Need for Higher Order Mode (HOM) coupler

Imagine worst case

1. the cavity resonant frequency is « tuned » to a spectral line of the beam

2. Generator switched off, $I_g=0$.

$$V\left(\frac{1}{2(R/Q)}\left(\frac{1}{Q_{ext}}+\frac{1}{Q_0}\right)-i\frac{\Delta\omega}{\omega(R/Q)}\right)=I_g-\frac{1}{2}I_{b.RF} \qquad \Rightarrow \Delta\omega=0; \Phi=0$$

$$\boxed{\Rightarrow V=-I_{b.RF}\cdot(R/Q)\cdot Q_{ext}=-2\cdot I_{DC}\cdot(R/Q)\cdot Q_{ext}}$$

This means that the beam is
decelerated.
Remedy: keep Q_{ext} as low as possible.

Output power (reflected):
$$\boxed{P_r=\frac{V^2}{2\cdot Z}=\frac{V^2}{2\cdot(R/Q)\cdot Q_{ext}}=2\cdot(R/Q)\cdot Q_{ext}\cdot I_{DC}^2}$$

1st example (LEP); RF Generator trip.
We obtain for the **accelerating mode** $\quad R/Q=232\,\Omega; Q_{ext}=2\cdot10^6; I_{DC}=6\,\text{mA}; P_r=33\,\text{kW}$

2nd example;
We obtain for the **higher order mode** with (R/Q) = 10 Ω, Qext = 20000
$$V=-2.4\,\text{kV}\Rightarrow P_r=14.4\,\text{W}$$

Higher order modes

Fig. 3 Examples of modes of a single cell with wide beam tubes

A typical HOM spectrum

Modes in SPL cavity

Numbers from Marcel Schuh

Cutoff tube diameter 140 mm

Monopole modes
Dipole modes
Cutoff
Cutoff

TM010
TE111
TM110
TM011
TM021

R/Q [Ω]
frequency [MHz]

JUAS 2020: SC RF - Caspers/Wendt/Bozzolan

How to deconfine HOMs[1]

Input coupler

Door knob

Gate Valve

Tuner

HOM damper

HOM damper

LHe

Mag.shield
LN₂ shield

Ion pump

0   1m
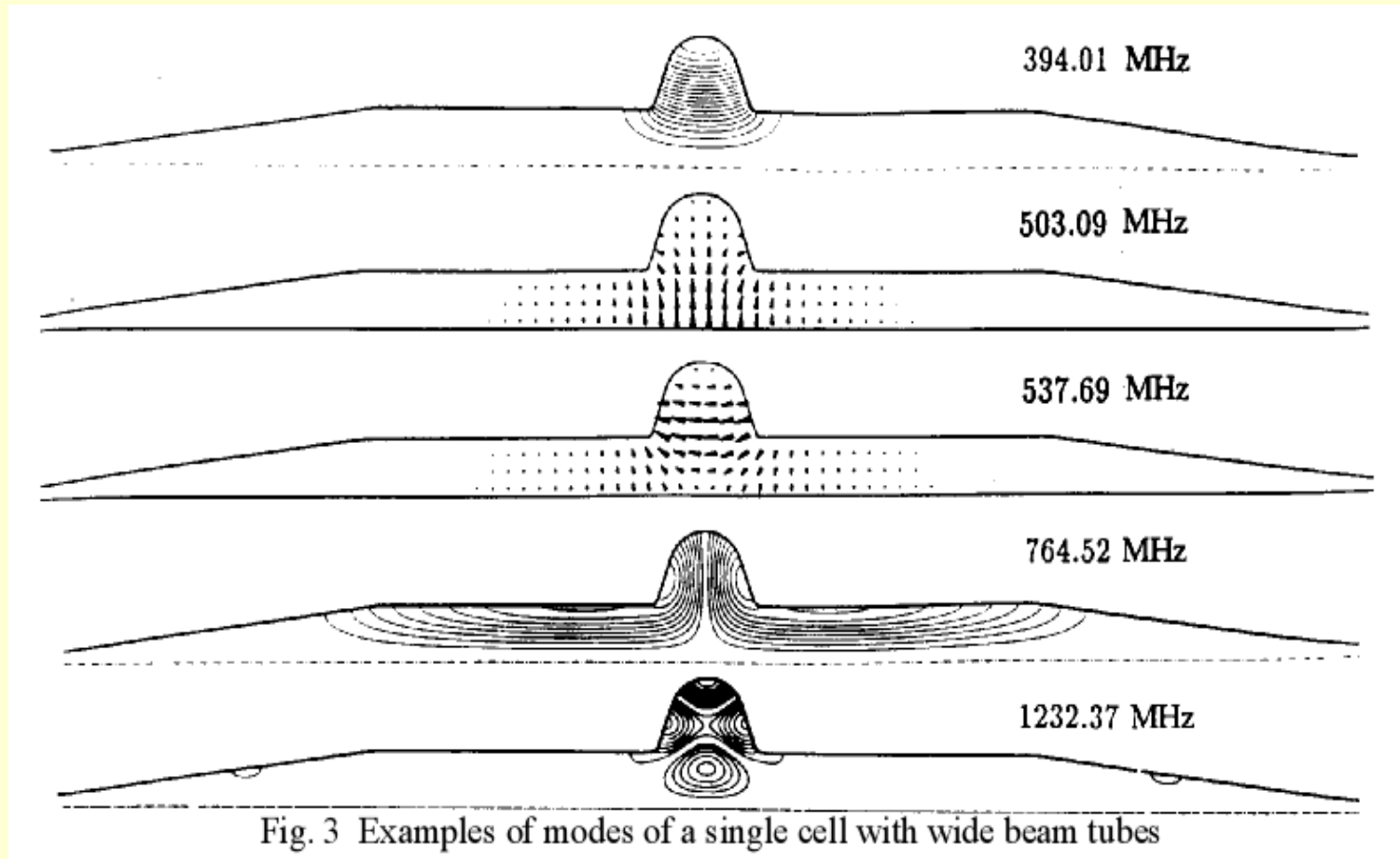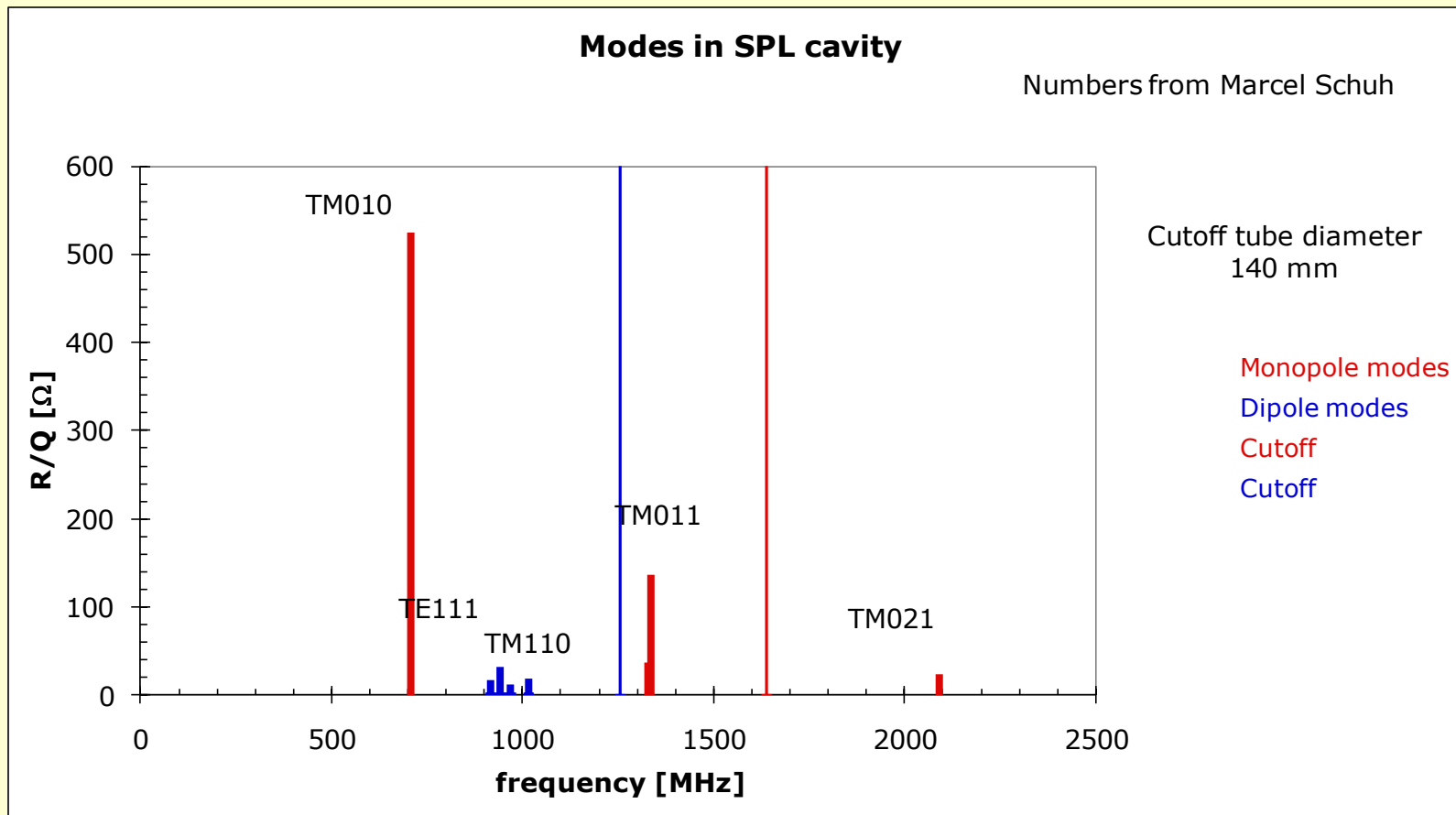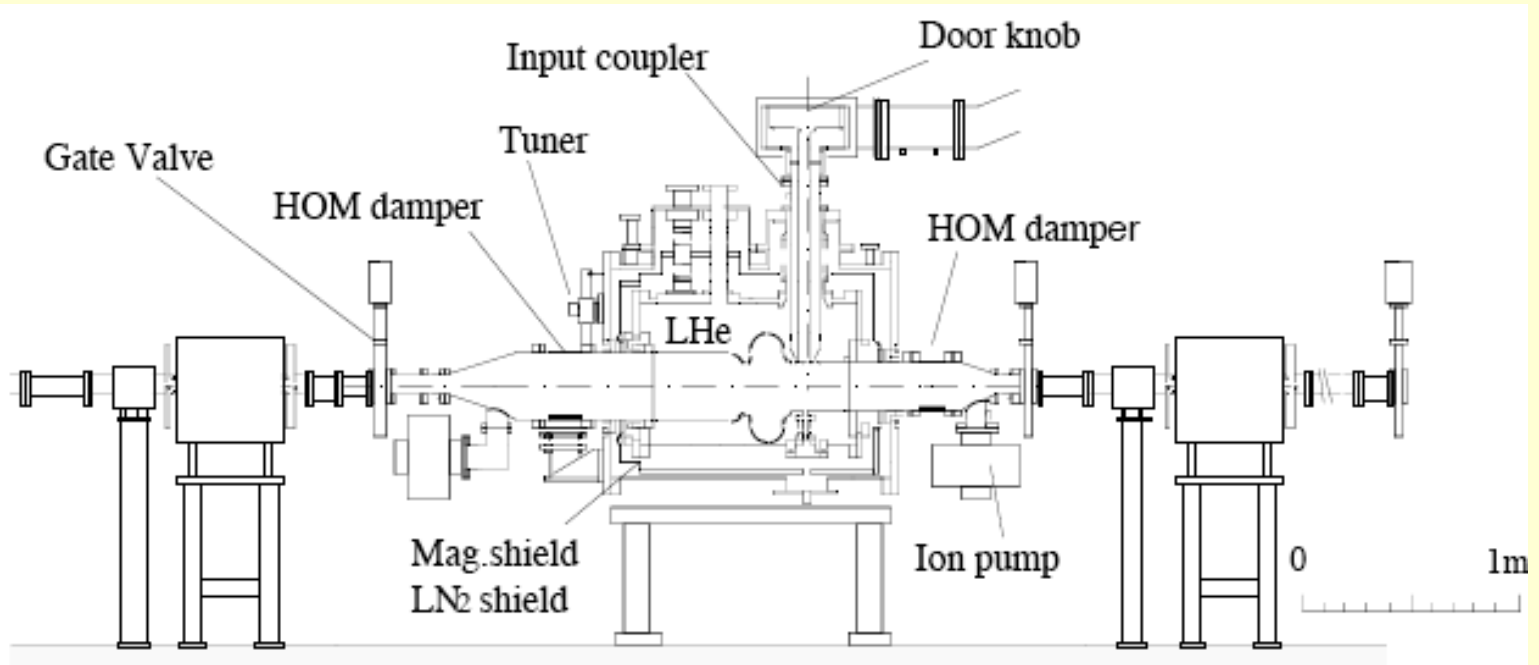
Figure: 1   A sketch of the prototype module in TRISTAN Accumulation Ring.

Open beam tube

OK for single cell cavity, but high cryo-load by thermal radiation

[1]http://www.lns.cornell.edu/Events/HOM10/Agenda.html

JUAS 2020: SC RF - Caspers/Wendt/Bozzolan

Damping HOMs 1/2: Beam tube loads

Ferrites

low power handling capacity if cold

higher power handling capacity if warm

mechanical and vacuum design not easy
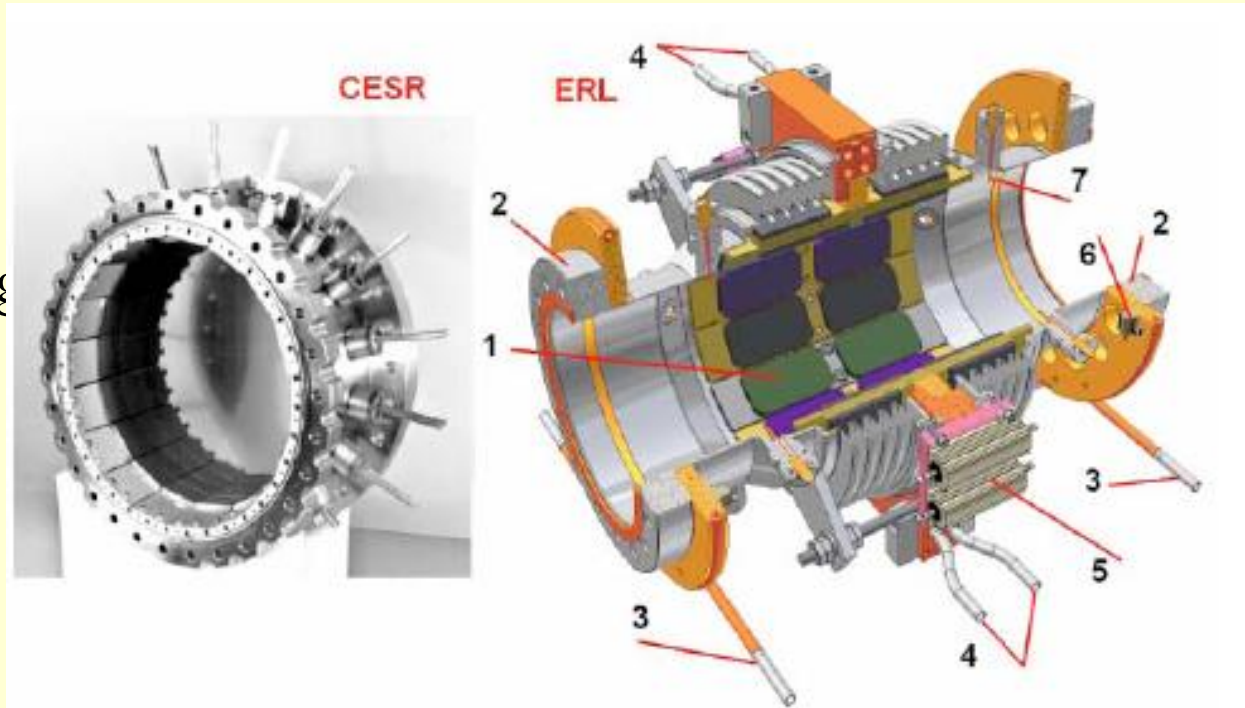
Figure 1: CESR and ERL HOM loads. 1 – absorber plates, 2 – flange to cavity, 3 – 5 K He cooling loop, 4 – 80 K cooling loop, 5 – 80 K heater, 6 – 5 K heaters, 7 – HOM pickup.

Damping HOMs 2/2: Resonant coaxial transmission line dampers

- Compensate internal impedances: The HOM coupler becomes a resonator coupled to the cavity resonator. It may have two eigenfrequencies.

  Obtainable Q_{ext}: 50

- Pros:
  - Couplers with several resonances possible (HERA, LEP, LHC, ILC are of this type)
  - Demountability
  - Fundamental mode rejection:
    - LEP: Fundamental mode E-field rejected by stop-filter in front of HOM coupler
    - Fundamental mode H-field rejected by loop plane perpendicular to cavity axis
    - Risk of detuning of notch filter

- BUT: High currents request for superconducting material prepared under ultra-clean conditions (like the cavity) and lHe cooling

- Prone to electron emission from inside cavity

JUAS 2020: SC RF - Caspers/Wendt/Bozzolan

Resonant coaxial transmission line dampers: Technical solution 1/3

LHC HOM coupler

10 cm

SNS HOM coupler

JUAS 2020: SC RF - Caspers/Wendt/Bozzolan

output
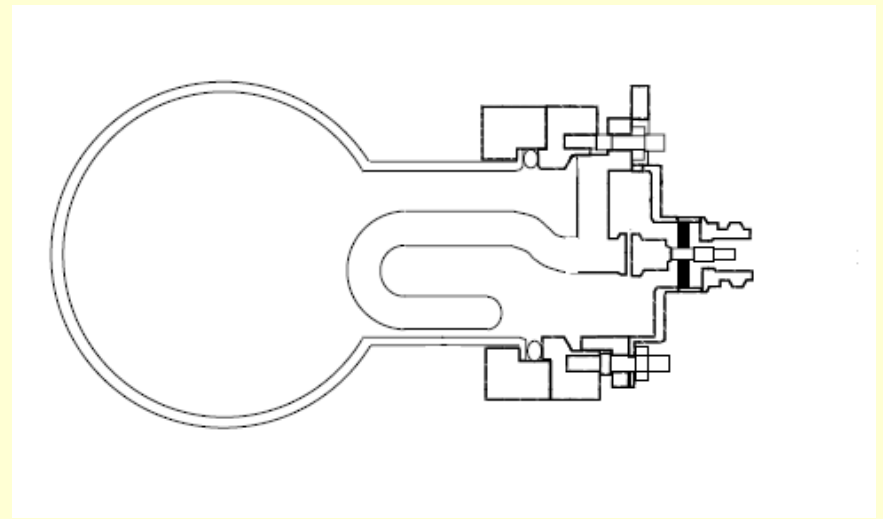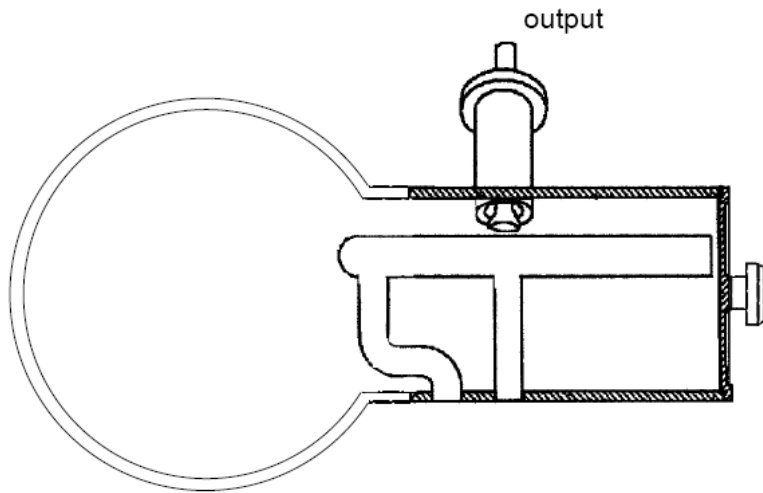
TESLA HOM coupler

The frequency tuner

The frequency of the cavity must be tuned to the harmonic spectral line of the bunched beam => need to develop a frequency tuner. Slater's theorem states that

$$\frac{\Delta f}{f} = \frac{1}{4U} \int_{\Delta V} \left(\varepsilon_0 E^2 - \mu_0 H^2 \right) dV$$

$$U = \frac{1}{4} \int_{V} \left(\varepsilon_0 E^2 + \mu_0 H^2 \right) dV$$
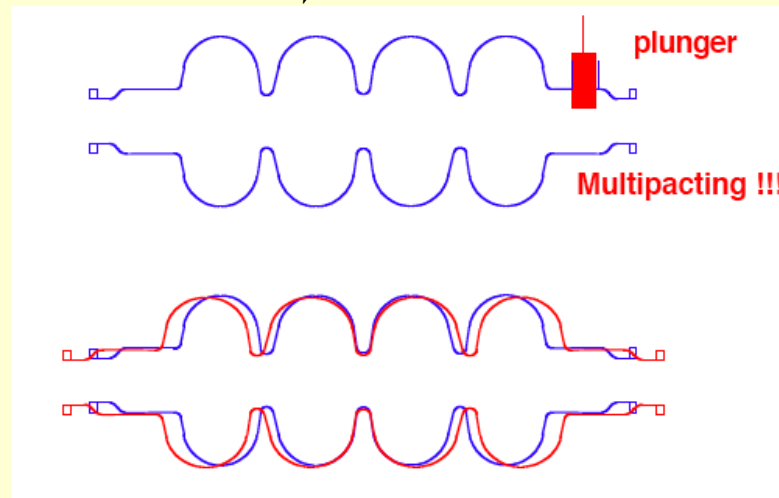
Mechanical oscillations
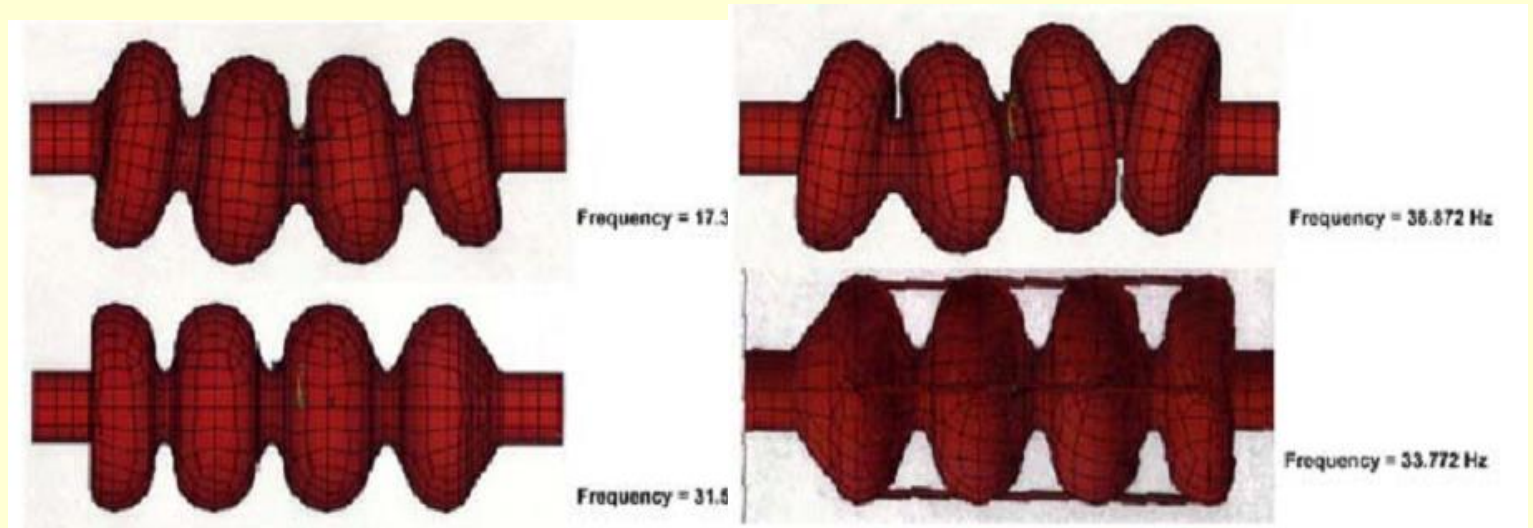
Fig. 20 Mechanical resonant modes of a 4-cell, 200 MHz cavity with 8 mm wall thickness. The low resonant frequencies spell trouble in the form of microphonics. Reducing the number of cells or stiffening is essential.

For example: at LEP, radiation pressure on the cavity walls of about 1000N in total possible

The LEP solution
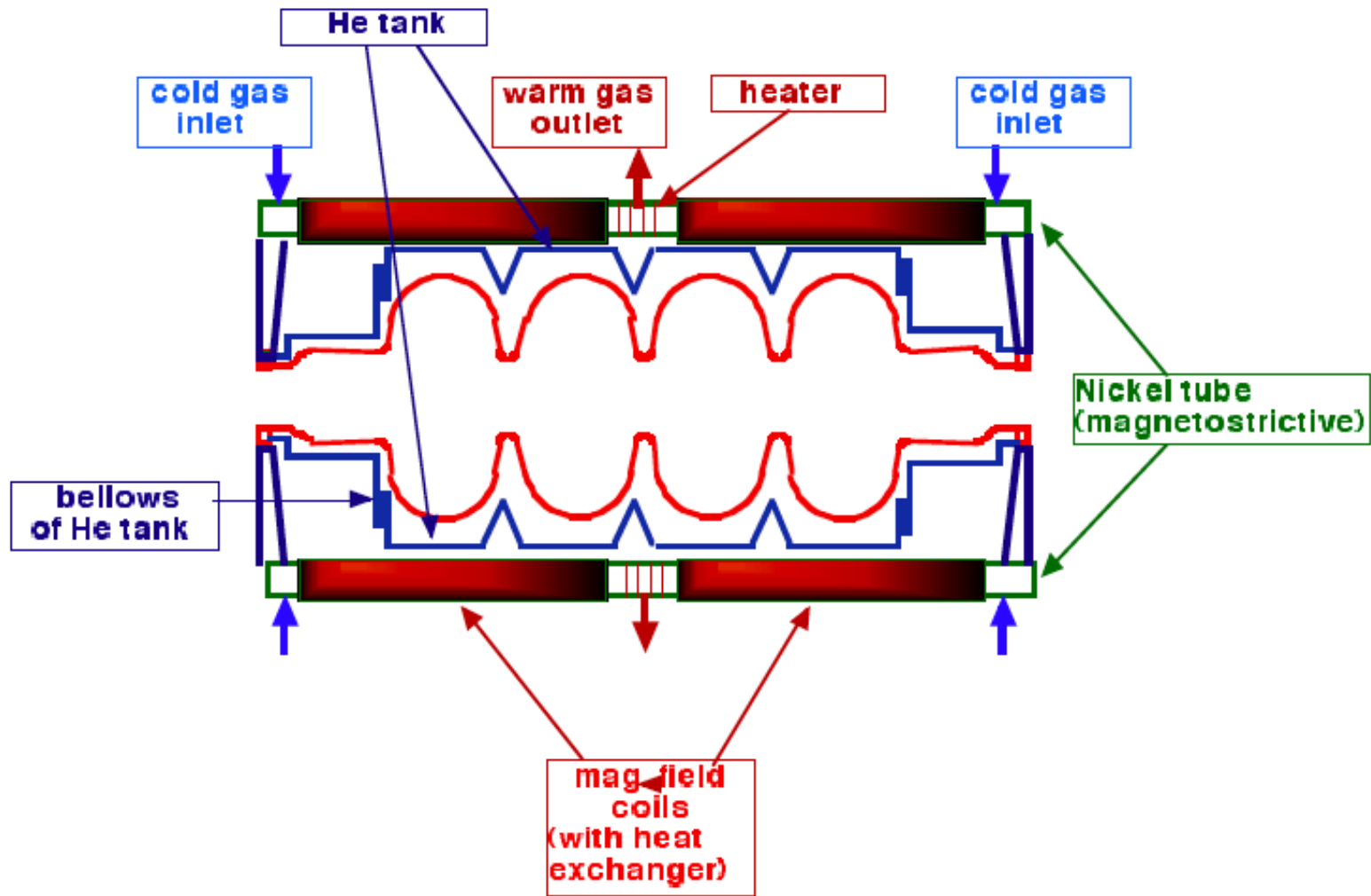
Integration into LEP cryostat 1/2

JUAS 2020: SC RF - Caspers/Wendt/Bozzolan
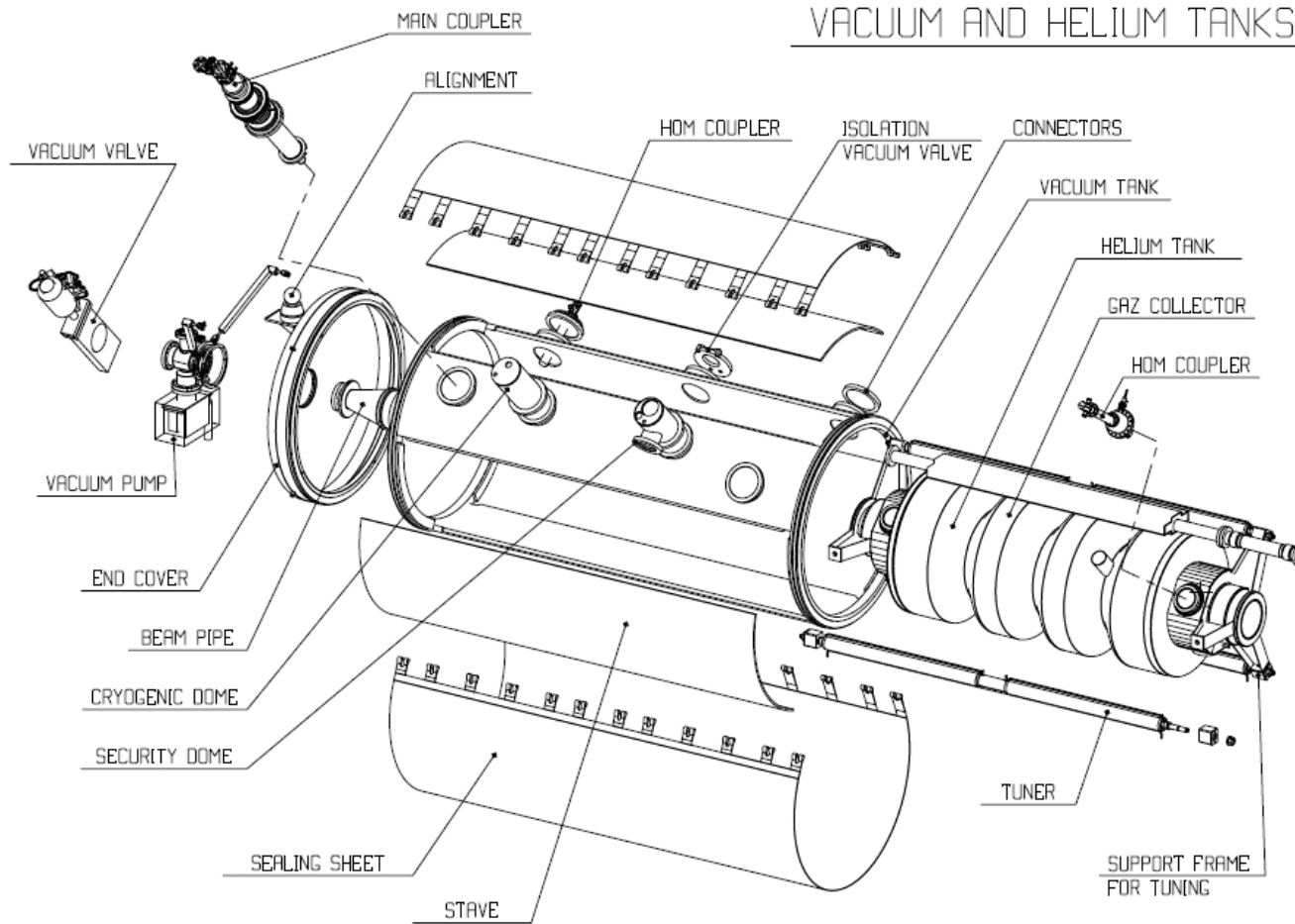
Comments:

The LEP cryostat could reliably be operated under CW conditions with beam and in pulsed conditions without beam in the present LHC tunnel environment (1.4 % slope).

It is worth noting that the lHe tank, the gas openings, and gHe collector were relatively small.

Pulsed operation: The thermal diffusivity $\kappa = \lambda/(c \cdot \rho)$ is such that it takes ~1 ms before the temperature pulse arrives at the niobium helium interface => advantage compared to CW operation.

This cryostat was tested under pulsed conditions with beam in the CERN SPS.

Cryomodules 1/2

JUAS 2020: SC RF - Caspers/Wendt/Bozzolan

Cryomodules

- installed in LEP tunnel

JUAS 2020: SC RF - Caspers/Wendt/Bozzolan
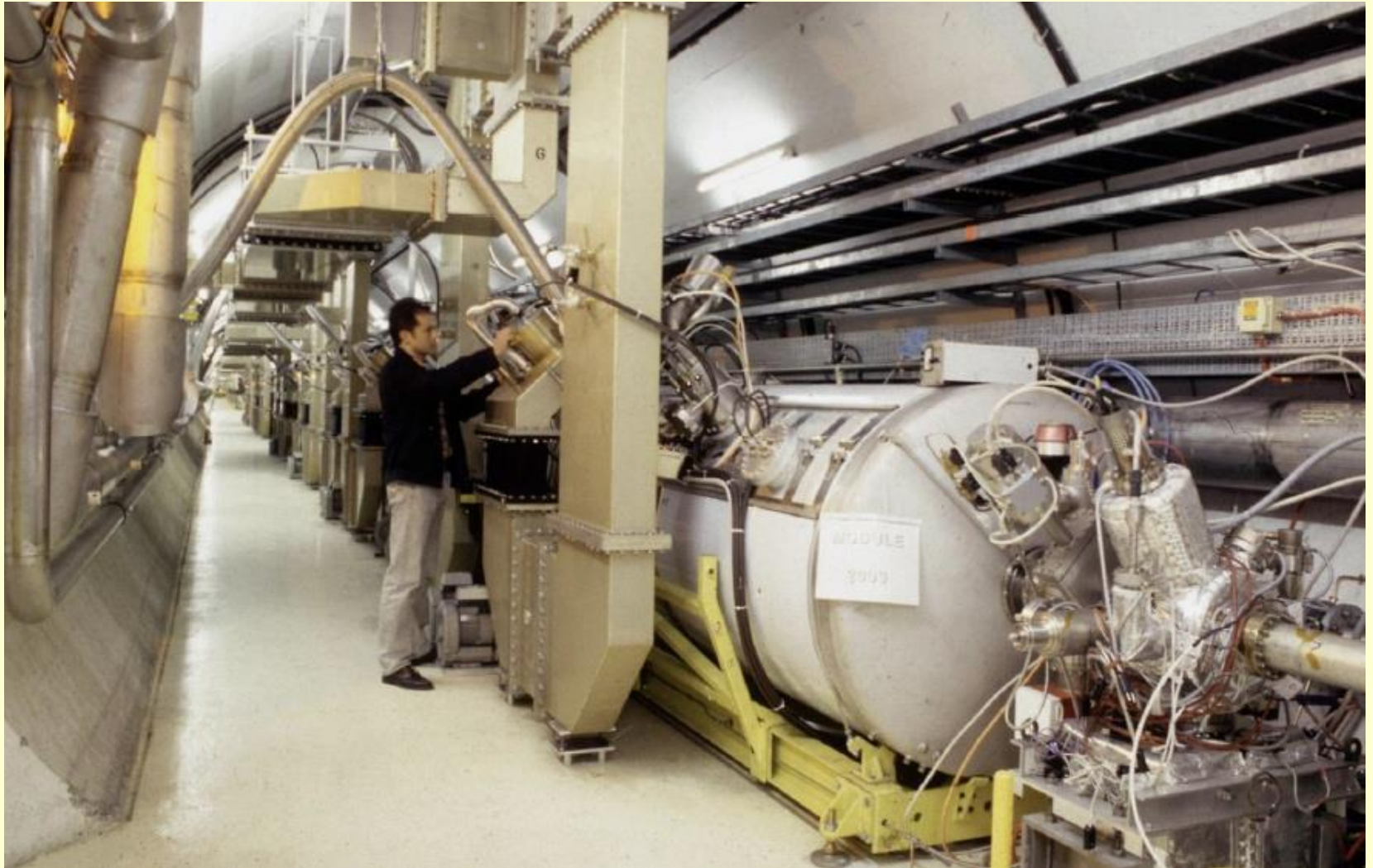
Summary and learning targets

- A lumped network circuit diagram allows an analytical description of the interaction of the RF cavity with the beam

- The cavity is designed to minimize the reflected RF power (which would be wasted anyhow in a load) by eliminating the « reactive beam loading » through tuning the frequency of the cavity and by matching the external Q to the nominal beam current.

- The beam consists of bunches passing the cavity in fractions of milliseconds[1] that may excite higher order modes (HOMs) of the cavity to high voltages, if not sufficiently damped by HOM couplers.

- Frequency tuners are in addition needed to damp frequency shifts from mechanical resonances excited by external noise sources (microphonics) or the interaction of the electromagnetic pressure with the cavity wall (Lorentz force detuning).

[1] for large storage rings such as LEP

JUAS 2020: SC RF - Caspers/Wendt/Bozzolan

Technological issues

- Cryogenics

- **<u>Anomalous losses:</u>**

  - Residual losses\magnetic shielding

  - Electron field emission

  - Electro polishing

  - Electron Multipacting (dust free assembly)

  - Heat removal (Quench - the role of large thermal conductivity, Coating a copper cavity with a thin niobium film)

  - Quality assurance and stochastic parameters

- Cavity production

- Improvement of cavity performance

- Summary

Basic Cryogenics

First law of thermodynamics:
The energy of a closed system stays constant.

$$dU = \delta Q + \delta W = 0$$

Second law of thermodynamics:
The entropy of a closed system can not decrease.

$$\delta Q = TdS$$

Schematic of cooling cycle, Kaeltetechnik A, S. Grohmann (ITTK, KIT)
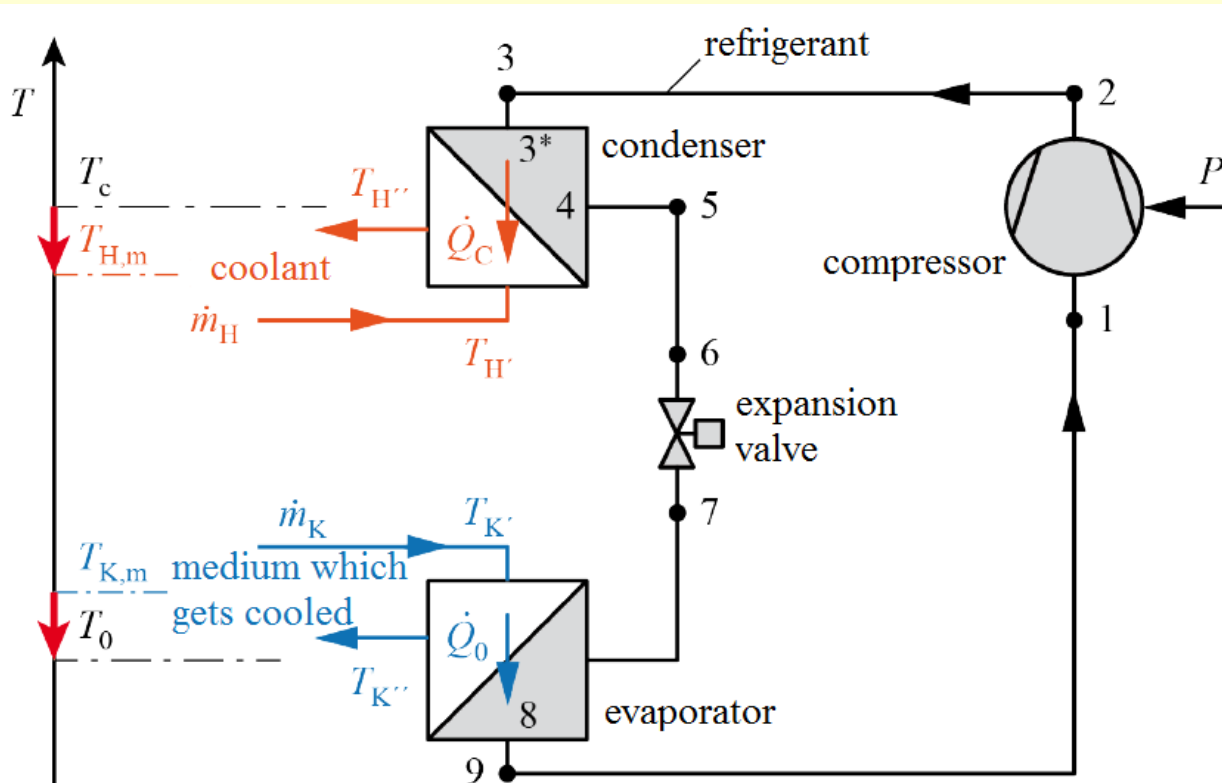
- Heat always flows from a warm region to a less warm region

- The most common cooling principle is decompression (throtteling)

Basic Cryogenics

Carnot efficiency
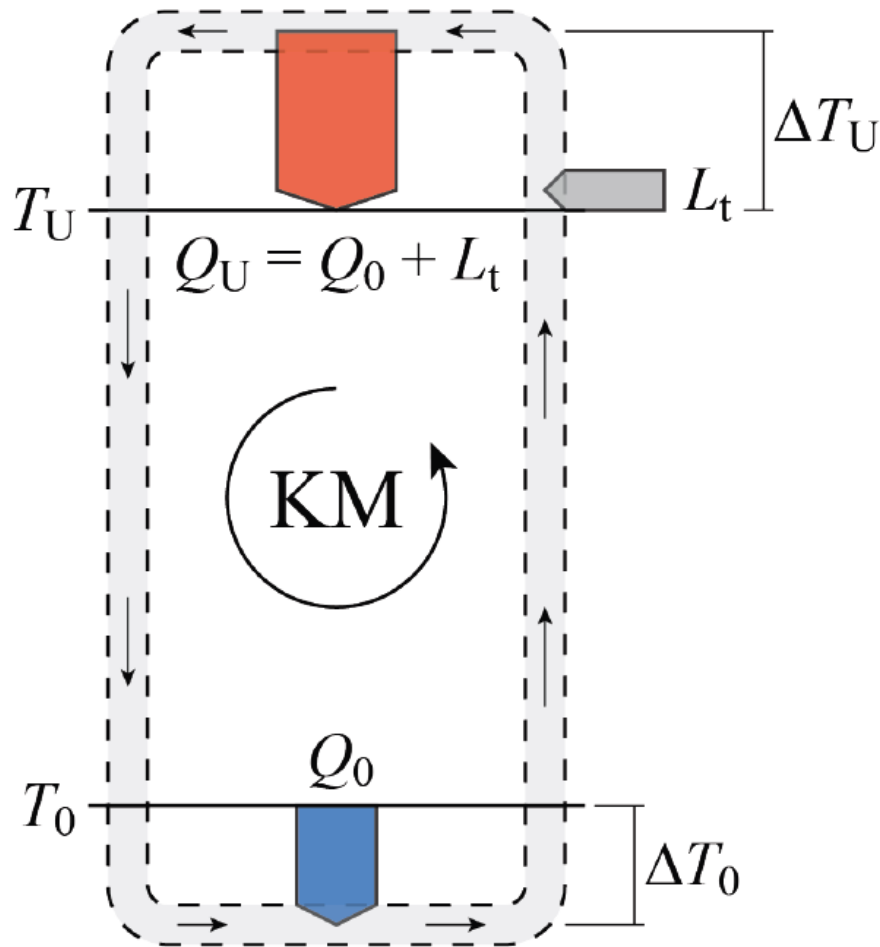
Schematic of cooling cycle, Kaeltetechnik A, S. Grohmann (ITTK, KIT)

- In the ideal case the ΔT's are zero.

- With the 1st law of thermodynamics the work of the compressor is given by

$$L_t = Q_U - Q_0 = Q_0(Q_U/Q_0 - 1)$$
$$= Q_0(T_U/T_0 - 1)$$

- The Carnot efficiency m_C for a refrigerator is defined as

$$\mu_C = Q_0/L_t = T_0/(T_U - T_0)$$

Basic Cryogenics

minimum energy for cooling and heating

$T_U = 20°C = 291.15K$

cooling | heating

cooling:
$$\frac{l_{min}}{q_0} = \frac{T_U}{T} - 1$$

heating:
$$\frac{l_{min}}{q_0} = 1 - \frac{T_U}{T}$$

minimum energy needed in J/J

temperature in K

JUAS 2020: SC RF - Caspers/Wendt/Bozzolan
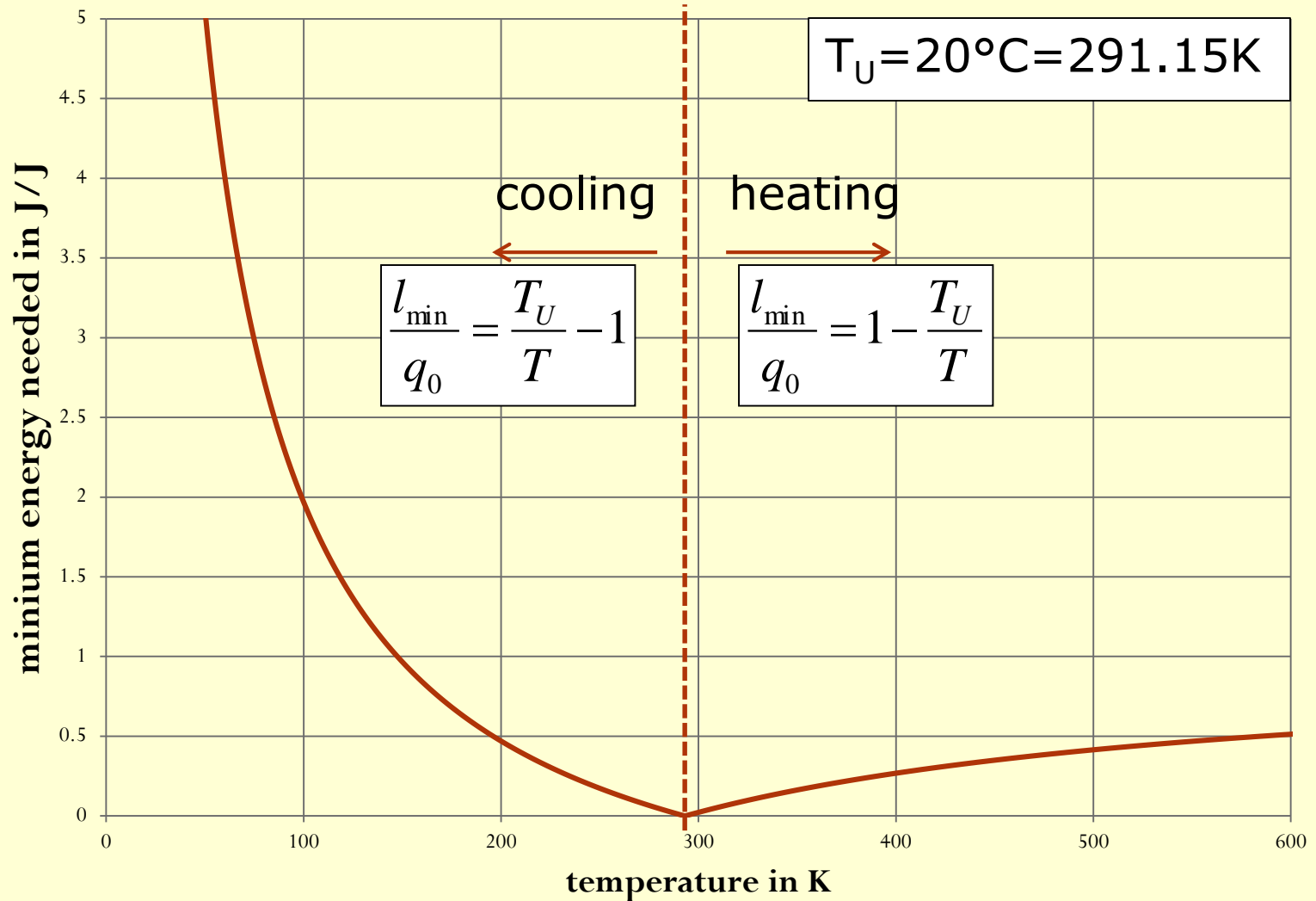
Basic Cryogenics cont.

pT-curve, Material properties
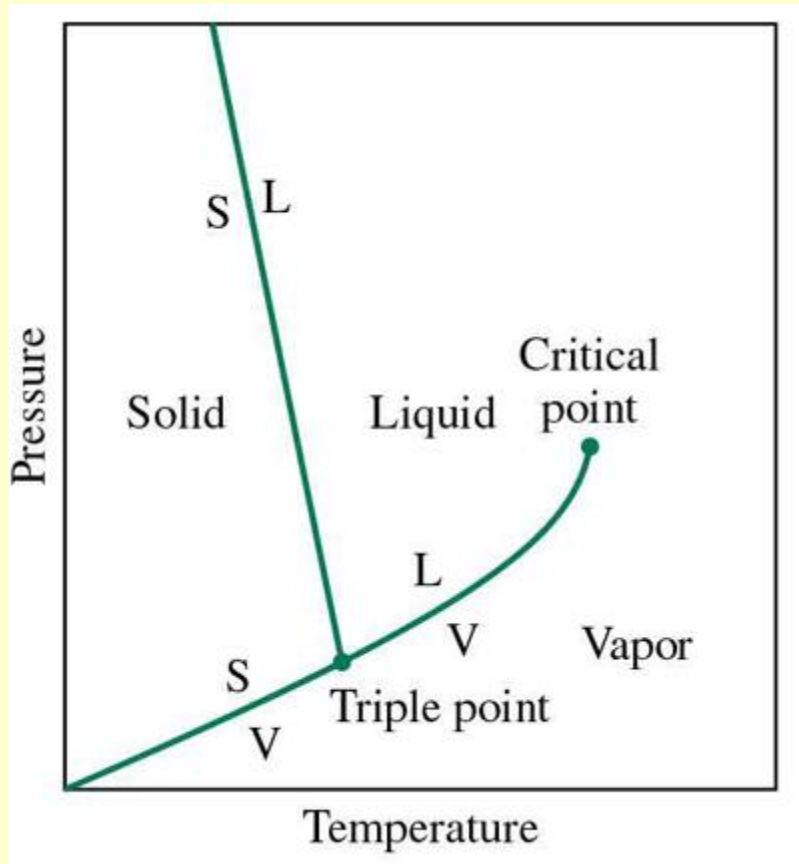
Schematic of a phase diagram,
http://moodle.zhaw.ch/mod/book/tool/print/index.php?id=63256
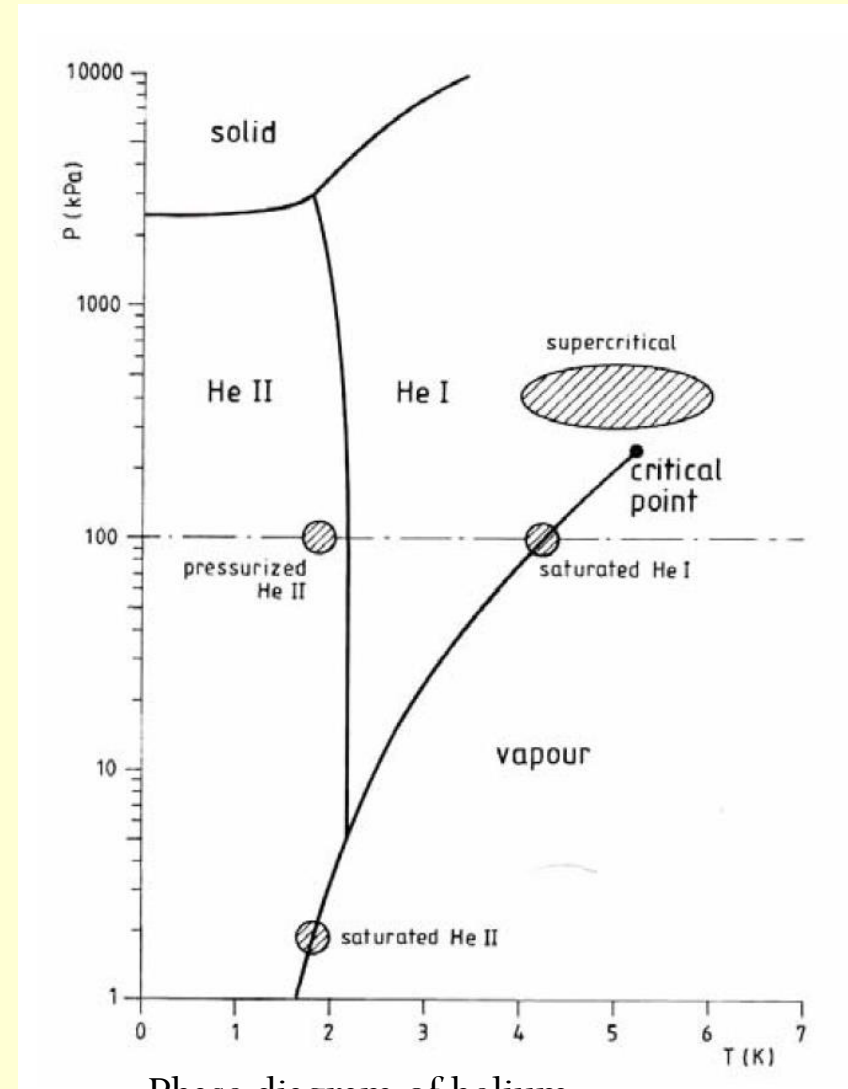
Phase diagram of helium,
CAS 2002, G. Vandoni

JUAS 2020: SC RF - Caspers/Wendt/Bozzolan

Basic Cryogenics cont.

He II and superfluidity

Schematic of fountain effect experiment

HEATER

PLUG

- One of the few macroscopic quantum phenomena
- Special effects
- Extremely low viscosity in thin channels
- Very high heat transport capability
- Can be described by two-fluid theory

Ratio of normal and superfluid densities of He II
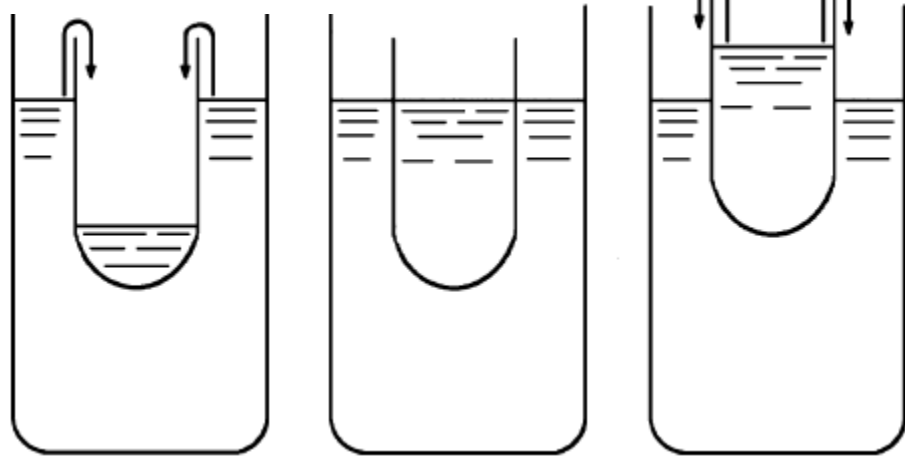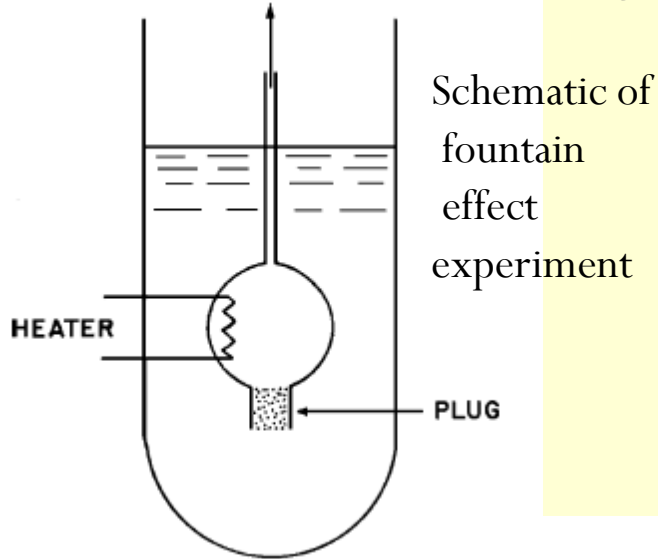
Schematic of film flow experiment

Thermal conductivity

Legend:
- He II
- He I
- He (G)
- N2 (L)
- H2 (L)
- Stainless Steel
- Al6063
- Diamond
- Water
- Copper
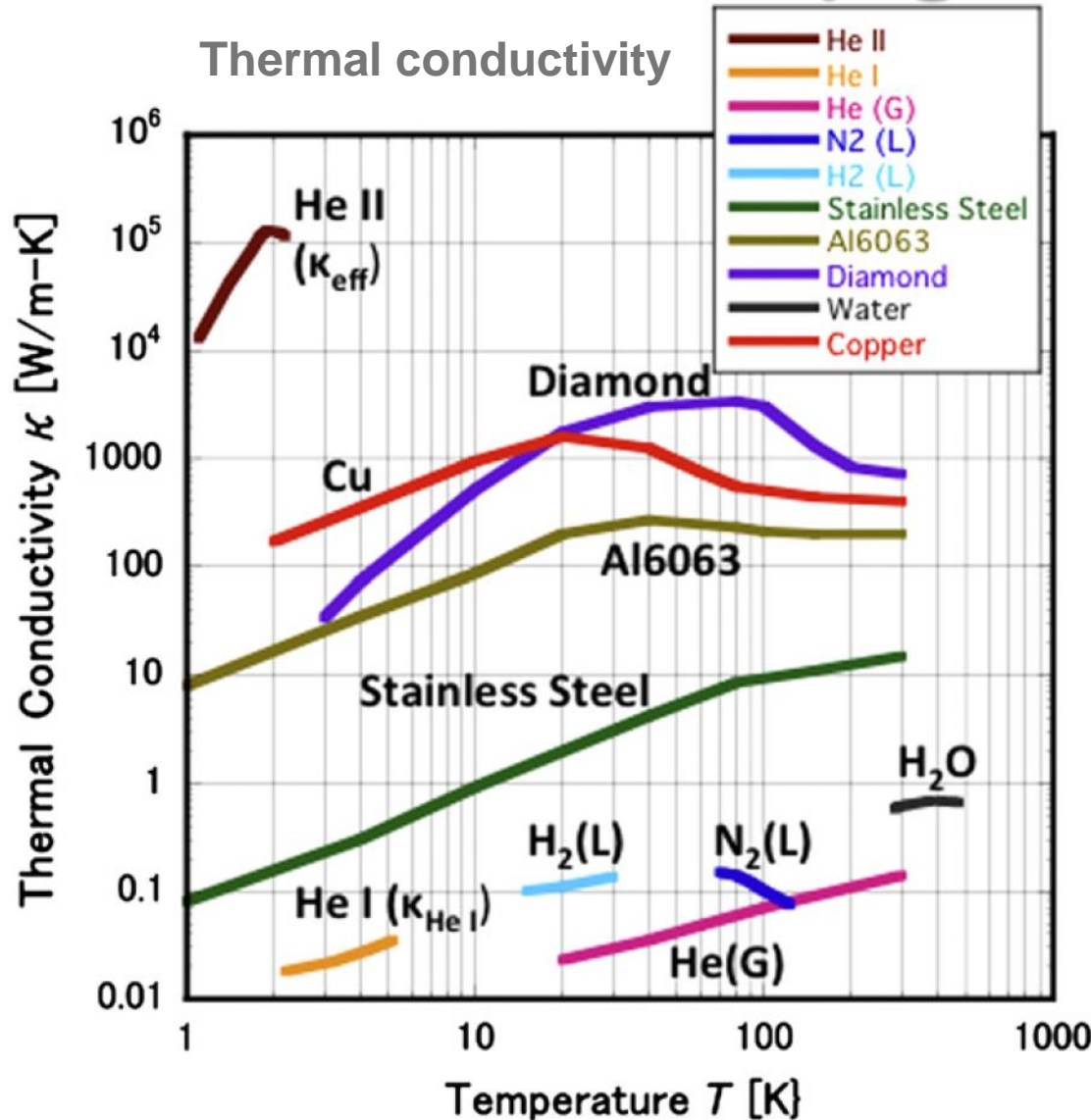
- The change in thermal conductivity in helium increases seven orders of magnitude at the lambda point

- At low temperatures many material properties can change very rapidly with temperature .

- e.g. heat capacity, electrical conductivity, vapour pressure

M. Murakami, Cryogenics, Volume 52, Issue 11, November 2012

SC vs. NC

For $T_1 = 300$ K and $T_2 = 4.2$ K, $\eta_c = 1/70$. The 'thermodynamic efficiency'

$$\eta_{td} = \dot{W}_c / \dot{W} \tag{4}$$

is the ratio of the power $\dot{W}_c$ needed to operate the compressor in the ideal case to the 'real' power $\dot{W}$. The total cryogenic efficiency is

$$\eta_{cr} = Q_2 / \dot{W} = \left(Q_2 / \dot{W}_c \right)\left(\dot{W}_c / \dot{W} \right) = \eta_c \eta_{td} \, . \tag{5}$$

With $\eta_{td} \approx 0.3$ for large units the total cryogenic efficiency is $\eta_{cr} = 4.5 \times 10^{-3}$. Unavoidably, in an sc accelerator some power P_{cr} flows into the liquid He, even in the absence of RF (standby heat load of cryostat). The efficiency η for a sc accelerator of RF-to-beam power conversion is then

$$\eta = \left[1 + \left(P_c + P_{cr} \right) / \left(P_b \eta_{cr} \right) \right]^{-1} \, . \tag{6}$$

As an example, for the sc cavity and cryostat for LEP with $P_c = 50$ W, $P_b = 50$ kW and $P_{cr} = 25$ W, we obtain a total efficiency of $\eta = 0.75$, which is larger by a factor of 5 than for a conventional RF system (Table 1).

Anomalous losses
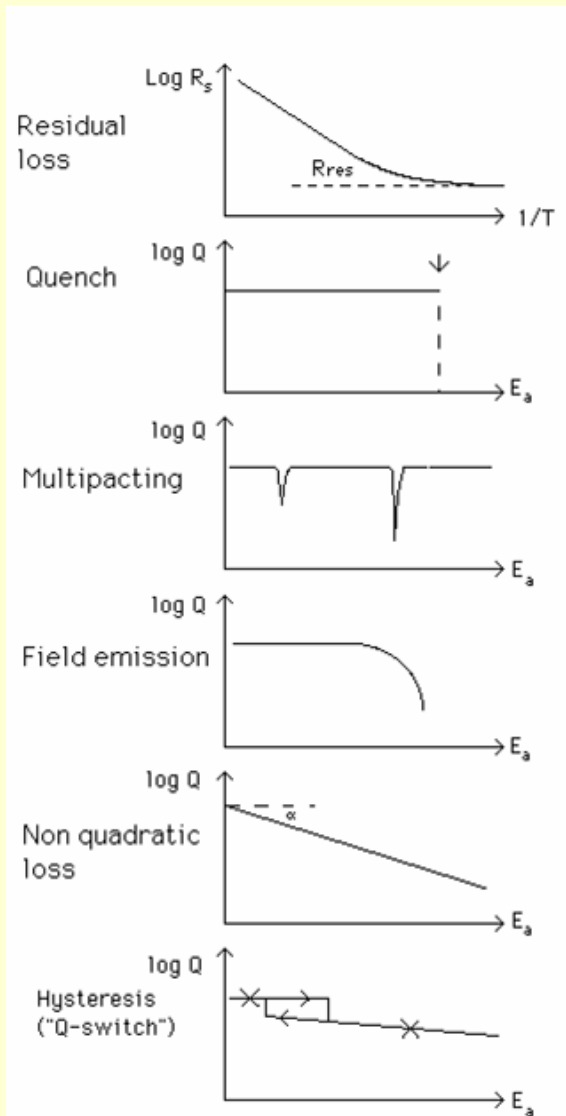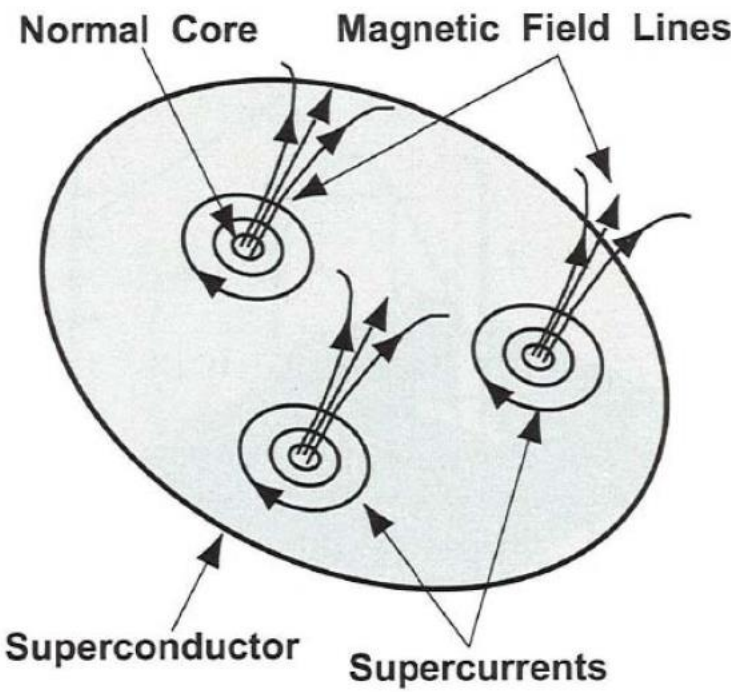
So-called « anomalous losses » account for all contributions to the RF losses that are not described by the intrinsic parameters of the superconducting material (critical temperature, critical field, BCS (or two fluid) surface resistance R_s, etc.).

These anomalous losses show up as heat and are visible in the R_s (T) and $Q_0(E_a)$ plots, as well as in the « temperature maps ».

JUAS 2020: SC RF - Caspers/Wendt/Bozzolan

Magnetic shielding

- Why do we need a magnetic shielding?

Normal Core   Magnetic Field Lines

$$R_{mag} = \frac{H_{ext}}{2H_{c2}} R_n$$

Superconductor   Supercurrents

$$R_{mag}[n\Omega] = 3H_{ext}[\mu T]\sqrt{f[GHz]}$$

Tobias.Junginger@quasar-group.org

JUAS 2020: SC RF - Caspers/Wendt/Bozzolan

Electron field emission 1/4
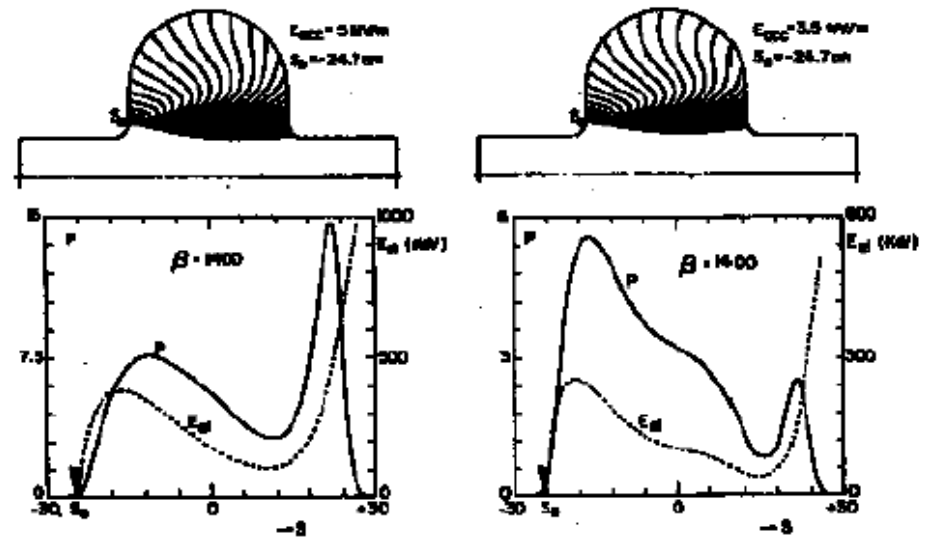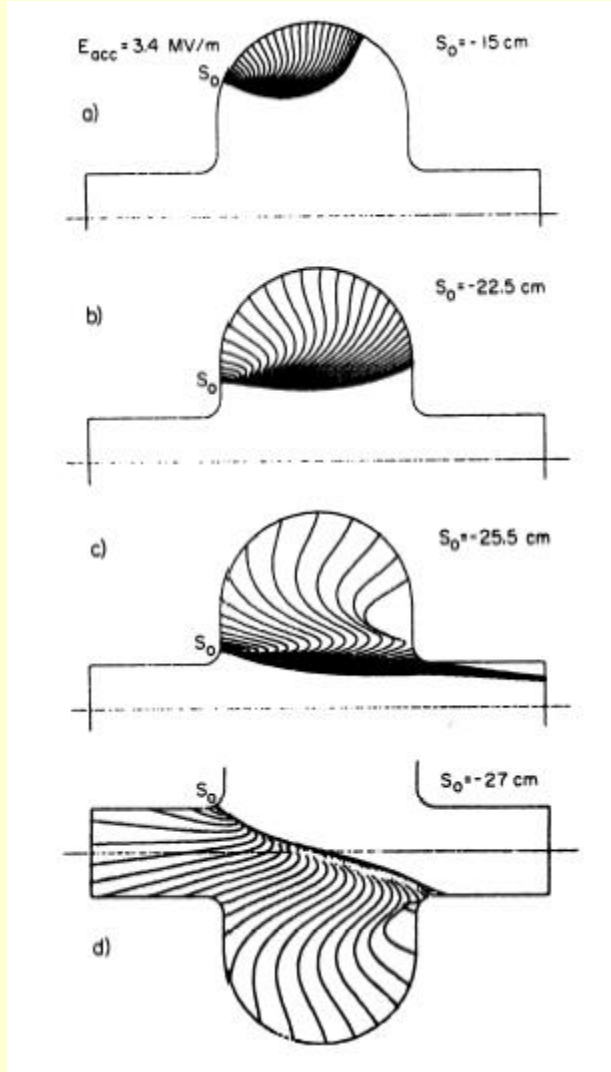
Impact energy and differential heat load

- Typical particulate emitters containing impurities
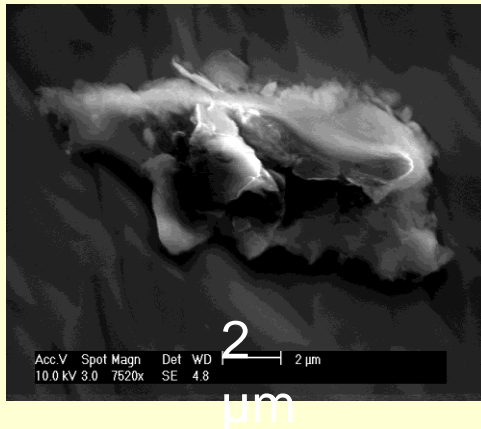
$E_{on}(2nA) = 140$ MV/m
$\beta = 31$, $S = 6.8 \cdot 10^{-6}$ µm²
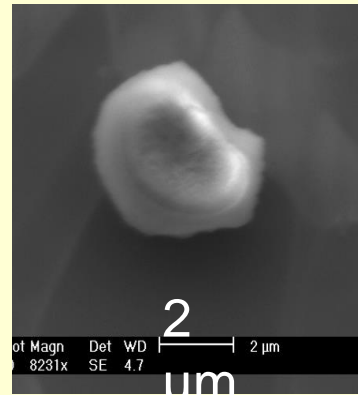
$E_{on}(2nA) = 132$ MV/m
$\beta = 27$, $S = 7 \cdot 10^{-5}$ µm²
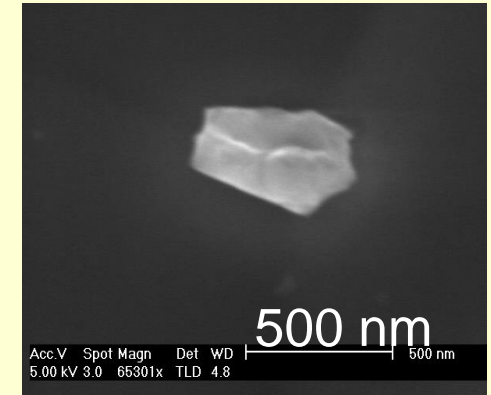
$E_{on}(2nA) > 120$ MV/m
$\beta = 46$, $S = 6 \cdot 10^{-7}$ µm²

Al Mg Nb

Al
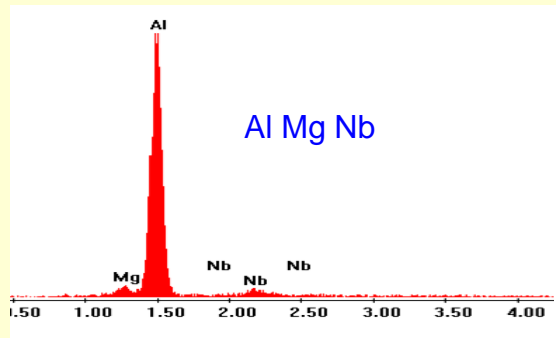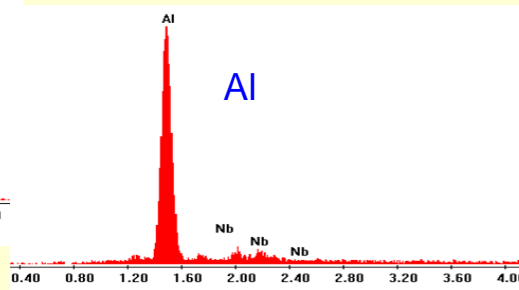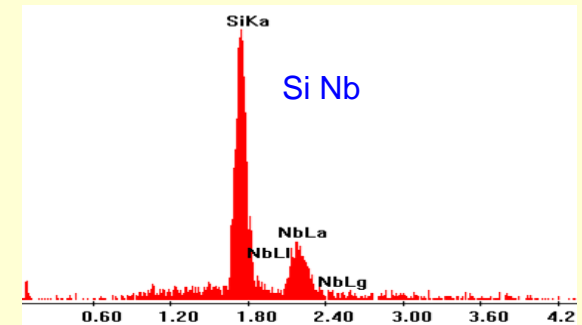
Si Nb

- Fowler Nordheim theory

Field emission of electrons from flat metal surfaces

Electron waves of bound states in a metal can tunnel through the potential barrier V(z) at the solid surface into vacuum by means of the quantum mechanical tunnelling effect
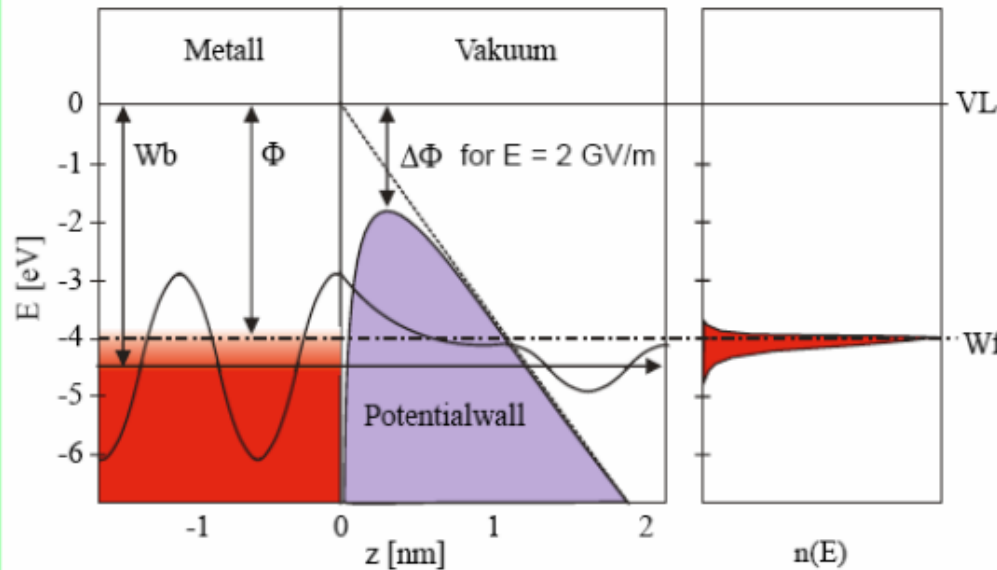
$V(z) = -e \cdot E \cdot z - e^2/(16\pi\varepsilon_0 \cdot z)$

work function Φ of metal

applied field E on surface

image charge correction

$\Delta\Phi = (e^3 E / 4\pi\varepsilon_0)^{1/2}$

Calculation of the current density j(E) within the Fowler-Nordheim theory results in

$$j(E) = \frac{AE^2}{\Phi t^2(y)} \exp\left(-\frac{B\Phi^{3/2} v(y)}{E}\right)$$

with constants A=154 and B=6830 and slight correction functions t(y) and v(y)

Φ=4eV at **E=2000 MV/m** $\Rightarrow$ **j= 1nA/μm²**

G. Müller, 15.11.2006   Bergische Universität Wuppertal   CARE06, Frascati

JUAS 2020: SC RF - Caspers/Wendt/Bozzolan

- Clean room preparation mandatory

JUAS 2020: SC RF - Caspers/Wendt/Bozzolan

Electropolishing: How it works

- The metal is immersed in an electrolyte and subjected to direct current. The metal part to be treated is made anodic and under certain conditions, a controlled dissolution of the metal is achieved.

JUAS 2020: SC RF - Caspers/Wendt/Bozzolan

from: L. Ferreira, B2FiftyTwo Seminar, Jan 2014
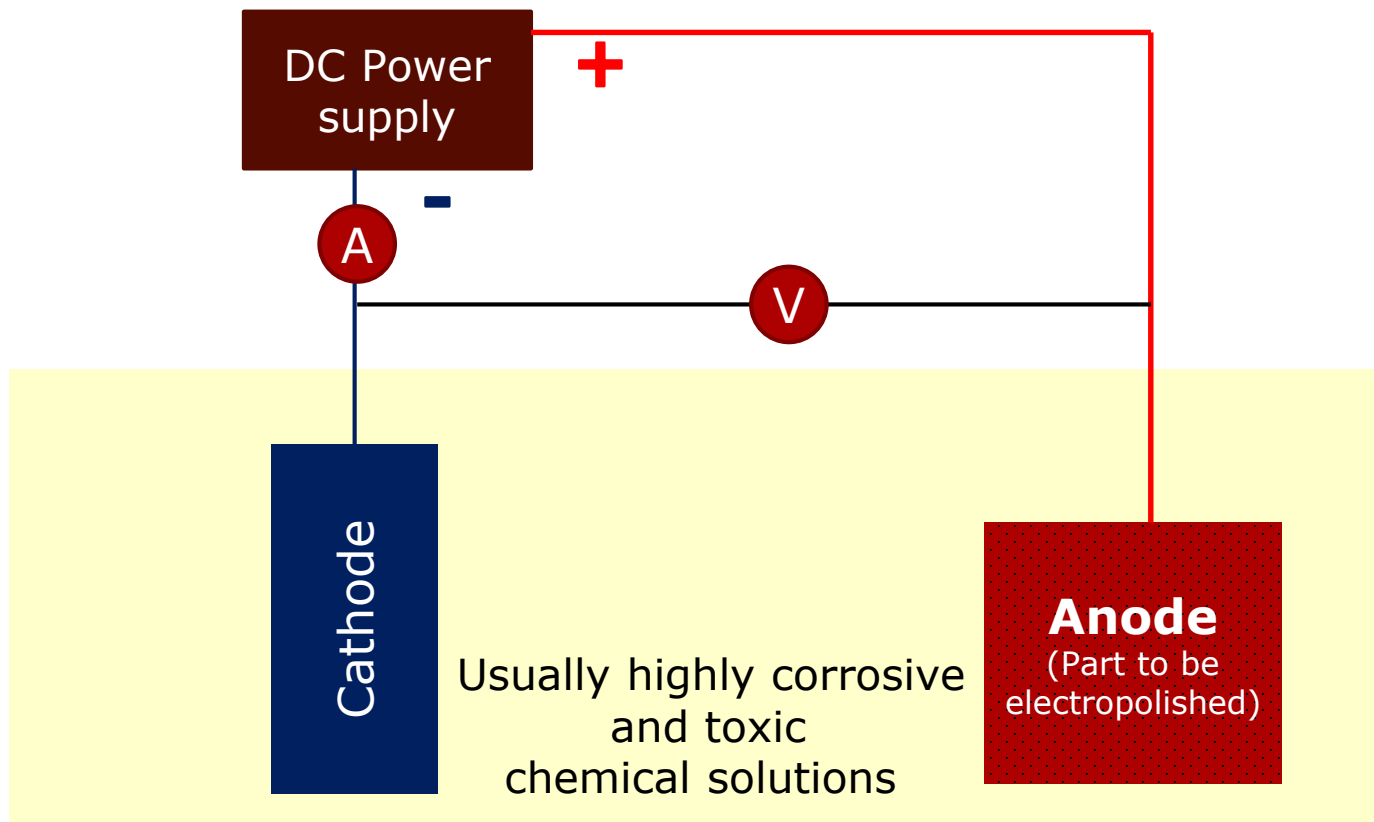
Electropolishing vs Mechanical based polishing

- Final roughness is function of initial surface finishing and removed thickness

hundreds μm

Mechanical polishing

Electropolishing
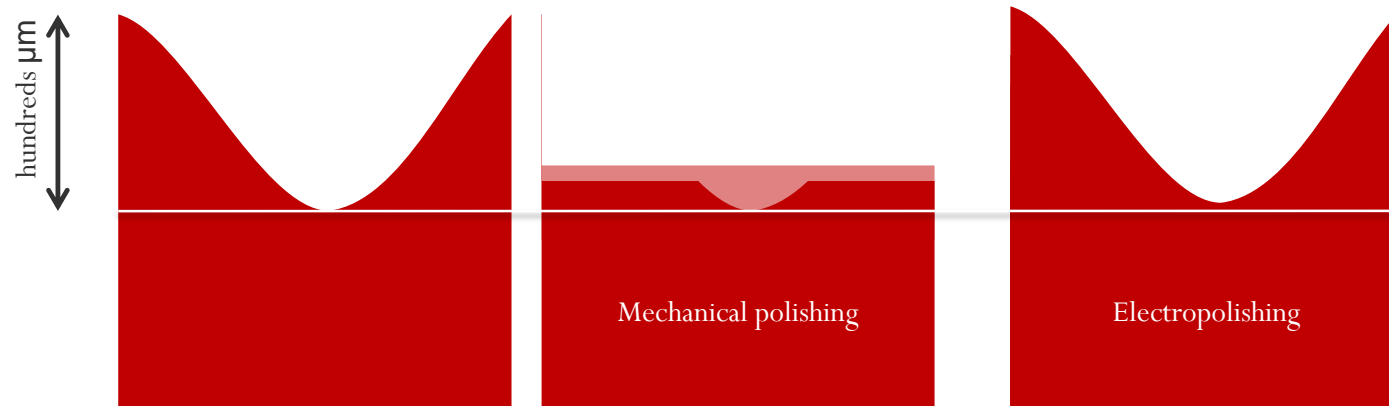
Disadvantages

- Usually highly corrosive and/or toxic solutions
  - Handling;
  - Process equipment;
  - Installation to process extracted fumes;
  - Installation to process waste water.

JUAS 2020: SC RF - Caspers/Wendt/Bozzolan

from: L. Ferreira, B2FiftyTwo Seminar, Jan 2014

Electron multipacting

Localized heating by multiple impact from electron current due to secondary emission in resonance with RF field.

Historically this phenomenon was a severe limitation for the performance of sc cavities.

The invention of the "circular" shape opened up the avenue for higher gradients.
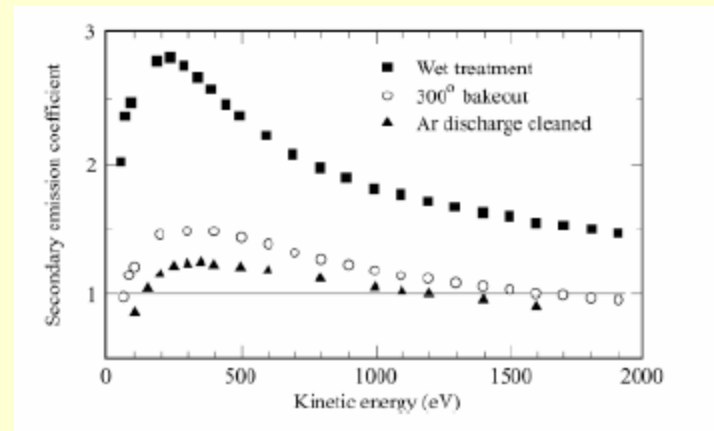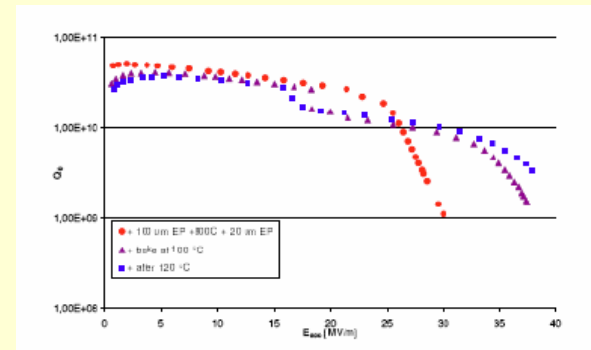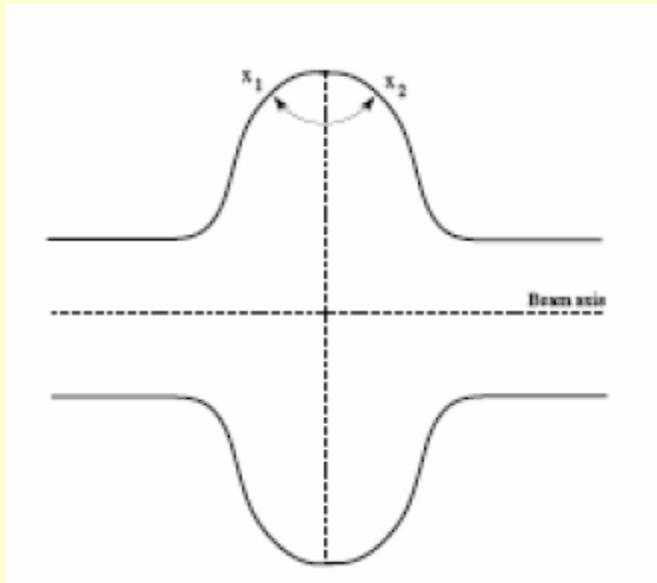
Field limitations – thermal breakdown

- Occurs at sub mm size defects with high resistance
- RF currents flow through the defects
- Defects heat up due to ohmic losses
- Area surrounding the defect is heated as well
- Thermal breakdown occurs if the surrounding area is heated above T_c

From H. Padamsee: CERN -2004 - 008

JUAS 2020: SC RF - Caspers/Wendt/Bozzolan
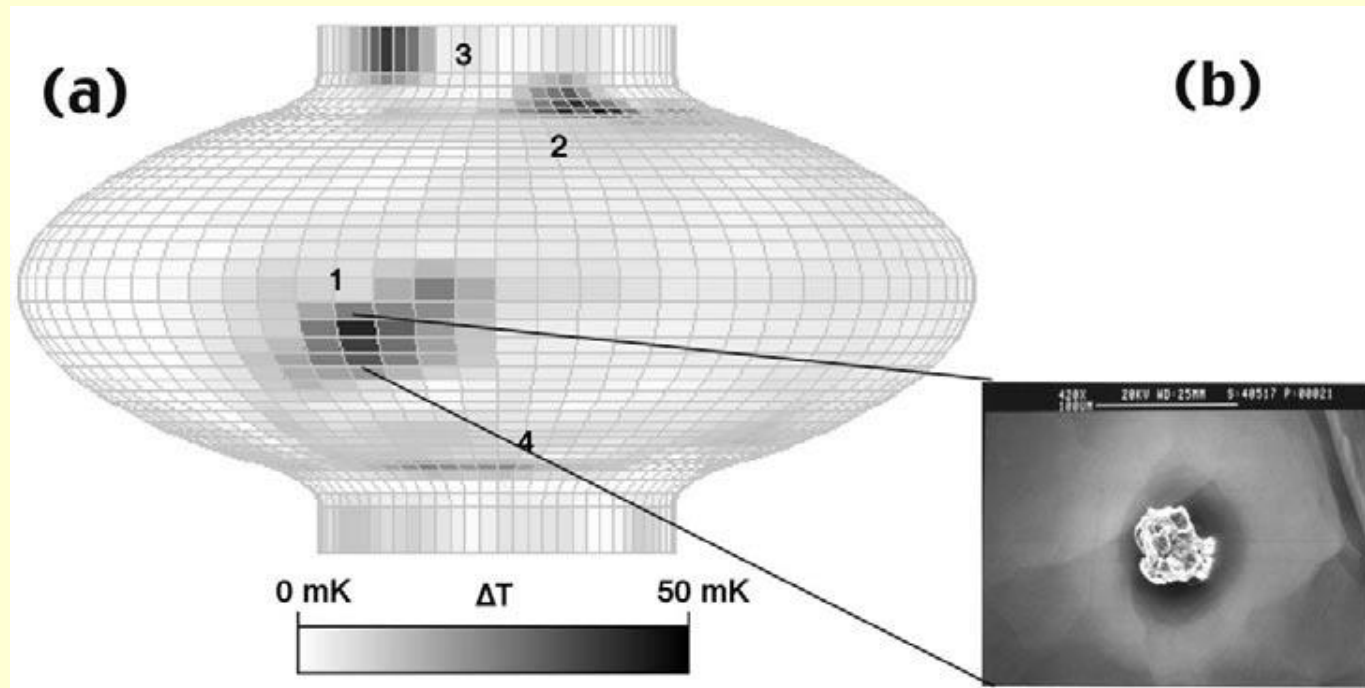
Heat removal

- Thermal Improvement of thermal conductivity for Niobium sheets
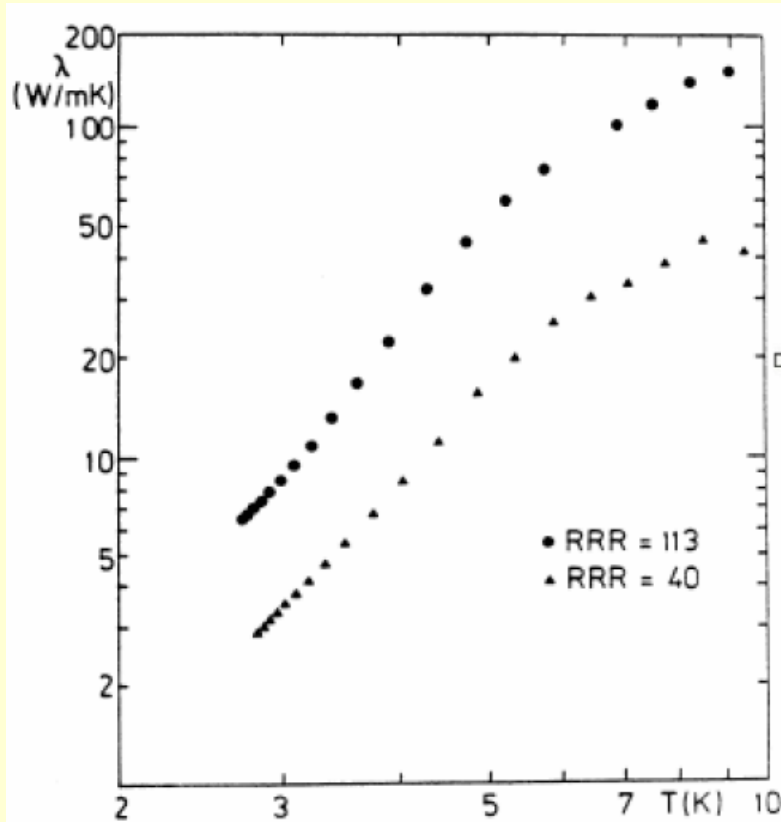
Fig. 1: Thermal conductivity of reactor grade niobium (RRR=40) and niobium of higher purity (RRR=113)

Cause for "quench":
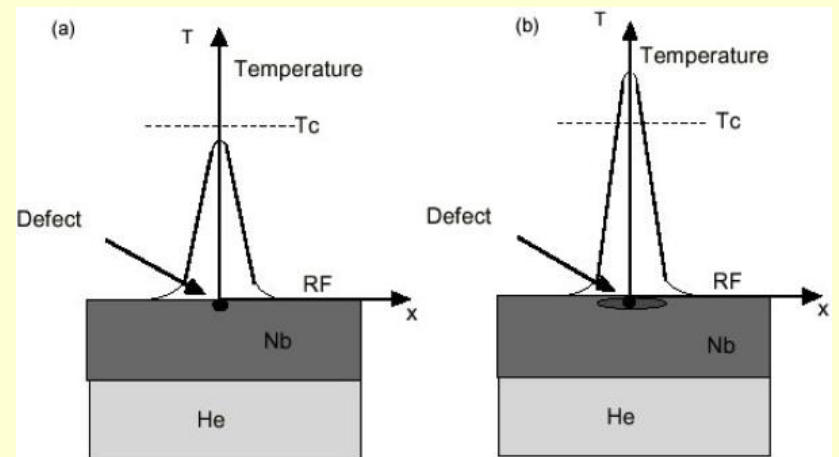
$$H_{max} \approx \sqrt{(4(T_c - T_B)\lambda/(R_n\, r))} .$$

RRR…. residual resistance ratio

Thin film Nb coating

- Coating a copper cavity with a thin Nb film
- Important role of high thermal conductivity substrate (Nb/Cu cavity)

JUAS 2020: SC RF - Caspers/Wendt/Bozzolan
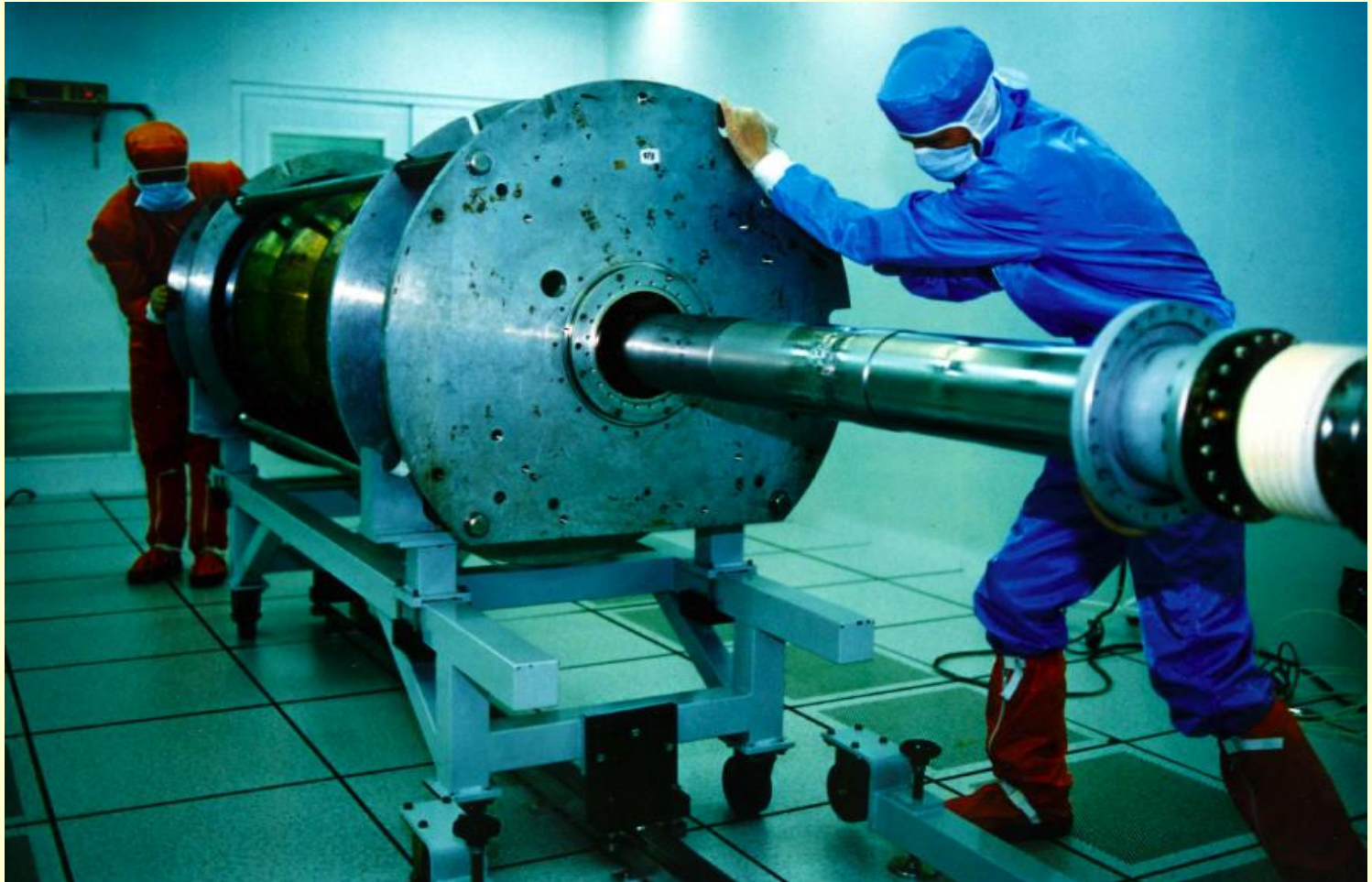
Improvement of quality assurance efforts: ORNL/JLAB results

Nevertheless, in spite of all technological efforts, performance of sc cavities is often stochastic

high β
$E_a = 18.2 \pm 2.6$ MV/m

low β
$E_a = 17.1 \pm 1.9$ MV/m
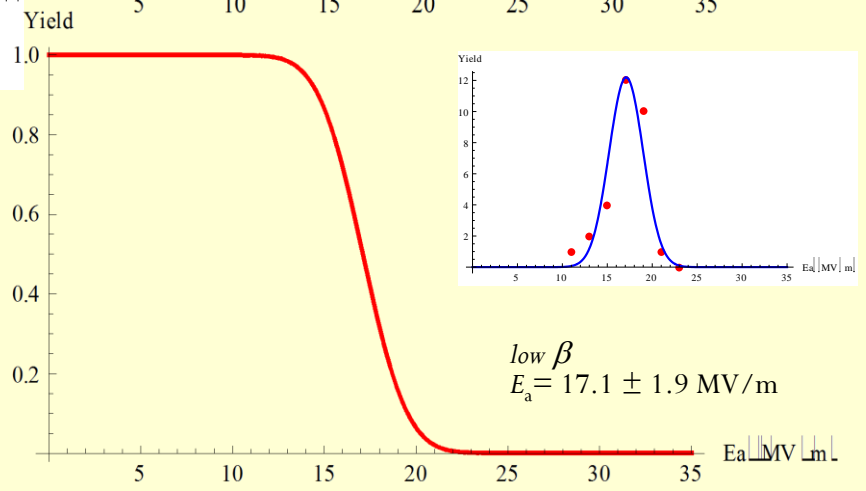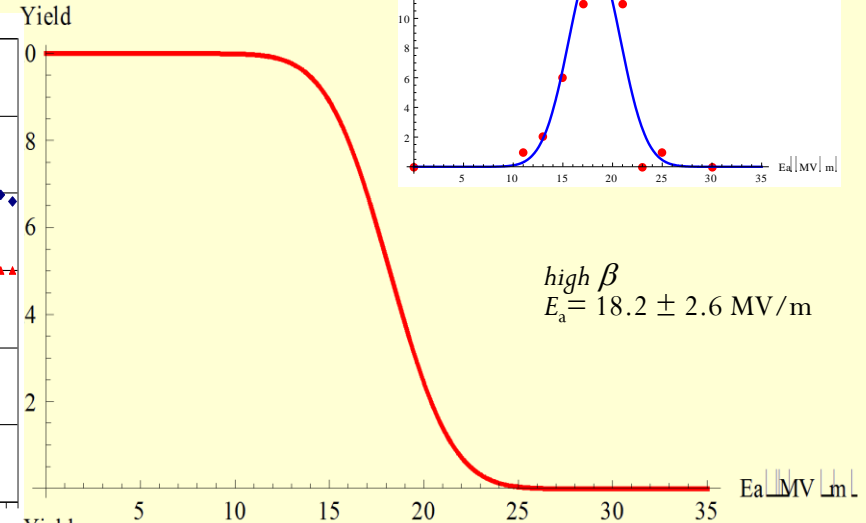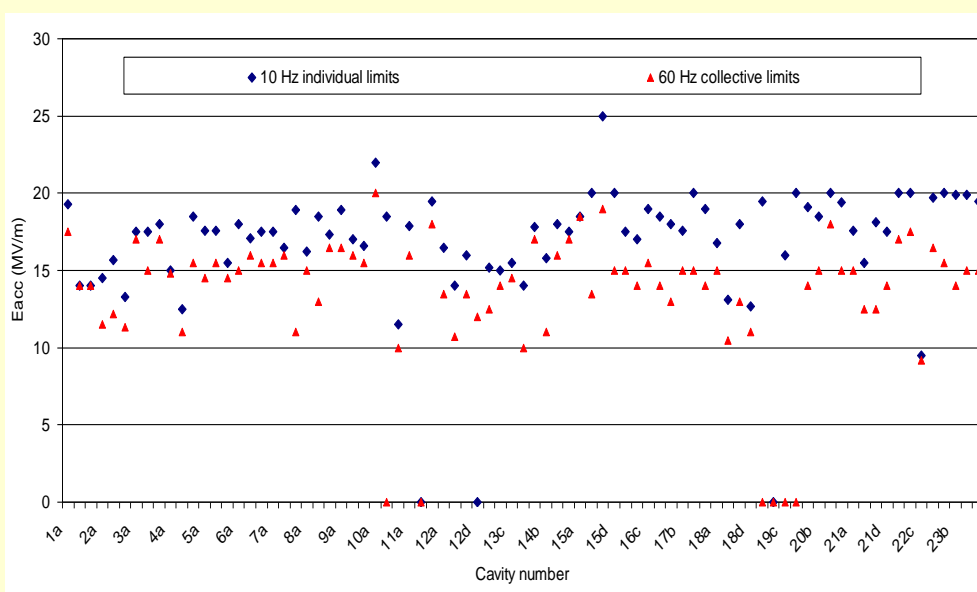
Source: I. E. Campisi and S.–H. Kim, **SNS Superconducting Linac operating experience and issues**,

Accelerator Physics and Technology Workshop for Project X, November 12-13, 2007

http://projectx.fnal.gov/Workshop/Breakouts/HighEnergyLinac/agenda.html

Stochastic parameters

Influencing quantity	Impact quantity	Physical explanation	Cure
Field emission sites (foreign particles sticking to the surface, size, density)	Q – value / acc. gradient γ radiation HOM coupler quench	Modified Fowler-Nordheim-theory	Electro-polishing Assembling in dust-free air Rinsing with ultrapure water (control of resistivity and particulate content of outlet water) and alcohol High pressure ultrapure water rinsing (ditto) "He- processing" Heat treatment @ $800 - 1400\,°C$
Secondary emission coefficient δ	Electron-multipacting	Theory of secondary electron emission	Rounded shape of cavity Rinsing with ultrapure water Bake-out RF - Processing
Unknown	Q – slope / Q-drop (Q – value / acc. gradient)	*Unknown*	Annealing $150\,°C$ Electro-polishing
Metallic normal-conducting inclusions in Nb	Acc. gradient	Local heating up till critical temperature of Nb	Inspection of Nb sheets (eddy current or SQUID scanning) Removal of defects ($\approx 1\,\mu m$) Sufficiently large thermal conductivity (30 - 40 [W/(mK)])
Residual surface resistance	Q – value / acc. gradient	*Unknown to large extent*	Quality assurance control of a multitude of parameters

JUAS 2020: SC RF - Caspers/Wendt/Bozzolan

PROCESS	WHY	COMMENTS
Forming		
EB Welding	Clean welding	Nb = getter material. If RRR/ 10 @ welding => Q_0/10
Ti purification	RRR enhancement	RRR 300-400 now commercially available
Chemical etching 100-200 μm **BCP EP**	Remove contamination and damage layer	Limitation : BCP ~ 30MV/m; EP => >40 mV/m but lack of reproducibility
Annealing 800°C, 2h (or 600°C, 10h)	Get rid of hydrogen	Source of H: wet processes H segregates near surface in form of hydrides (= bad SC)
Chemical etching 5-20 μm	Remove diffusion layer (O, C, N)	Diffusion layer < ~1μm in bulk, a little higher at Grain Boundaries
Specific rinsing	e.g. remove S particles due to EP	Under evaluation HF, H_2O_2, ethanol, degreasing,…
High pressure rinsing (HPR)	Get rid of dust particles	Not always enough (recontamination during assembly)
Assembling	Ancillaries : antennas, couplers , vacuum ports…	**In clean room, but recontamination still possible**
Baking, 120°C, 48h	Decrease high field losses (Q-drop)	Unknown mechanism, first 10 nm of the surface in concern.
Post processing	Get rid of "re-contamination" ?	Under evaluation: dry ice cleaning, plasma
Test RF	Cavity's performance	First naked cavity in vertical cryostat, then dressed in horizontal cryostat/ accelerating facility
He processing, HPP	Decrease field emission	RF power with/ without He to destroy field emitters (dust particles) NB field emission : principal practical problem in accelerators

JUAS 2020: SC RF - Caspers/Wendt/Bozzolan

Frascati, (Practical) Limitations & possible solutions ,CAS 2013

Improvement of cavity performance

Lilje & Schmueser
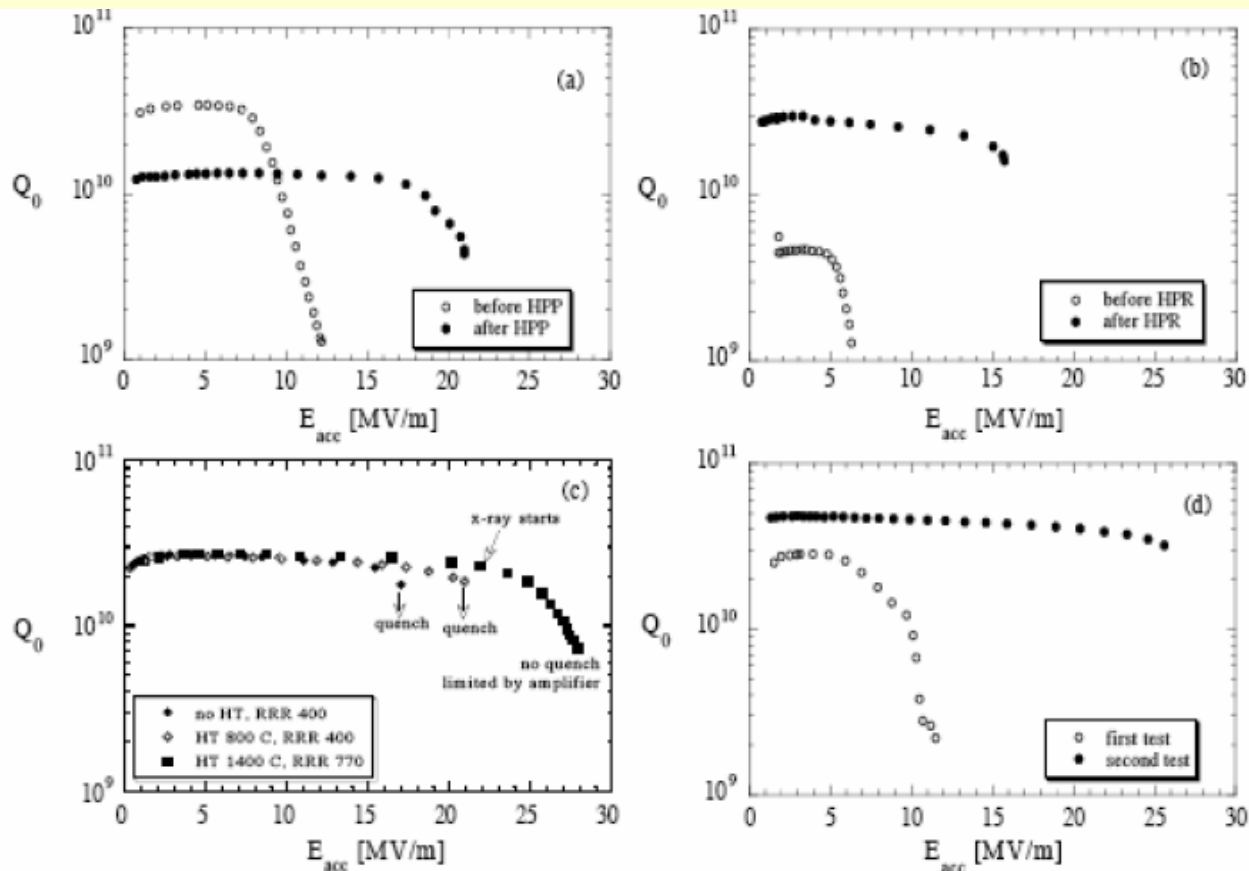
Figure 27: Improvement in cavity performance due to various treatments: (a) high power processing, (b) high pressure water rinsing, (c) successive application of 800°C and 1400°C heat treatment, (d) removal of surface defects or titanium in grain boundaries by additional BCP. All tests were done at 1.8 K [Aune et al. 2000].

Summary and learning targets

- The choice of the technology (normal conducting vs. superconducting) depends on a variety of parameters: mass of accelerated particle, beam energy, beam current, mains power consumption, etc.

- If superconducting, the typical interval of RF frequencies is between 300 MHz and 3 GHz.

- The technically most suitable superconducting material being niobium, choosing lower frequencies allows operation at $4.2 - 4.5$ K, the boiling temperature of lHe, higher frequencies request operation at $1.8 - 2$ K. However, the cryogenic installation is much more demanding.

- The production of sc cavities requests careful application of quality control measures during the whole cycle of assembly in order to avoid the degradation of performance by « anomalous losses ».

- The « anomalous losses » contribute to an extra heat load, which is expensive to cool and which may limit the performance.

JUAS 2020: SC RF - Caspers/Wendt/Bozzolan

Diagnostics

- Many features of the cavity can be tested by RF-measurements.

- But losses, which occur in the form of localized heat can only be detected by additional diagnostics.

- The classical approach is temperature mapping.

JUAS 2020: SC RF - Caspers/Wendt/Bozzolan

- Temperature mapping equipment (~ 1980)

JUAS 2020: SC RF - Caspers/Wendt/Bozzolan
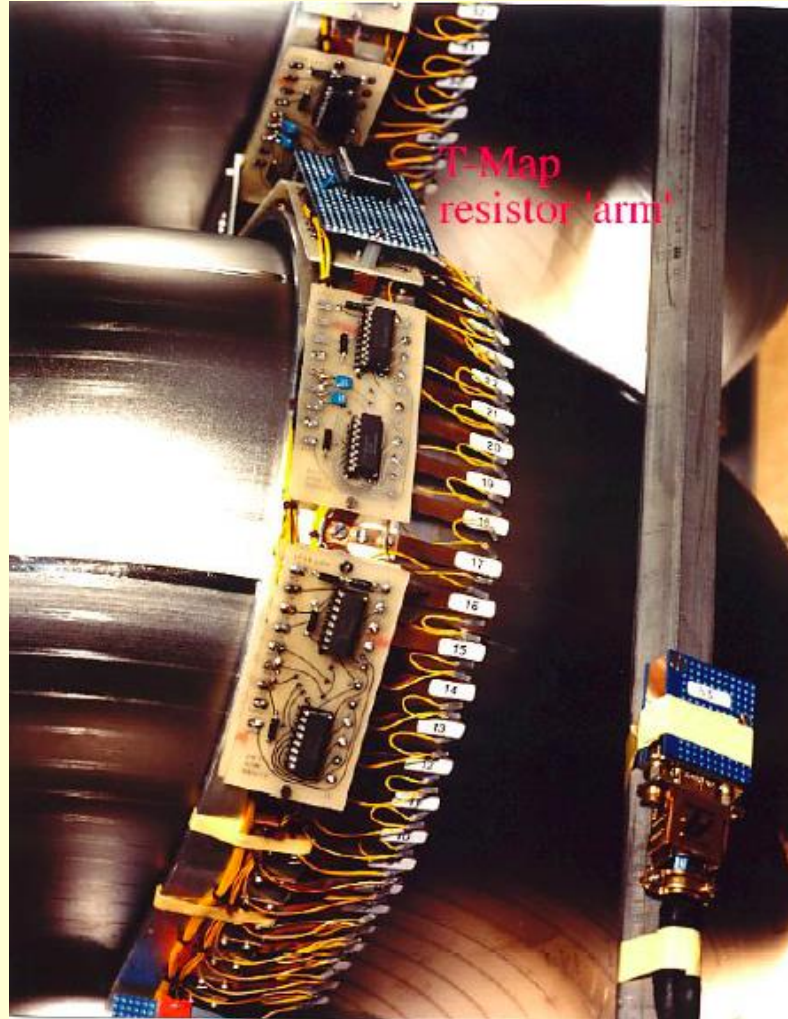
- Temperature mapping results (today)
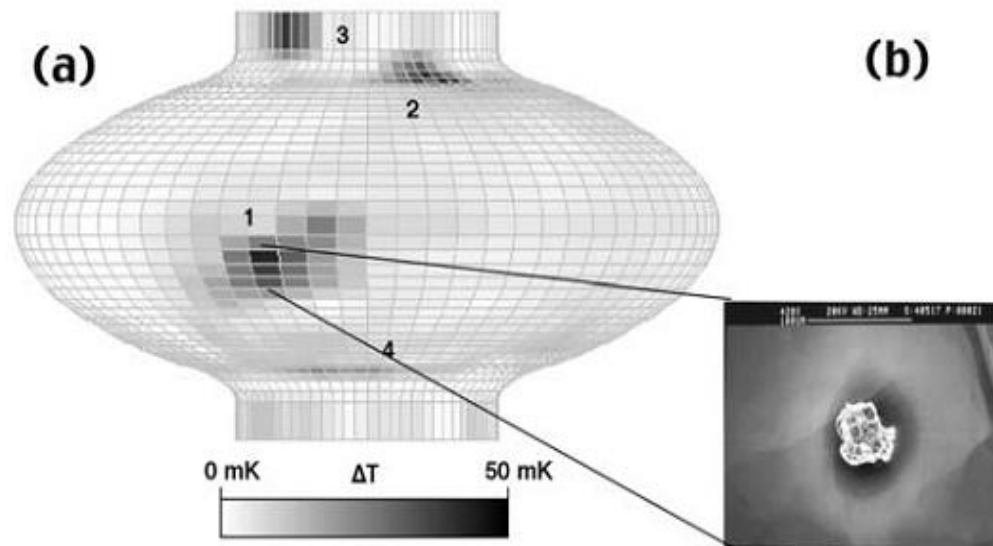
Fig. 16 (Left) Temperature map at 400 Oe of a 1.5 GHz, single cell cavity showing heating at a defect site, labelled #1 and field emission sites labelled #2, 3, and 4. (b) SEM micrograph of the RF surface taken at site #1 showing a copper particle [5].

From H. Padamsee: CERN -2004 - 008

- T-mapping for the diagnosis of anomalous losses
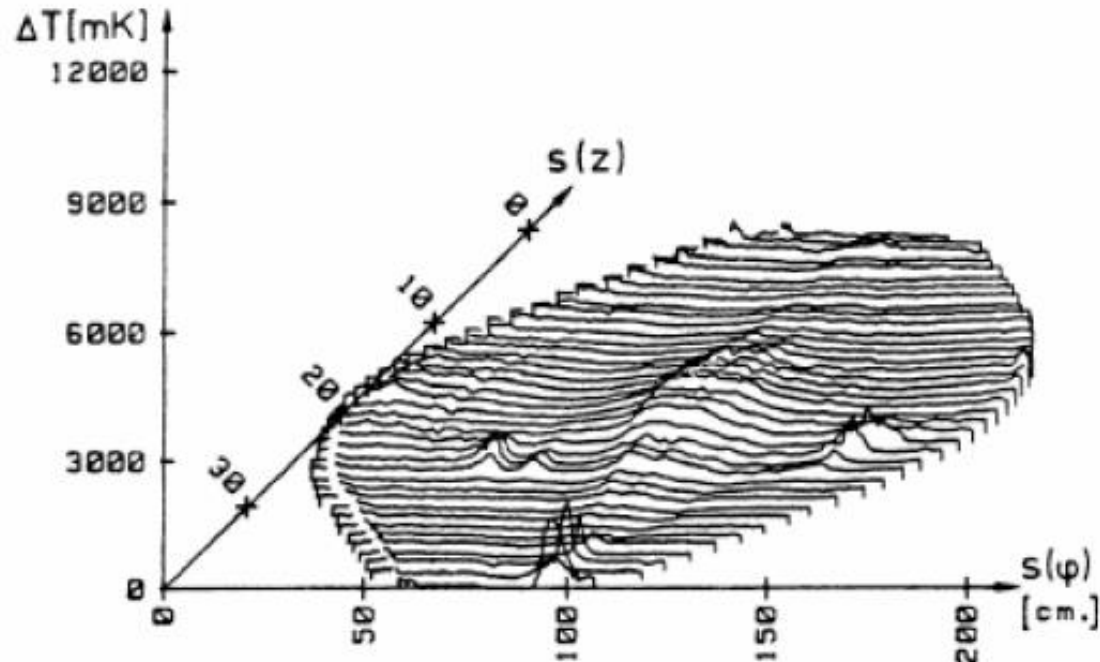
Fig. 4: Temperature map of a 500 MHz cavity at E_{acc} = 12.5 MV/m. The temperature increase ΔT of the outer cavity surface is plotted against the surface coordinates s(z) and s(ϕ)(z=length in arbitrary units along a meridian, ϕ = azimuthal location)

- T-mapping for electron field emission diagnosis

JUAS 2020: SC RF - Caspers/Wendt/Bozzolan
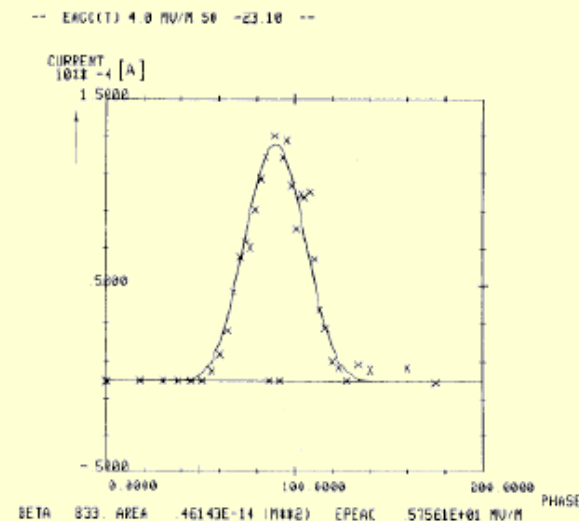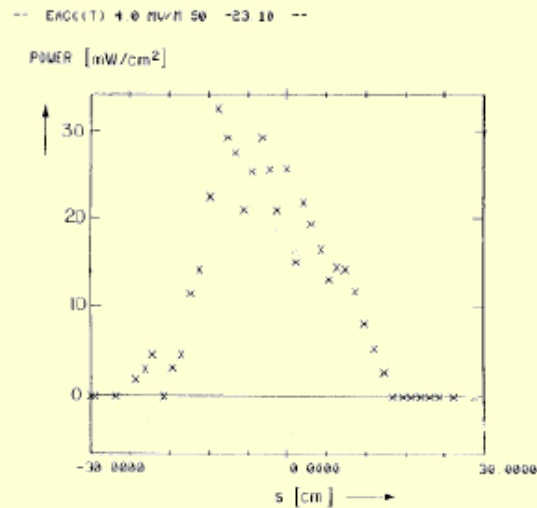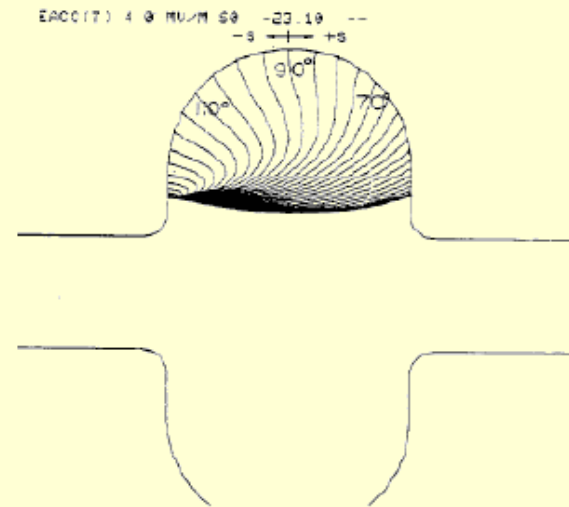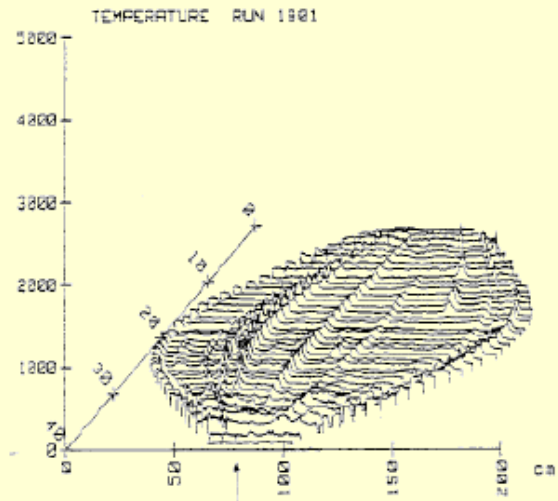
- Second sound in superfluid helium

First used by K. Shepard at Argonne NL for detecting the quench location in split ring resonator

OST oscillating superleak transducer

gold

normal fluid

glue

superfluid

120V
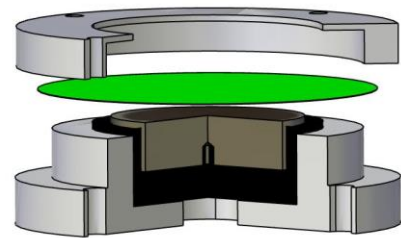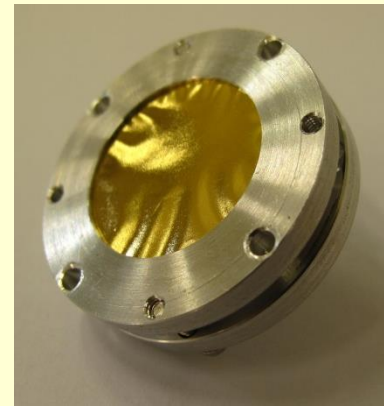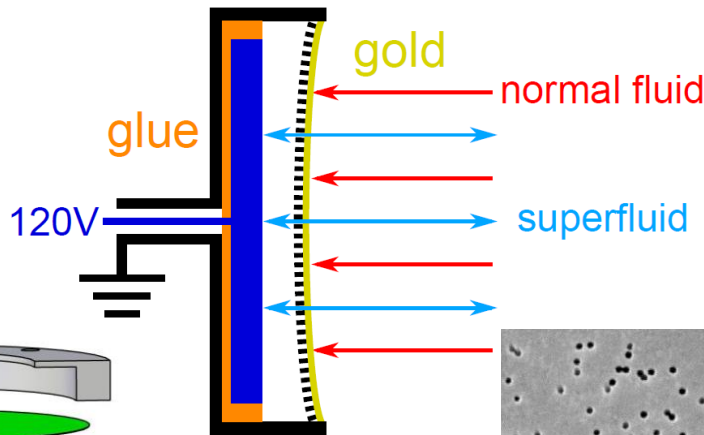
Hannes Vennekate

Mohammed Fouaidy

1µm | EHT = 20.00 kV   SPL   WD = 10 mm
Detector = SE1   Au coated membrane   Date :21 Feb 2011
Mag = 5.00 K X   Shiny side   Maud Scheubel EN/MME-MM
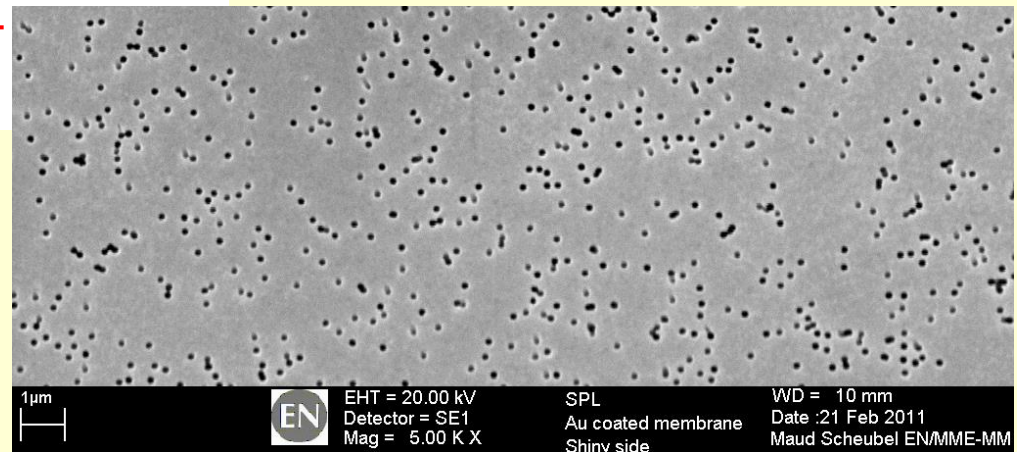
Diagnostics

- Detection and localisation of quenches on superconducting RF cavities by the measurement of the second sound with OSTs

- The localisation of a quench can be done with a relatively small number of sensors

OST 1

OST 2

JUAS 2020: SC RF - Caspers/Wendt/Bozzolan
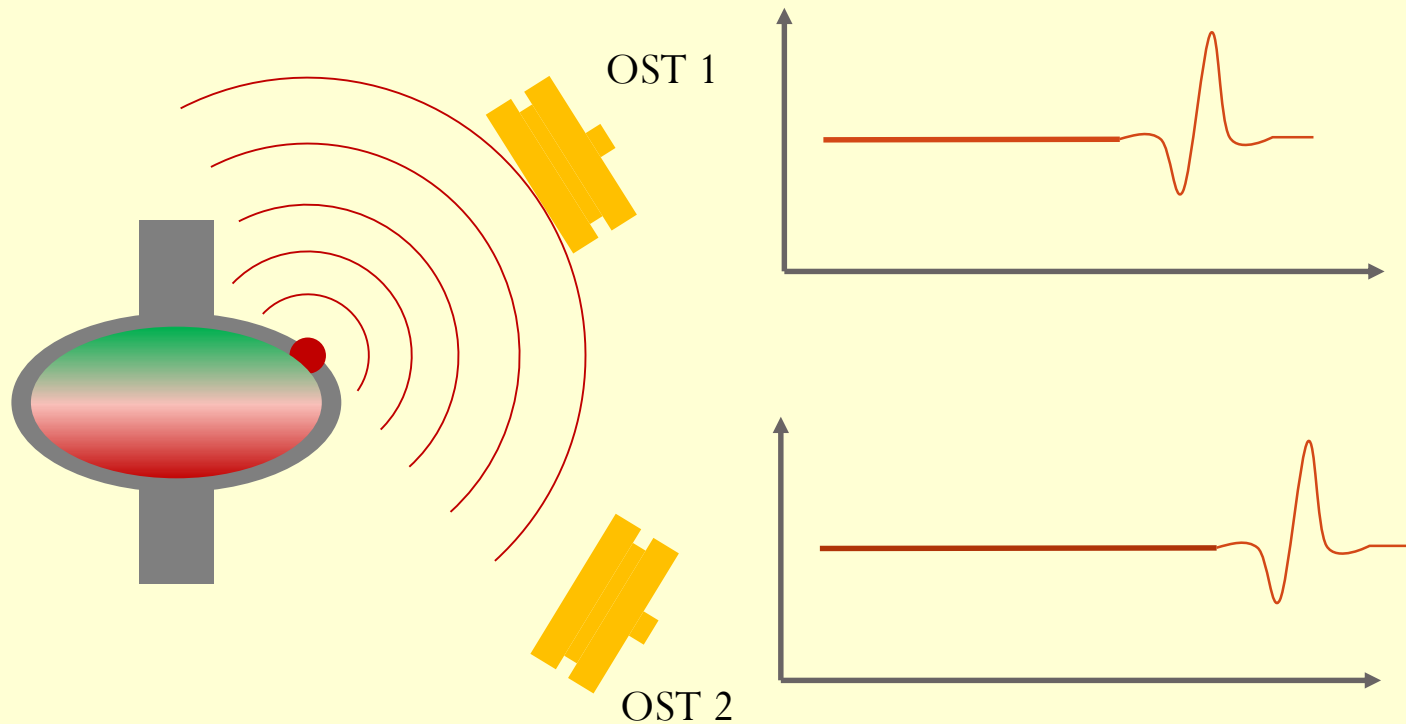
OST signal
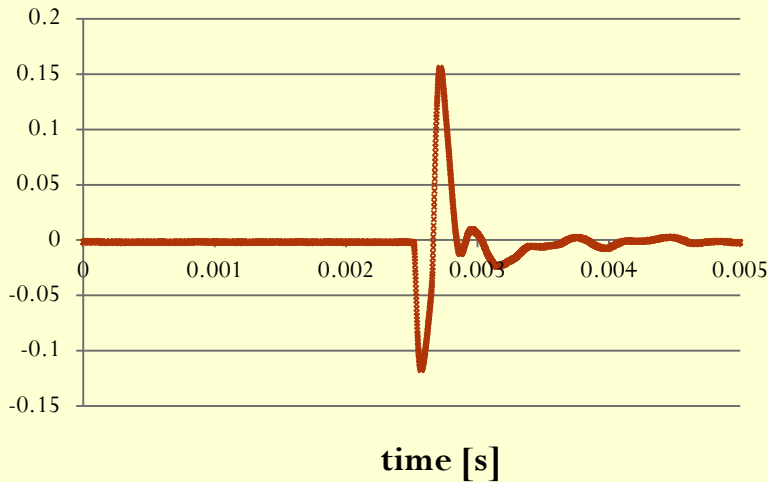
Speed of second sound in helium

Green line: values from Hepak (helium property programm)
Red line: temperature from measurement
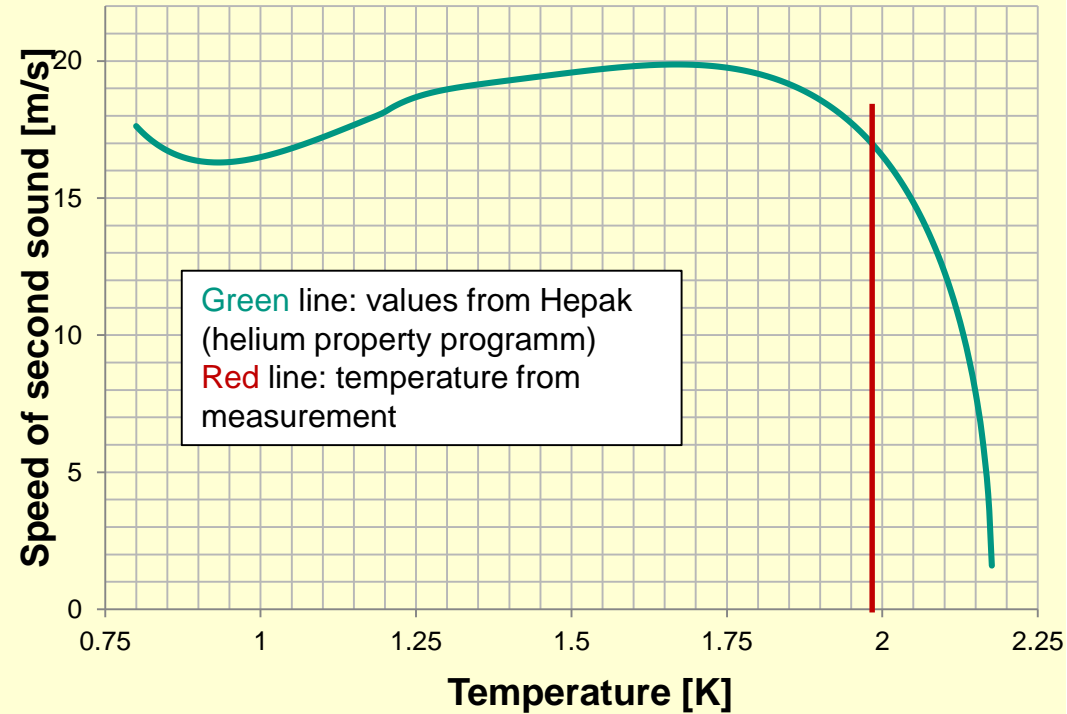
- This measurement was done at 1.977 K
- $v_2(1.977\ K) = 17.14\ m/s$
- Signal of the measurement at t=2.52 ms
- Distance to heater $v_2t = 4.32$ cm

135

State of the art SRF research

- Reaching ultimate performance with bulk Nb cavities
  - Maximizing the quality factor Q_0
  - Reaching high accelerating gradients E_{acc}

- Beyond Niobium: New materials
  - High temperature superconductors
  - Low temperature superconductors: Nb based materials

JUAS 2020: SC RF - Caspers/Wendt/Bozzolan

High Q versus high E_{acc}

- High Q is crucial for cw applications (e.g. light sources)
  - moderate E_{acc} (12 – 20 MV/m)
  - Cryogenics is cost driver
  - High Q reduces cryogenic load

    $(P_{diss} \sim {E^2 acc}/{Q})$
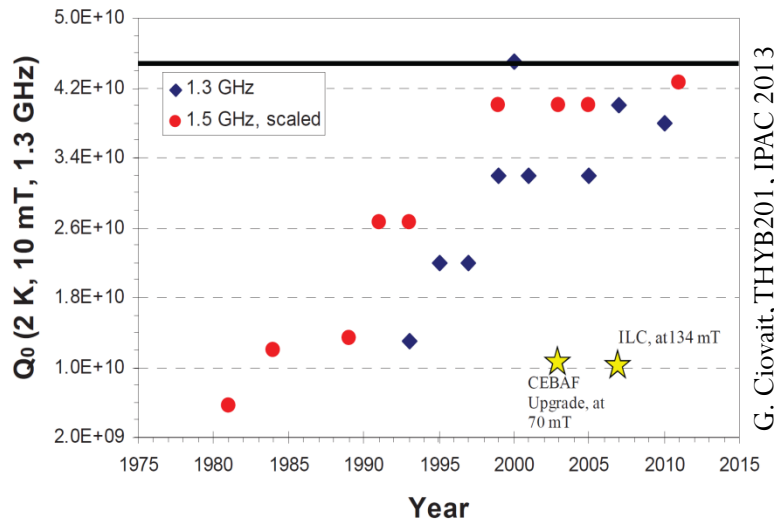
- High E_{acc} is crucial for pulsed applications (e.g. particle physics)
  - Machine size is cost driver.

JUAS 2020: SC RF - Caspers/Wendt/Bozzolan
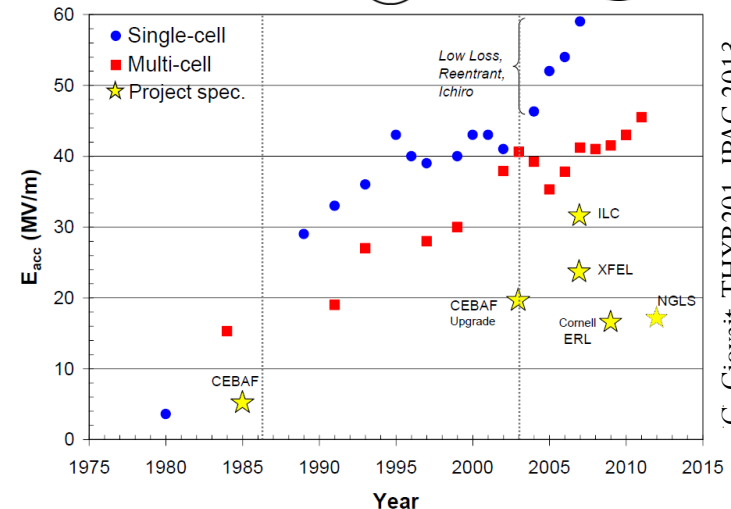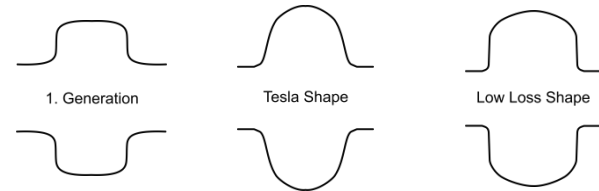
Maximizing Q: Ideal and Reality

- In the ideal case: Is Q constant up to the theoretical limit?

- Recent theoretical calculations yield increasing Q for increasing rf field.[See B.P. Xiao et al., Physica C 490 (2013)]

JUAS 2020: SC RF - Caspers/Wendt/Bozzolan
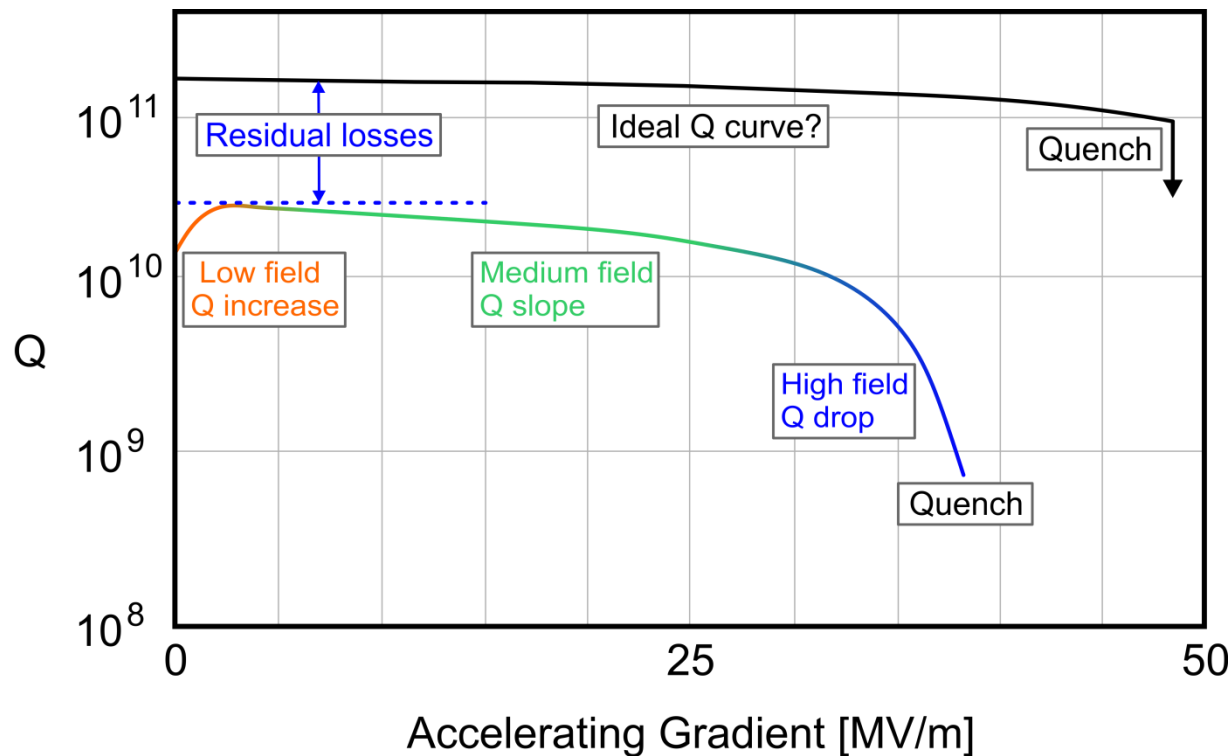
Maximizing Q: Improving treatments

- Baking at 800°C with injection of N_2 degrades cavity performance.

- After the removal of several μm by EP, the performance increases and exceeds baseline.

- Q slope reverses to "anti Q slope".

- Comparison with Argon suggest interstitial effect instead of NbN formation.
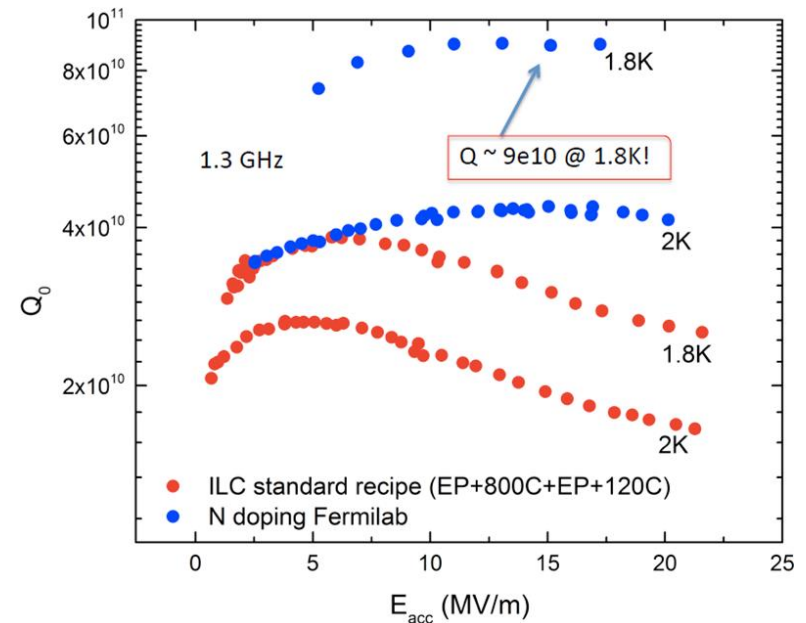
A. Grassellino, TUIIOA3, SRF 2013

- Experimental data in good agreement with B.P. Xiao's field dependent model.

Maximizing Q: Improving cooling procedures

- Cooling speed through T_c and spatial temperature gradients impact the residual resistance.

- Measurements of the ambient field suggest that changes in flux trapping and the creation of thermal currents cause changes in R_{res}.
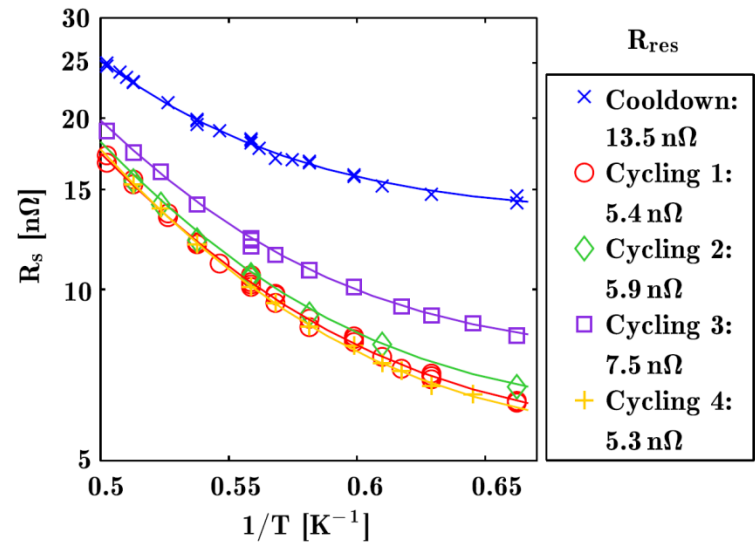
Vogt et al, PRST-AB 16.102002 (2013)

Achieving maximal gradients

- World record $E_{acc} = 59$ MV/m ($Q = 4 \cdot 10^9$)
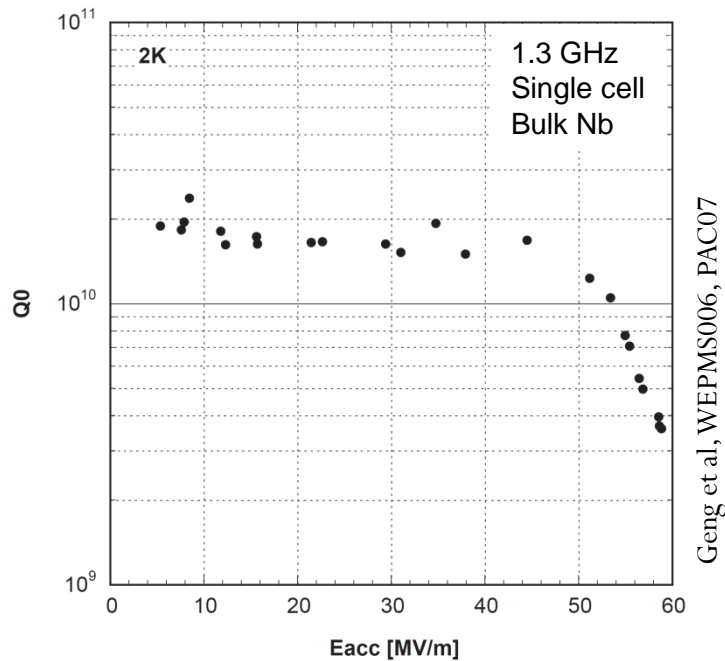
- High performing cavities are limited by field emission or quench

- Avoiding emission sites by
  - Centrifugal barrel polishing: grinds larger defects
  - Improved Electro-polishing: smoothens surface on sub-μm scale
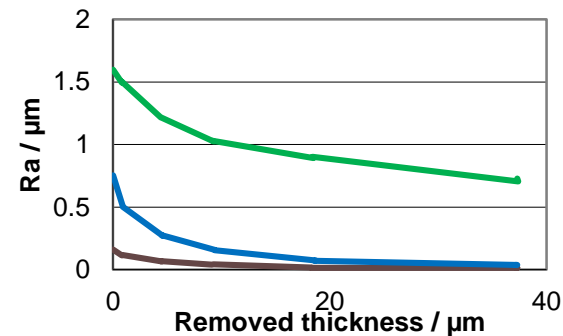 - Cleaner handling: avoid (re-) contamination

Surface Preparation

- Centrifugal barrel polishing:
  - Mechanical removal and smoothening of the surface with abrasive "stones".
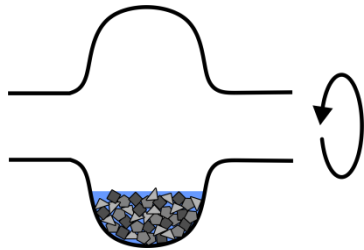
P. Michelato, SRF Tutorials, 2013

  - Produces a new damage layer that need to be etched.

- Electro-Polishing:
  - *Best* surface finish for cavities
 - Final roughness depends on initial surface finish

from: L. Ferreira, B2FiftyTwo Seminar Jan 2014

- Clean handling:
  - Any preparation of the surface and the final assembly needs to be done in a clean room (ISO 4).
  - Re-contamination has to be avoided.

JUAS 2020: SC RF - Caspers/Wendt/Bozzolan

Materials beyond Nb: Potential Benefits

- Higher Q due to lower BCS surface resistance:
  - Reduces cryogenic dynamic losses (operation costs)
  - Allows operation at higher temperature (reduces cryogenic static losses)
- Higher accelerating gradients:
  - Reduces installation costs due to more compact accelerators
- Reduced materials costs
  - Inexpensive materials, well formable, high thermal conductivity
- Simplified fabrication and assembly
  - Separating cavity shape from rf surface (Coatings)
  - More flexibility in design of cryomodules

Zoo of Superconductors

JUAS 2020: SC RF - Caspers/Wendt/Bozzolan
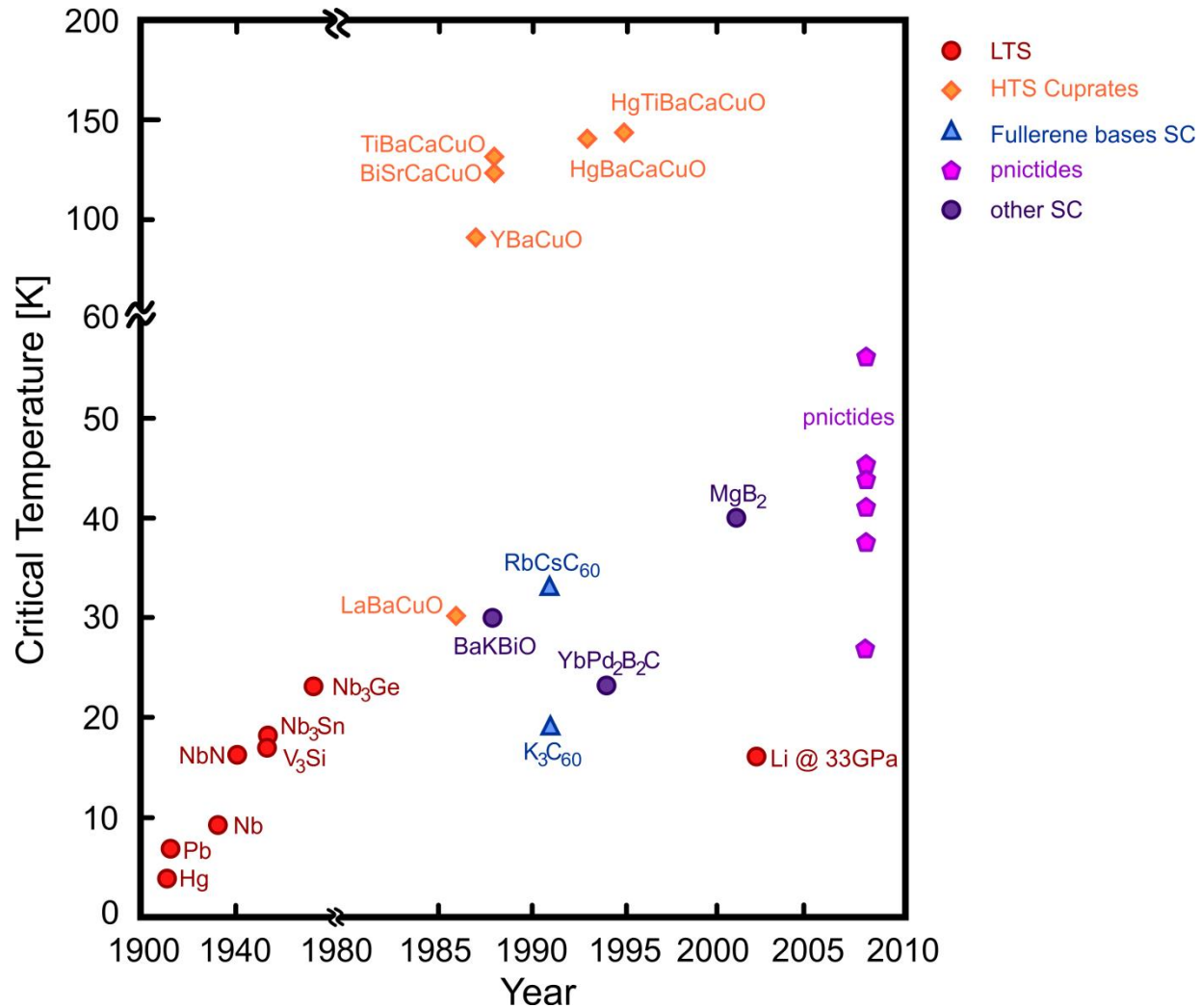
Materials beyond Niobium: Requirements

- High critical temperature T_c: $R_{BCS} \propto e^{(-\Delta/kT)}$; $T_c \propto \Delta$

- Small penetration depth λ: $R_{BCS} \propto \lambda^3$

- High critical field H_c: Operation at high gradient

- High thermal conductivity: prevent quenches

- Compound phase should be stable over a broad composition range

- Compound phase needs to be stable from $2 - 300$ K

- Material should be inert and formable

Classes of superconductors

|	Nb	Low Temp. SC	MgB$_2$	YBCO
T$_c$ [K]	9.2	10 - 20	39	> 90
λ [nm]	40	60-180	140	150-1000
H$_c$ [mT]	200	200-600	430	1400
κ	0.8	20-130	40	100
remarks			2 sc gaps	Ceramic, anisotropic

- High temperature superconductors are not suitable for srf applications

- Not all parameters are known for all potential candidates.

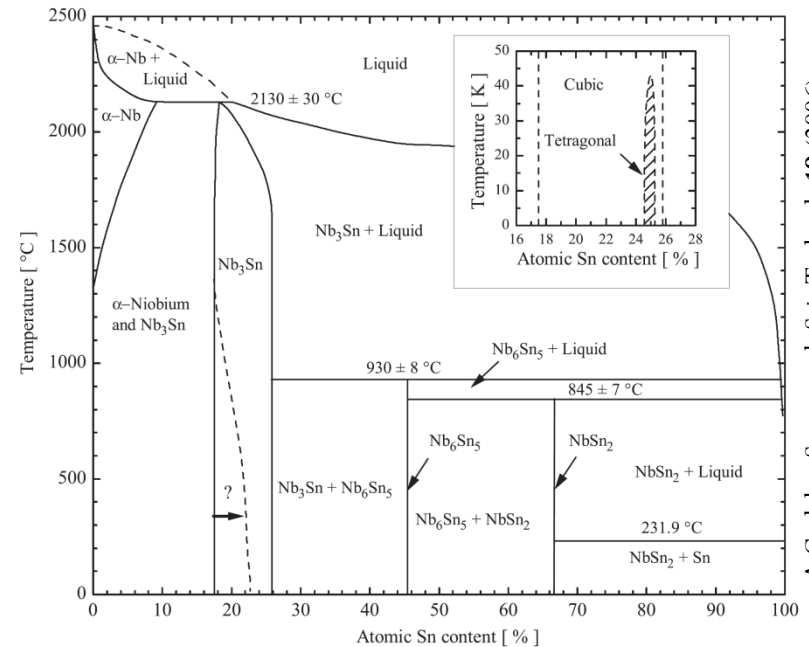# LTS: A15 & B1 compounds
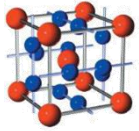
A15 structure A_3B

- A atoms: transition elements
- B atoms: non transition or transition elements
- Stable and high T_c: **Nb_3Sn**, V_3Ga, V_3Si, Mo_3Re
- A15 compounds are not formable due to extreme brittleness
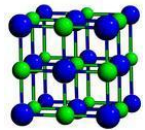
B1 structure AB

- A atoms: metallic
- B atoms: non-metallic
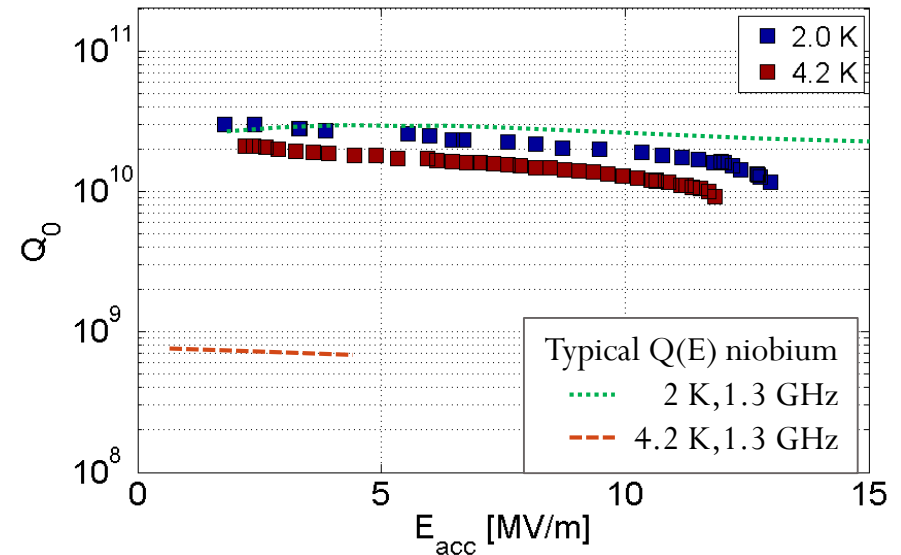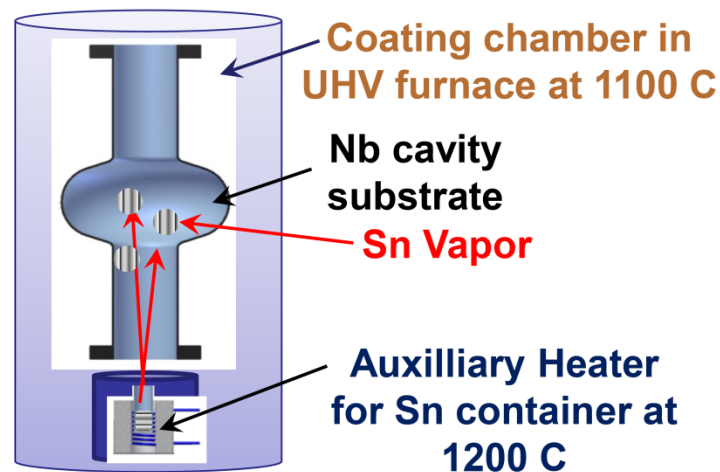- Stable and high T_c: NbC, **NbN**

Phase diagram of the Nb-Sn system

A Godeke, Supercond. Sci. Technol. **19** (2006) R68–R80

A15 compounds: Nb$_3$Sn

- Low thermal conductivity would favor coating a copper cavity with Nb$_3$Sn.

- Only successful fabrication so far: Sn vapor diffusion into Nb cavity, alloying Nb$_3$Sn (Wuppertal 1985, Cornell 2013)

Both pictures from: *Nb3Sn for SRF Application*
M. Liepe (Cornell), WEIOA04, SRF 2013

Summary

- For now, only high Q at moderate E_{acc} or high E_{acc} at moderate Q can be achieved.

- The high Q research tries to understand loss mechanisms and develops new recipes to minimize the residual resistance.

- Maximum E_{acc} can only be achieved by high-end surface preparation. Improving polishing and cleaning procedures is mandatory for multicell cavities and serial production.

- New materials have lower BCS surface resistance (higher Q) and/or higher critical field (higher E_{acc}).

- HTS are not suitable for rf applications.

- Nb_3Sn is the most promising alternative material so far.

ACKNOWLEDGMENT

- A lot of 'material' from CERN will be used but this does not mean that 'material' from other institutions is considered inferior.

- Other material was taken from contributions to the CERN Accelerator Schools, CAS [1] (CERN-2006-002, CERN-2005-03, CERN-2005-04, CERN-2004-08, CERN-1996-03, CERN-1992-03, as well as earlier ones and other sources mentioned).
  - R. P. Feynman et al., Lectures on Physics Vol. II
  - P. Schmüser et al.; The Superconducting TESLA Cavities; Phys. Rev. Special Topics - AB 3 (9) 092001
  - A. W. Chao & M. Tigner, Handbook of Accelerator Physics and Engineering, World Scientific
  - Alexey Ustinov, Lecture on superconductivity, University Erlangen-Nürnberg (from which I used some slides w.r.t. Superconductivity)

(http://www.pi.uni-karlsruhe.de/ustinov/group_hp/fluxon.physik.uni-erlangen.de/pages/lectures/WS_0708/Superconductivity-2007-01.pdf)

- and an excellent textbook of the field: H. Padamsee, J. Knobloch, and T. Hays, RF Superconductivity for accelerators & H. Padamsee, RF Superconductivity, Weinheim 2008, resp.

[1] http://cdsweb.cern.ch/collection/CERN%20Yellow%20Reports

Last but not least I thank my colleagues E. Haebel and J. Tuckmantel for many discussions, clarifications, and presentation material.

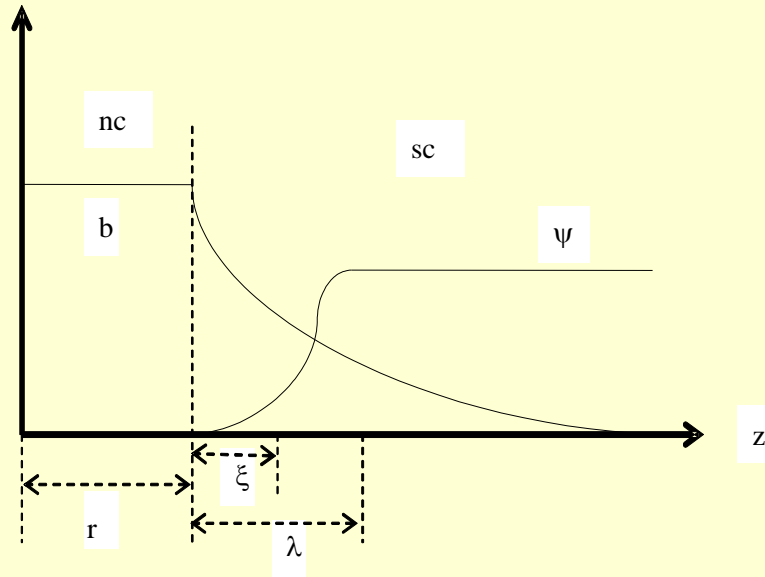# BACKUP SLIDES

Surface tension at nc-sc interface

Fig. 1: Interface between normal to superconducting metal for a type II superconductor with $\lambda > \xi$. b denotes the (microscopic) magnetic field and ψ describes the wave function of the superconducting condensate.

Inspecting Fig. 1, the energy balance DE between the condensation energy E_C and the diamagnetic energy E_B for a planar interface area A and an applied magnetic field B, is

$$\Delta E = \Delta E_c - \Delta E_B =$$

$$= \frac{1}{2\mu_0} B_{th}^2 A(r + \xi) - \frac{1}{2\mu_0} B^2 A(r + \lambda)$$

JUAS 2020: SC RF - Caspers/Wendt/Bozzolan

For a type II superconductor, as the penetration of magnetic fields starts from small filaments of cylindrical shape located parallel to the interface, a more realistic way to describe the energy balance is based on a small half-cylinder of radius r instead of a plane, which will become normal:

$$\Delta E = \Delta E_c - \Delta E_B = \frac{1}{2\mu_0} \cdot B_{th}^2 \cdot \frac{\pi}{2} \cdot (r + \xi)^2 - \frac{1}{2\mu_0} \cdot B^2 \cdot \frac{\pi}{2} \cdot (r + \lambda)^2 < 0 \, ,$$

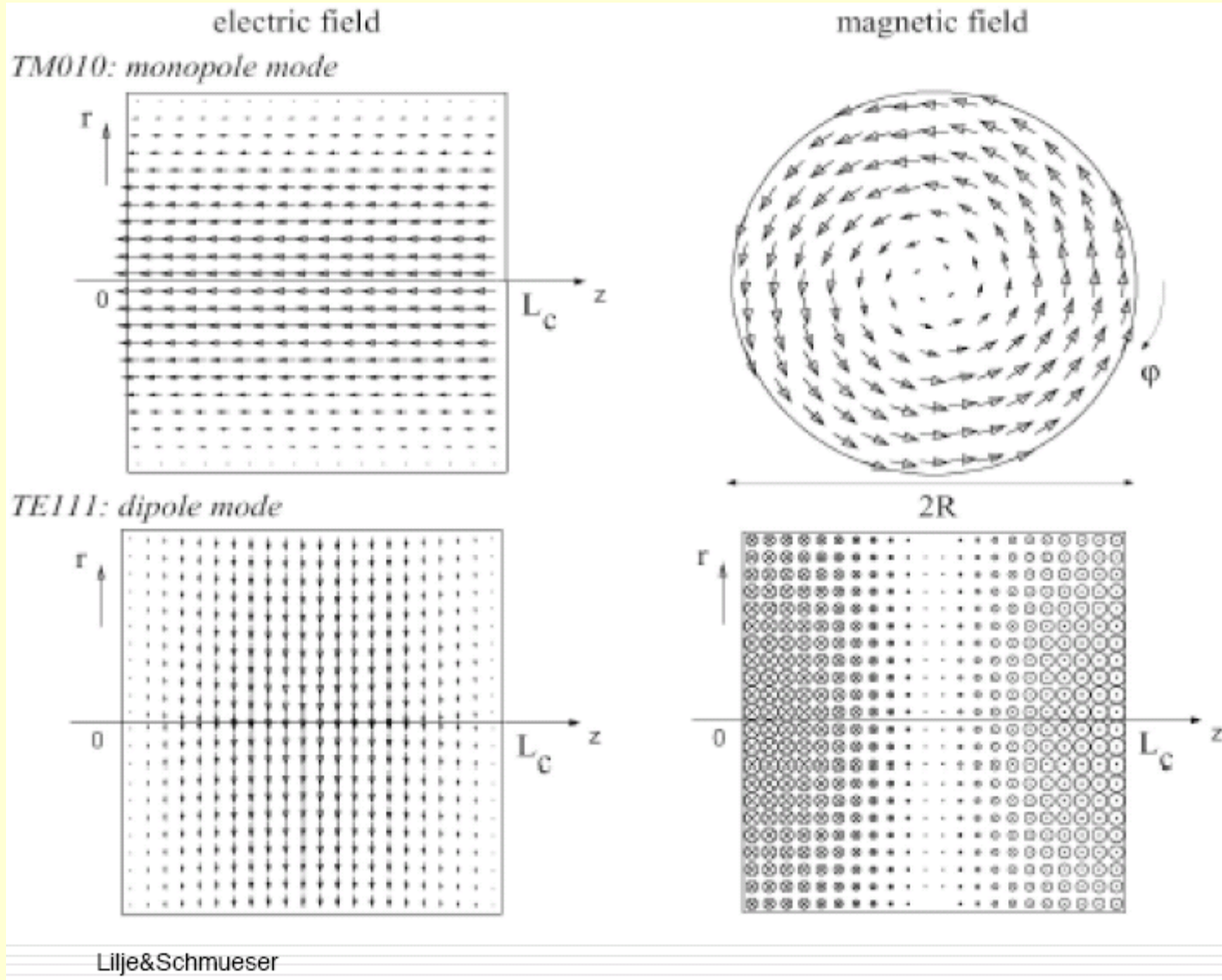from which the threshold B^*_{c1} of the magnetic field for penetration is defined as

$$B^*_{c1} \geq \frac{r + \xi}{r + \lambda} \cdot B_{th} \xrightarrow{r \to 0} \overbrace{\frac{\xi}{\lambda}}^{1/\kappa} \cdot B_{th} = \frac{1}{\kappa} \cdot B_{th} \, .$$

In a type II superconductor, the lowest value of the applied magnetic field B which induces penetration as filaments of magnetic field into the bulk is called the lower critical field B_{c1}, for which the microscopic theory gives as exact result:

$$B_{c1} = \frac{\ln \kappa}{\sqrt{2} \cdot \kappa} \cdot B_{th}$$
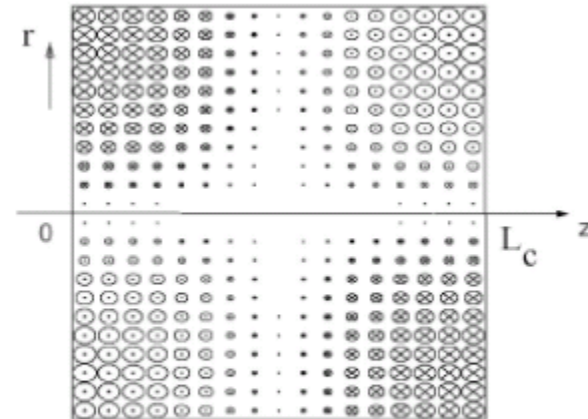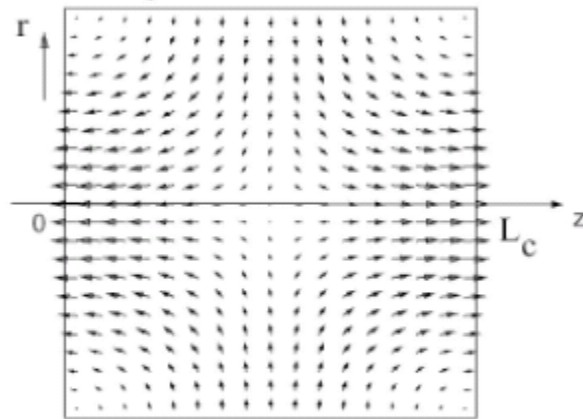,

very close to the previous one. In a type I superconductor, the lowest value of the applied magnetic field B which induces bulk penetration of magnetic field is called the thermodynamic critical field B_{th}

Different mode families 1/2

electric field — magnetic field

TM010: monopole mode

TE111: dipole mode

2R

Lilje&Schmueser

JUAS 2020: SC RF - Caspers/Wendt/Bozzolan
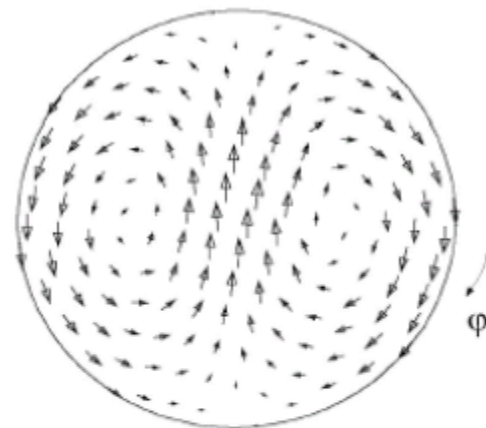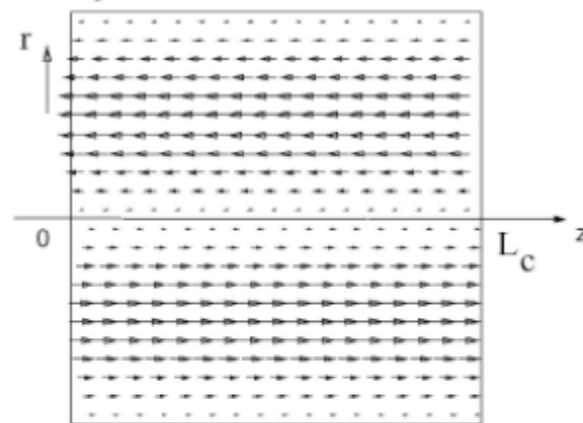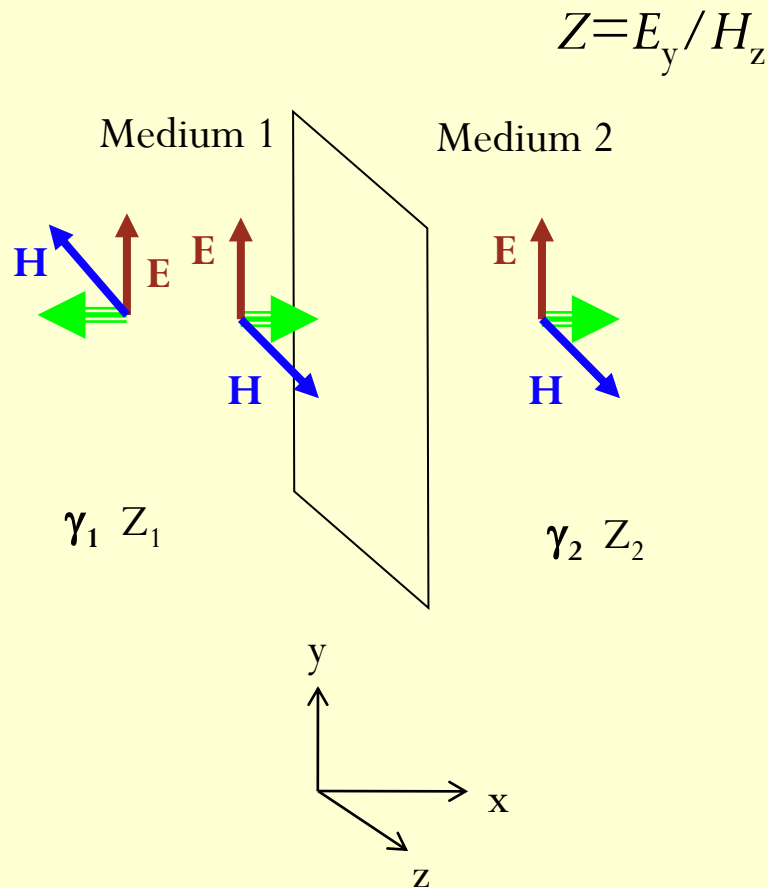
TM011: monopole mode

TM110: dipole mode

Figure 1: Electric and magnetic field in a pillbox cavity for several resonant modes (Courtesy of M. Liepe).

Lilje&Schmueser

Introduction of the notion of reflection and transmission factors.

$$Z = E_y / H_z$$

$$E_{yi} = \hat{E} e^{-\gamma_1 x} e^{i\omega t}$$

$$H_{zi} = \frac{\hat{E}}{Z_1} e^{-\gamma_1 x} e^{i\omega t}$$

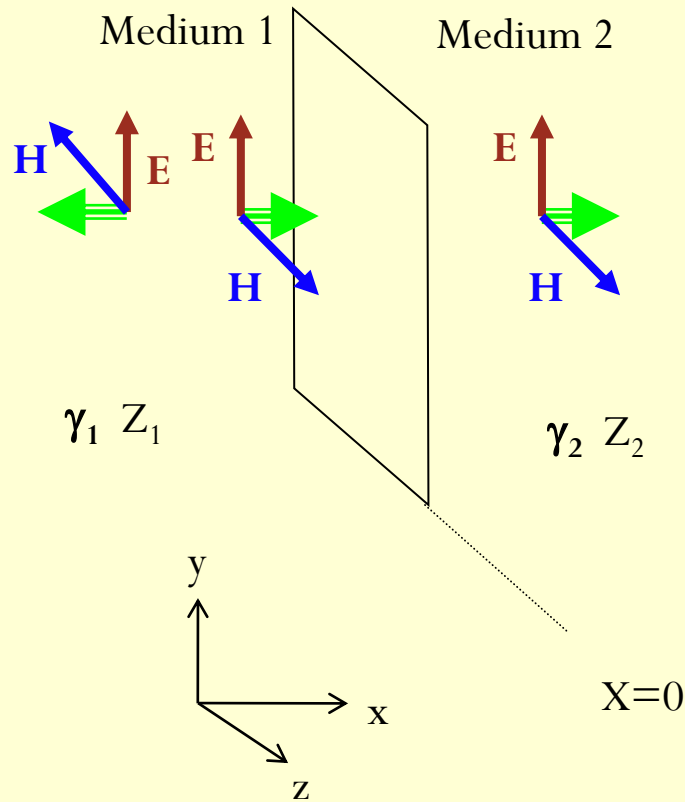$$E_{yr} = \rho \hat{E} e^{\gamma_1 x} e^{i\omega t}$$

$$H_{zr} = -\rho \frac{\hat{E}}{Z_1} e^{\gamma_1 x} e^{i\omega t}$$

$$E_{yt} = \tau \hat{E} e^{-\gamma_2 x} e^{i\omega t}$$

$$H_{zt} = \tau \frac{\hat{E}}{Z_2} e^{-\gamma_2 x} e^{i\omega t}$$

Medium 1   Medium 2

H   **E**   **E**   **E**

H   **H**

γ_1 Z_1 γ_2 Z_2

y

x

z

JUAS 2020: SC RF - Caspers/Wendt/Bozzolan

From continuity at the interface:

$$\left.\begin{array}{l} E_{yi} + E_{yr} = E_{yt} \\ H_{zi} + H_{zr} = H_{zt} \end{array}\right\} x = 0$$

Medium 1   Medium 2

H   **E**   **E**   **E**

H   **H**

$\gamma_1 \ Z_1$ $\gamma_2 \ Z_2$

y

x

z

X=0

$$1 + \Gamma = \tau$$

$$\frac{1}{Z_1} - \Gamma \frac{1}{Z_1} = \tau \frac{1}{Z_2}$$
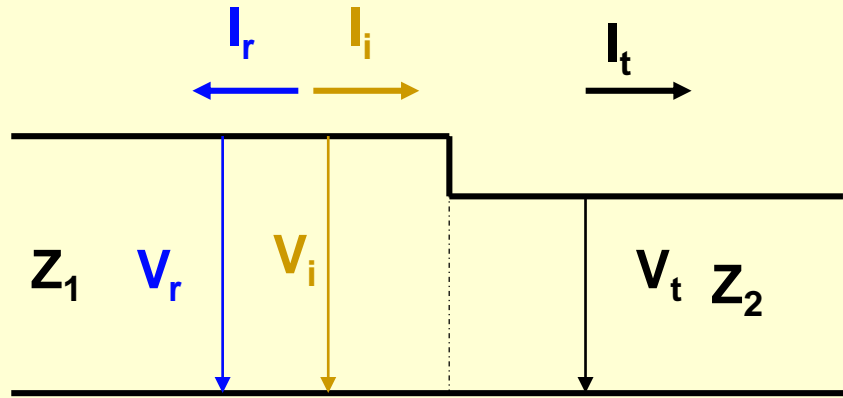
$$\frac{Z_2}{Z_1}(1 - \Gamma) = \tau$$

$$1 + \Gamma = \frac{Z_2}{Z_1}(1 - \Gamma)$$

$$\Gamma = \frac{Z_2 - Z_1}{Z_2 + Z_1}$$

$$\tau = \frac{2Z_2}{Z_2 + Z_1}$$

157

Response of a cavity to RF

- Apply transmission line theory (to a one-port impedance):

$$V_t = V_i + V_r$$

$$I_t = I_i - I_r$$

$$\boxed{V_t = \tau \cdot V_i} \qquad \boxed{V_r = \Gamma \cdot V_i}$$

$$V_r = Z_1 \cdot I_i$$

$$V_t = Z_2 \cdot I_t$$

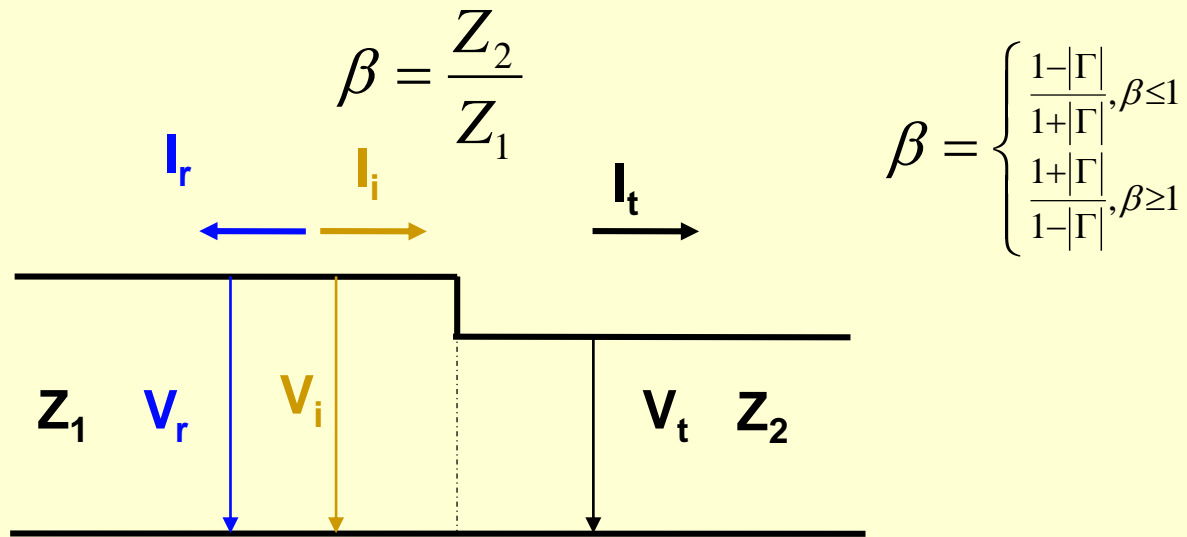Reflexion factor ρ Transmission factor τ

$$\Rightarrow \Gamma = \frac{Z_2 - Z_1}{Z_2 + Z_1} \qquad\qquad \Rightarrow \tau = \frac{2 \cdot Z_2}{Z_2 + Z_1}$$

$$\tau - \Gamma = \frac{2 \cdot Z_2 - (Z_2 - Z_1)}{Z_1 + Z_2} = 1$$

JUAS 2020: SC RF - Caspers/Wendt/Bozzolan

- Reflexion factor Γ depends on position, the coupling factor β does not:

$$\beta = \frac{Z_2}{Z_1}$$

$$\beta = \begin{cases} \frac{1-|\Gamma|}{1+|\Gamma|}, \beta \leq 1 \\ \frac{1+|\Gamma|}{1-|\Gamma|}, \beta \geq 1 \end{cases}$$

$$|\Gamma| = \left|\frac{Z_2 - Z_1}{Z_2 + Z_1}\right| = \left|\frac{Z_2/Z_1 - 1}{Z_2/Z_1 + 1}\right| = \begin{cases} \frac{\beta-1}{\beta+1}, \text{if } \beta \geq 1 \\ \frac{1-\beta}{1+\beta}, \text{if } \beta \leq 1 \end{cases}$$

$$|\tau| = |1 + \Gamma| \underset{\rho \geq 0}{=} 1 + |\Gamma| = 1 + \frac{\beta-1}{\beta+1} = \frac{2\beta}{1+\beta}$$

$$|\tau| = |1 + \Gamma| \underset{\rho \leq 0}{=} 1 - |\Gamma| = 1 - \frac{1-\beta}{1+\beta} = \frac{2\beta}{1+\beta}$$

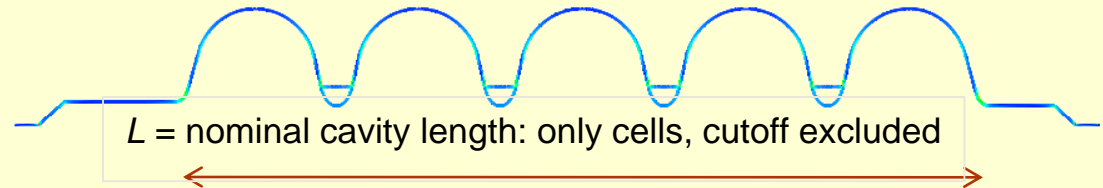- Determination of Q_0 and accelerating voltage/gradient

$$V_t = \tau \cdot V_i = \frac{2\beta}{1+\beta} V_i \Rightarrow V_t^2 = \frac{4\beta^2}{(1+\beta)^2} V_i^2 = \frac{8\beta^2}{(1+\beta)^2} \cdot \underbrace{Z_1}_{(R/Q)\cdot Q_0/\beta} \cdot \underbrace{\frac{V_i^2}{2Z_1}}_{P_i} \qquad 1)$$

$$\Rightarrow V_t = \sqrt{\frac{8\beta}{(1+\beta)^2} \cdot (R/Q)\cdot Q_0 \cdot P_i}$$

$$\frac{1}{Q_L} = \frac{1}{Q_0} + \frac{1}{Q_{ext}} = \frac{1+\dfrac{Q_0}{Q_{ext}}}{Q_0} \Rightarrow Q_0 = \left(1 + \underbrace{\frac{Q_0}{Q_{ext}}}_{=\beta}\right)\cdot Q_L = (1+\beta)\cdot \underbrace{Q_L}_{\omega\tau}$$

$$\beta = \begin{cases} \dfrac{1-|\Gamma|}{1+|\Gamma|}, & \beta \le 1 \\ \dfrac{1+|\Gamma|}{1-|\Gamma|}, & \beta \ge 1 \end{cases}$$
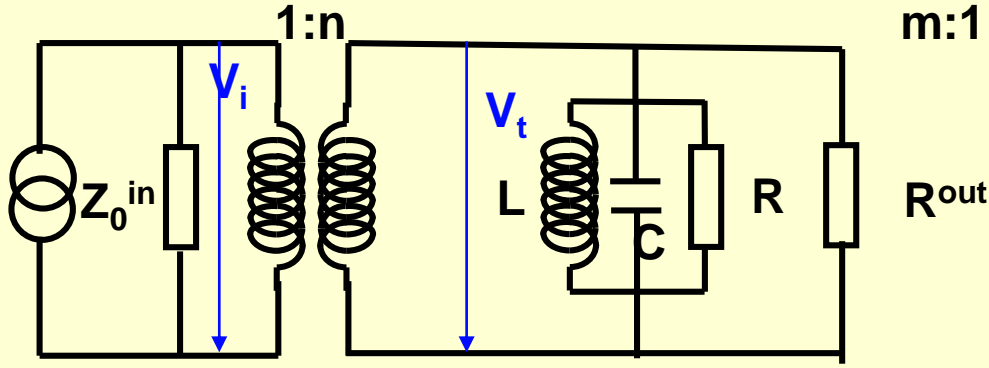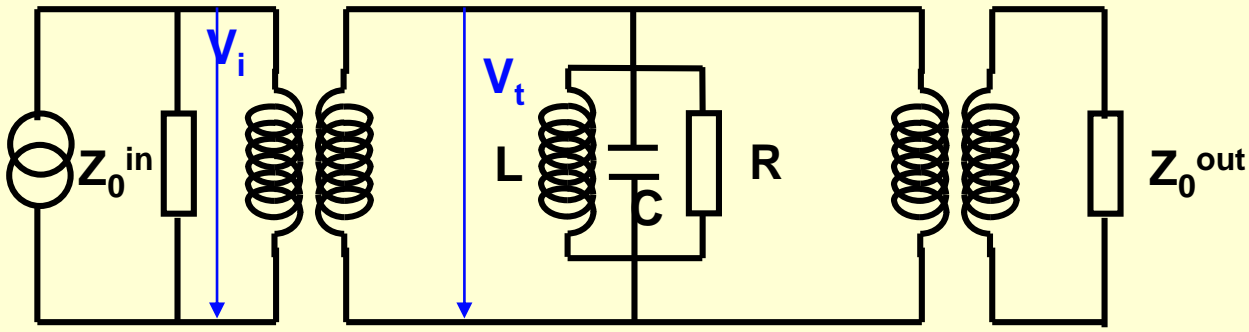
$$E_{acc} = V_t / L$$

L = nominal cavity length: only cells, cutoff excluded

1) Remember

$$Z_1 = \frac{Z_1}{Z_2}\cdot Z_2 = \frac{Z_2}{\beta} = \frac{R}{\beta} = \frac{1}{\beta}\cdot\underbrace{\frac{R}{V_c^2/2}}_{P_c}\cdot\omega U \cdot \frac{V_c^2}{2\omega U} = \frac{1}{\beta}\cdot\underbrace{\frac{\omega U}{P_c}}_{Q_0}\cdot\underbrace{\frac{V_c^2}{2\omega U}}_{R/Q} = \frac{(R/Q)\cdot Q_0}{\beta}$$

underbrace $\frac{Z_1}{Z_2}$: $1/\beta$
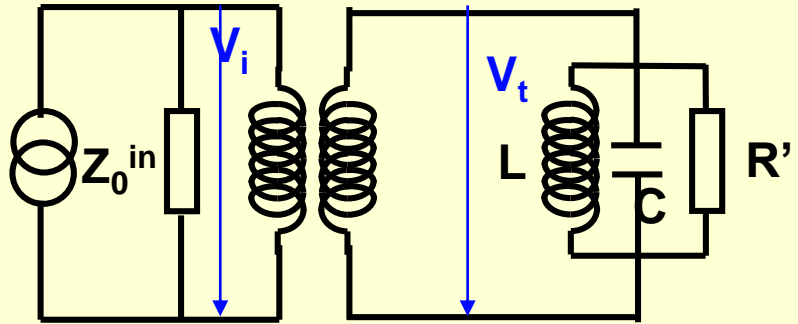
- The response of a **two port cavity** is equivalent to that of a one-port cavity
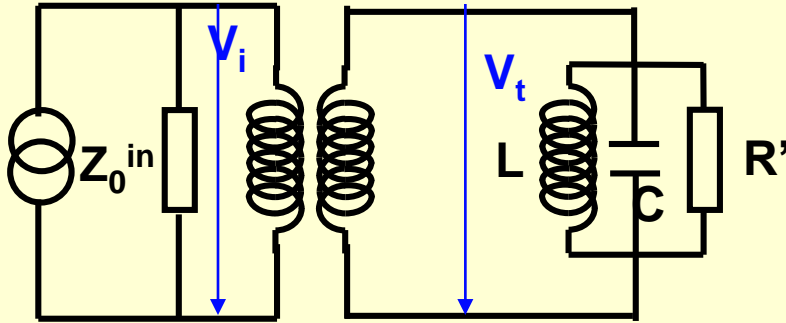

$$R^{out} = m^2 Z_0^{out}$$

$$m^2 = \frac{(R/Q) \cdot Q_{ext}^{out}}{Z_0^{out}}$$

$$\frac{1}{R'} = \frac{1}{R} + \frac{1}{R^{out}}$$

$$V_t = \tau \cdot V_i = \frac{2\beta'}{1+\beta'} V_i \Rightarrow V_t^2 = \frac{4\beta'^2}{(1+\beta')^2} V_i^2 = \frac{8\beta'^2}{(1+\beta')^2} \cdot \underbrace{Z_0^{in}}_{(R/Q)\cdot Q_0'/\beta'} \cdot \underbrace{\frac{V_i^2}{2Z_0^{in}}}_{P_i}$$

$$\Rightarrow V_t = \sqrt{\frac{8\beta'}{(1+\beta')^2} \cdot (R/Q)\cdot Q_0' \cdot P_i}$$

$$Q_0' = (1+\beta') \cdot \underbrace{Q_L}_{\omega\tau} \qquad E_{acc} = V_t / L \qquad \beta' = \begin{cases} \frac{1-|\Gamma|}{1+|\Gamma|}, \beta' \leq 1 \\ \frac{1+|\Gamma|}{1-|\Gamma|}, \beta' \geq 1 \end{cases}$$

$$\frac{1}{Q_0} = \frac{1}{Q_0'} - \frac{1}{Q_{ext}^{out}} \qquad Q_{ext}^{out} = \frac{\omega U}{P_{out}} = \frac{V^2}{2\cdot(R/Q)\cdot P_{out}}$$
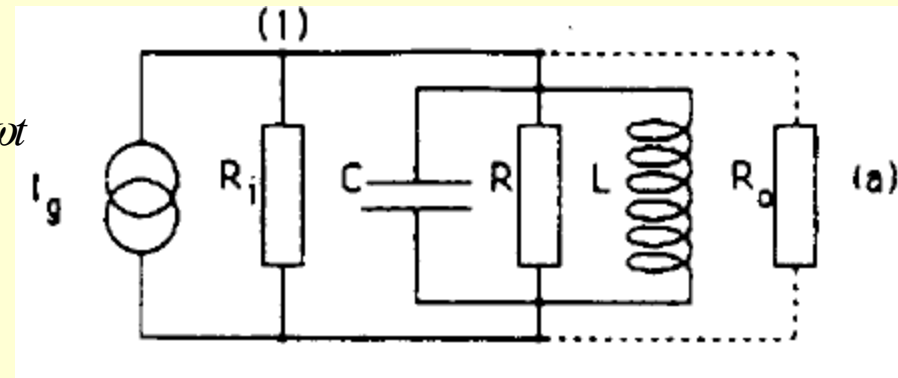
1. Apply Kirchhoff's current law at node (1)

$$\frac{V}{R_i} + \frac{1}{L}\int V(t) + C\frac{dV}{dt} + \frac{V}{R} = I_{g0} \cdot \cos\omega t$$

2. Differentiate and transform lumped circuit elements into cavity parameters by using preceding "Table 7"

$$\frac{d^2V}{dt^2} + \frac{\omega_0}{Q_L}\frac{dV}{dt} + \omega_0^2 V = -I_{g0}\cdot\left(\frac{R}{Q}\right)\cdot\omega\cdot\omega_0\cdot\sin\omega t$$

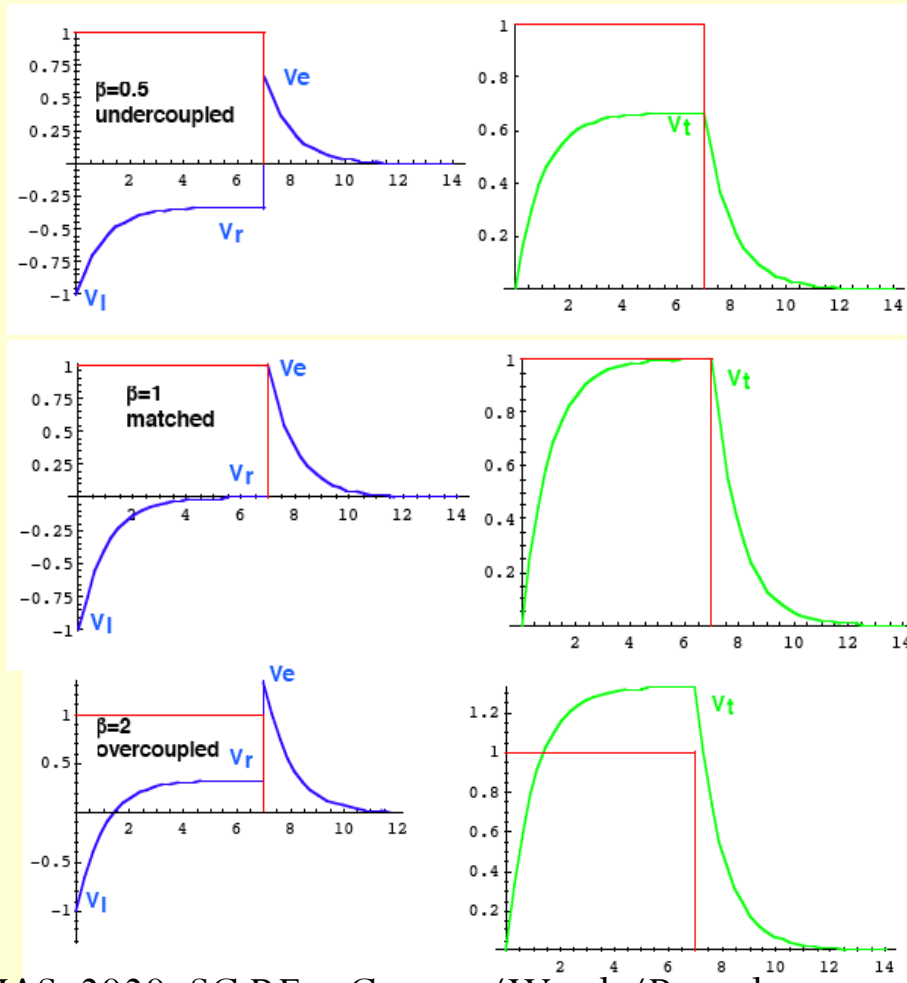3. Find the general solution of the homogeneous differential equation

$$V(t) = e^{-\frac{\omega_0 t}{2Q_L}} \cdot \left(c_1 \cdot e^{i\sqrt{1-1/(2Q_L)^2}\cdot\omega_0 t} + c_2 \cdot e^{-i\sqrt{1-1/(2Q_L)^2}\cdot\omega_0 t} \right)$$

4. Find the solution of the inhomogeneous differential equation

$$V(t) = V_0 \cdot \cos\omega_0 t \cdot \left\{ 1 - e^{-\frac{\omega_0 t}{2Q_L}} \right\}$$

JUAS 2020: SC RF - Caspers/Wendt/Bozzolan

Transient response

- Determination of Q_0 and accelerating voltage/gradient (2)
- Oscilloscope signal for voltage measurement

$$V_t = V_i + V_r$$

Remember: $V_e = V_i + V_r$

$$|\rho| = \left|\frac{V_r}{V_i}\right| \Rightarrow 1^{\text{st}}\text{method}:$$

$$\beta = \frac{1 - \left|\dfrac{V_r}{V_i}\right|}{1 + \left|\dfrac{V_r}{V_i}\right|} = \begin{cases} \dfrac{|V_i| - |V_r|}{|V_i| + |V_r|}; \beta \leq 1 \\[2mm] \dfrac{|V_i| + |V_r|}{|V_i| - |V_r|}; \beta \geq 1 \end{cases}$$

$$2^{\text{nd}}\text{method}: \beta = \frac{1 - \left|\dfrac{V_r}{V_i}\right|}{1 + \left|\dfrac{V_r}{V_i}\right|} = \frac{1 - \left|\dfrac{V_i - V_e}{V_i}\right|}{1 + \left|\dfrac{V_i - V_e}{V_i}\right|} =$$

$$= \frac{|V_e|}{2 \cdot |V_i| - |V_e|} = \frac{1}{2 \cdot \left|\dfrac{V_i}{V_e}\right| - 1}$$

JUAS 2020: SC RF - Caspers/Wendt/Bozzolan